POST-OROGENIC UPLIFT, YOUNG FAULTS, AND MANTLE REORGANIZATION IN THE APPALACHIANS

Jesse Stuart Hill

A dissertation submitted to the faculty of the University of North Carolina at Chapel Hill in partial fulfillment of the requirements for the degree of Doctor of Philosophy in the Department of Geological Sciences.

Chapel Hill
2018

Approved by:

Kevin Stewart

James Hibbard

Jonathan Lees

Tamlin Pavelsky

Karl Wegmann

ABSTRACT

Jesse Stuart Hill: Post-orogenic uplift, young faults, and mantle reorganization in the Appalachians
(Under the direction of Kevin G. Stewart)

The Appalachians have a complex history involving a wide range of geologic processes. In recent decades the story of how this ancient orogen has been built up and broken down through multiple cycles of collision and rifting has become richer with investigations into the apparent enigma of mountain building in the absence of obvious tectonic forces. There are features that cannot be explained if the Appalachians are simply the remnants of a once Andean-scale range that has eroded steadily since it was in proximity to a plate margin, such as fracture zones that cut through the mountains that have been studied but not well understood, or active seismic zones that do not seem to belong in a passive margin setting. Many landscapes in the mountains resemble those found near plate margins and have led previous workers to conclude that parts of the Appalachians are the result of a Cenozoic topographic rejuvenation. In this dissertation, I use a multi-faceted approach to propose an explanation of how and why the southern and central Appalachians have uplifted in recent geologic time. In chapter 1, I use an automated analysis of longitudinal stream profiles and flow directions to show how fractures and faults associated with topographic lineaments crossing the mountains can influence erosional processes and landscape development in the Blue Ridge of western North Carolina. In chapter 2, I present the first documented evidence of a seismically active, Cenozoic brittle fault zone associated with blocky uplift of the Appalachians. In chapter 3, I link young landscapes to mantle delamination and attempt to explain why there is a mismatch of topography along the geologic provinces.

ACKNOWLEDGMENTS

I am forever grateful to Kevin Stewart for his guidance, patience, and willingness to nurture my curiosity with an open mind. He gave me the luxury to search for new ideas, even if most of them did not yield tangible results. It's been a great adventure. The mapping project was funded with EDMAP Award G15AC00156, under the supervision of the STATEMAP initiative. Additional funding for chapters 1 and 2 came from the J. Robert Butler Scholarship and Martin Research Fund, awarded through the Geological Sciences department at UNC-Chapel Hill. George Allen and I had insightful conversations about the concepts behind chapter 1. Thanks to Rick Wooten, Bart Cattanach, and Nick Bozdog of the NCGS for their time in the field and for helping put the pieces together around the Boone fault. Michelle Gavel and Emma Blackwell worked as field assistants during the mapping project. James Bear was very gracious with his time and insight at the Vulcan quarry in Boone. A special thanks to the people of Watauga County for their hospitality and access to their land. David Greenawald always stopped what he was doing to help me improve figures and concepts. Birk Biryol shared his raw tomographic data with me and helped me understand many geophysical conundrums. Jonathan Lees and Tamlin Pavelsky taught me the value of making my own tools and avoiding a black box whenever possible. Jim Hibbard showed me the complexity of Appalachian geology and that there is more than a lifetime of questions to pursue here. Karl Wegmann and Sean Gallen opened my eyes to using geomorphology to understand hidden structural stories. Thanks to Tallulah for sticking with me through it all. Last but definitely not least, I want to thank Deborah Harris, who helped me laugh on a daily basis.

TABLE OF CONTENTS

LIST OF FIGURES

CHAPTER 1: AUTOMATIC KNICKPOINT DETECTION AND COMPARISON OF STREAM DIRECTIONS RELATIVE TO INTERNAL FABRICS ALONG WESTERN NORTH CAROLINA BLUE RIDGE STREAMS

1.1. Introduction

When a stream profile is thrown out of equilibrium due to a lowering in base level, a wave of erosion moves towards the headwaters as over-steepened sections of streams called knickpoints. Knickpoints propagate upwards until they either reach the headwaters or are eliminated by erosion along their upstream ascent. Many workers use knickpoint-migration rates to estimate timing and magnitude of uplift but few consider how bedrock heterogeneities may alter erosive processes. In this study, we focus on the southern Appalachian Mountains, an ancient orogen with multiple internal rock fabrics such as metamorphic foliation and post-orogenic fracture sets. We use an automated technique to estimate knickpoint abundance and stream flow directions along ~100 streams from 15 basins ranging from 12 - 346 km^2 in drainage area from Graham and Swain counties, western North Carolina. We analyzed ~6m-horizontal-resolution LIDAR to test the idea that lithologic differences across northeast-striking, Paleozoic and older structures drive knickpoint formation, and that streams flow along paths controlled by structures parallel and perpendicular to the regionally northeast-trending mountain belt. Although we detected some knickpoints along streams draining northwest, perpendicular to mapped bedrock contacts, east-flowing and south-flowing streams are the most abundant and contain the most knickpoints. We propose that knickpoints and hillslopes in our study area are migrating headwards by blocky failure along high-angle, lineament-parallel fractures rather than metamorphic foliation. We attempt to connect uplifted plateaus and peaks, transient knickpoints, and neotectonic structures to a Neogene

rejuvenation of a landscape often considered sculpted by differential erosion of Paleozoic and older bedrock features.

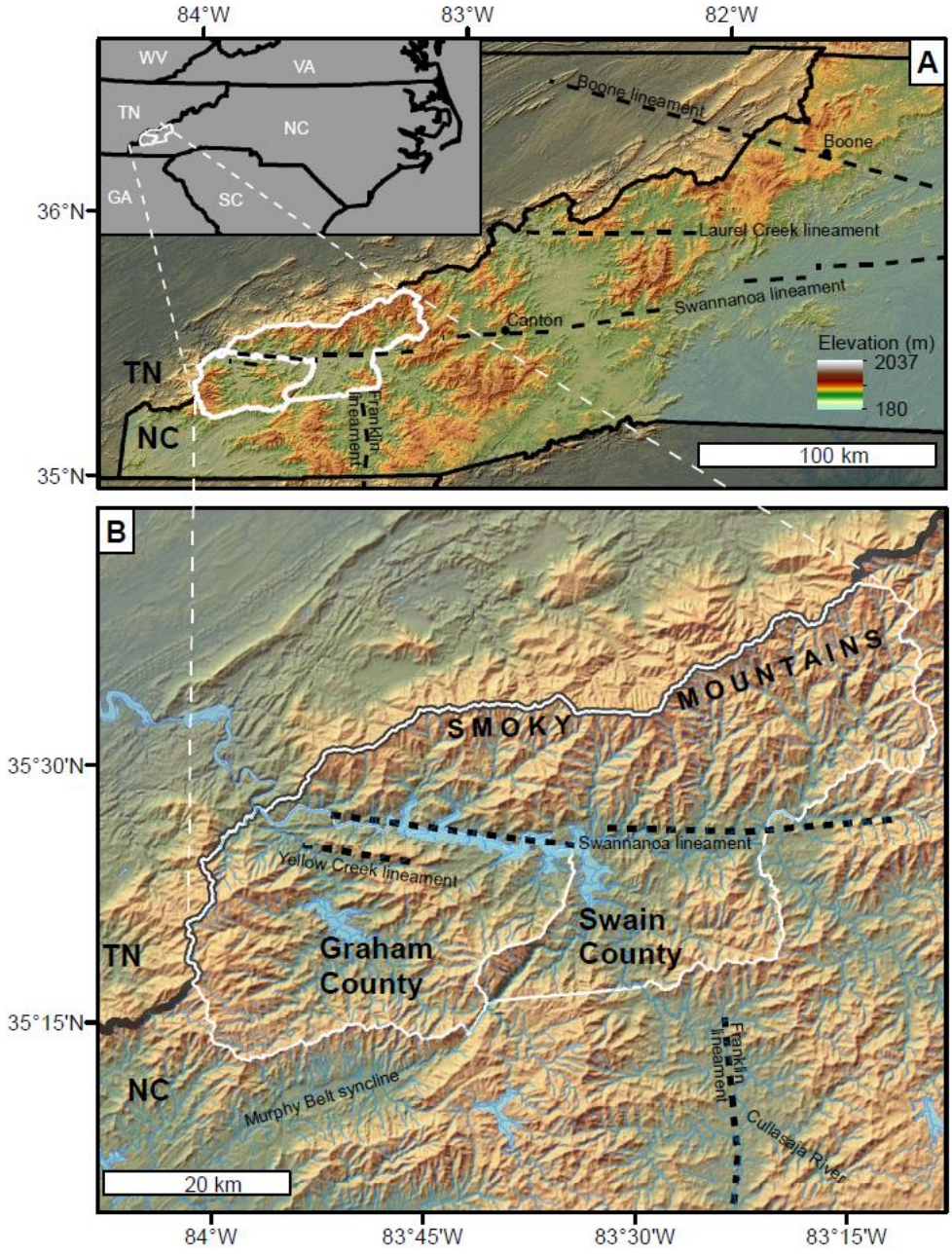

Figure 1.1: (A) Digital elevation model of western North Carolina showing locations of Graham and Swain counties (white outline) and major topographic lineaments (black dashes). Inlay map shows location within the state. (B) Digital elevation model showing relevant geologic features. Note the location of the Murphy Belt Syncline and the Cullasaja River. Although the orogenic belt trends NE-SW, there is a family of lineaments running E-W, parallel to the major Swannanoa lineament.

Knickpoints form through numerous mechanisms, and their profile cannot be directly attributed to their mode of genesis. Previous authors linked knickpoints to base level changes related to either tectonics (Snyder et al., 2000; Kirby and Whipple, 2001; Miller et al., 2006; Wobus et al., 2006; Gallen et al., 2013) or climate fluctuations (Pazzaglia et al., 1998; Whipple, 2001). Other studies have explained knickpoints by lithologic controls such as rock hardness (Hack, 1982; Goldrick and Bishop, 1995; Hancock et al., 1998; Duvall et al., 2004), sediment flux and grain size (Whipple and Tucker, 2002; Sklar and Dietrich, 2004), and attitude of layering relative to stream flow direction (Miller, 1991; Bishop and Goldrick, 1992). Hillslope failure adjacent to streams can deposit material into valleys, forming natural dams resembling knickpoints (Stock and Dietrich, 2006; Korup, 2006). When base level falls, transient knickpoints and adjacent hillslopes migrate headwards as coupled erosive systems that separate steepened, more active landscapes downstream from lower-relief, less active headwaters (Gallen et al, 2011).

Knickpoints can be valuable tools for understanding tectonic histories, but it is necessary to eliminate non-tectonic mechanisms of formation before using knickpoints to estimate uplift timing or magnitude. One common method for distinguishing headwards-migrating, tectonically driven knickpoints from stationary, lithologically controlled ones is to compare knickpoint locations to underlying bedrock units (e.g. Crosby and Whipple, 2006; Gallen et al, 2011; Miller et al, 2013). This method of comparison can be problematic if bedrock heterogeneities exist between mapped contacts. One solution to these problems is to investigate the knickpoints in the field but traversing entire stream networks on foot is not always feasible. To address this issue and to test the idea that metamorphic fabrics interact with fractures to form knickpoints along stream segments draining perpendicular to the strike of foliation, we use an automated, GIS-based technique to compare the directions of entire stream networks with directions of the streams at knickpoints. We use this automated process to determine if the stream directions match the strikes of bedrock contacts,

metamorphic foliation, or any of the multiple fracture sets in the study area. We compare the retreat directions of knickpoint with overall stream direction at ~100,000 LIDAR-derived points from Graham and Swain counties, North Carolina, that drain into a major topographic lineament, which is the local base level (Figure 1.1). We also sort knickpoints by elevation, rock type, and relation to meso-and macro-scale structures in the study area and present a conceptual uplift model explaining both the remote sensing and field observations as a result of differential erosion and neotectonics.

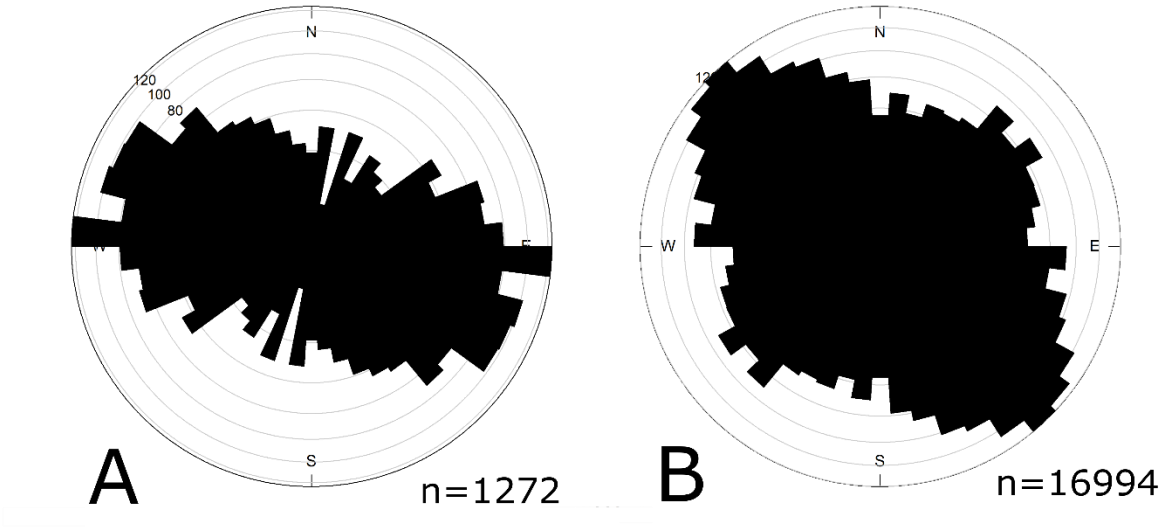

Figure 1.2: (A) Rose diagram showing strikes of joints found within the Swannanoa lineament, indicating that fractures strike generally parallel to the E-W lineament. (B) Rose diagrams of strikes of joints collected by the North Carolina Geological Survey in the Blue Ridge province, indicating the regional joints strike generally perpendicular to the main orogenic belt.

1.2 Geologic background and setting

During the Paleozoic, the supercontinent Pangea was assembled as multiple NW-directed accretionary events formed the NE-striking metamorphic fabrics (e.g. Hibbard et al., 2010). During the Triassic, Pangea began to break apart as the Atlantic Ocean was born (e.g. Manspeizer et al., 1989; Thomas, 2006). In the Jurassic, dike emplacement marked the last major plate boundary tectonic event of the Appalachians (Beutel et al., 2005), but not the last record of exhumation. Since then at least four pulses of offshore sedimentation occurred, likely related to uplift and erosion, with the largest event happening in the Middle Miocene (Poag and Savon, 1989; Pazzaglia and Brandon, 1996).

Numerous lines of evidence support the hypothesis that the southern Appalachians were uplifted in the Miocene (e.g.: Hack, 1982; Nystrom, 1986; Dennison et al., 1997; Stewart and Dennison, 2006). Miocene coarse-grained conglomerates in the Coastal Plain contain clasts from the Piedmont and Blue Ridge (Nystrom, 1986), plus there is a band of Miocene rocks lying unconformably above folded Oligocene strata around the southern terminus of the mountain belt in Georgia (Dennison and Stewart, 2006; Stewart, 2015). Many of the high plateaus in western North Carolina, Virginia, West Virginia, and Pennsylvania are likely erosional surfaces uplifted in the Middle Miocene that are currently being dissected by clusters of knickpoints at ~900-1150 m elevation (Gallen et al., 2013, Miller et al., 2013; Hill, 2013). This type of headward-migrating incision resembles an erosional process normally found near active plate margins (e.g. Whipple, 2001; Wobus et al., 2006).

The geomorphology of western North Carolina does not always correspond to lithology, likely because the mountains are responding to uplift that occurred in the Miocene (e.g., Hack, 1982; Nystrom, 1986; Dennison et al., 1997; Stewart and Dennison, 2006). By analyzing profiles of the Cullasaja River, Gallen et al. (2013) estimated the eroded volume of material between a

relict landscape projected from the headwaters and the modern-day profile to reconstruct the timing and magnitude of uplift. They observed 52 knickpoints along 44 stream profiles at locations consistent with a knickpoint retreat simulation and proposed that NW-flowing streams draining from a high plateau in southwestern North Carolina are actively dissecting a relict landscape uplifted ~480 m in the Middle Miocene. To eliminate the explanation that the Cullasaja knickpoints are lithologically controlled, Gallen et al. (2011) showed that knickpoint locations do not correspond to bedrock contacts on a 1: 500,000 scale geologic map. The Cullasaja River drains to the northwest, perpendicular to the NE-striking regional metamorphic fabric and bedrock contacts. In our previous work in the region (Hill, 2013), we observed the sharpest knickpoints in NW-draining basins whose streams flow against the NE-striking metamorphic foliation, possibly because differential erosion occurs in bedrock units not included on the currently available, low-resolution geologic maps. In their work in sedimentary rocks in south-central Indiana, Miller et al. (1991) focused on the interaction of stream dip and bedding, and found the highest relief knickpoints occur in thick units dipping against streams or at lower dips than the stream, especially where vertical joints allowed for blocky failure along bedrock discontinuities.

The data in this study come from Graham and Swain counties, North Carolina, where streams drain into the ~250 km long E-W Swannanoa lineament, just south of the Smoky Mountains (Figure 1.1). This area is composed mostly of Proterozoic rocks metamorphosed into quartzites, gneisses and schists during a series of Paleozoic orogenies, with the dominant metamorphic fabric being the NE-striking foliation (Southworth et al., 2012). The metamorphic foliation is overprinted by a series of E-W trench valleys that strike parallel and are likely associated with the Swannanoa lineament. There are three similar sets of lineaments (E-W, N-S, and WNW-ESE) that cut the southern Appalachian mountain belt and contain lineament-parallel fractures and faults (Hack, 1982; Dennison et al., 1997; Gay, 2000; Stewart and Dennison, 2006;

Hill, 2013). The Franklin lineament is a N-S trending trench spanning ~50 km southward from the Swannanoa lineament to northern Georgia (Figure 1.1). Local fracture sets strike parallel to the E-W and N-S trenches, especially in areas proximal to the lineaments (Hill, 2013). These directions differ from the NW-SE regional joint set that strikes perpendicular to and is likely related to the NE-trending foliation (Figure 1.2).

During our previous work in this area we found topographic lineaments separating high plateaus from steep peaks and noted different stream geometry on either side of the lineaments (Hill, 2013). Streams on the northern side of the Swannanoa lineament (Figure 1.1), within the Great Smoky Mountains, are graded and near equilibrium with fewer knickpoints, while streams to the south, within the Cheoah River basin, are far from equilibrium and have many knickpoints. In addition to the three high-angle fracture sets, we found minor dip-slip faults that commonly had strikes parallel to the lineaments. We found high-angle, WNW-striking, dip-slip faults within a lineament swarm near Boone, NC (Figure 1.1) that were likely not formed during the Paleozoic or Mesozoic, but more likely during Late Cenozoic uplift and topographic rejuvenation (Hill et al, 2016). The Boone lineament swarm serves as the local base level for numerous streams that contain knickpoints from ~900-1100 m, located 200-300 m above the valley floor. There appears to be at least a spatial connection between knickpoints and the lineaments, and we suspect there may be a genetic link as well.

1.3 Methods

1.3.1 Automated Knickpoint Selection

Manual selection of knickpoints by visual analysis of longitudinal stream profiles is time-intensive, subjective, and difficult to repeat. Existing automated-knickpoint-selection tools do not distinguish lithologically controlled from transient knickpoints and require analysis of the entire digital elevation model (e.g. Gonga-Saholiariliva et al., 2011), while others require manual removal of anthropogenic features such as dams by visual comparison to satellite imagery (e.g Queiroz et al., 2014). We focus only on information extracted from the longitudinal profile and can resolve both of these issues automatically. We base our technique on the idea that no single criterion always works to find knickpoints in real-world systems due to noise and natural variation between drainage basins. Rather than using only one parameter derived from the profile, we define a knickpoint numerically four different ways and select only knickpoints that match all of our criteria.

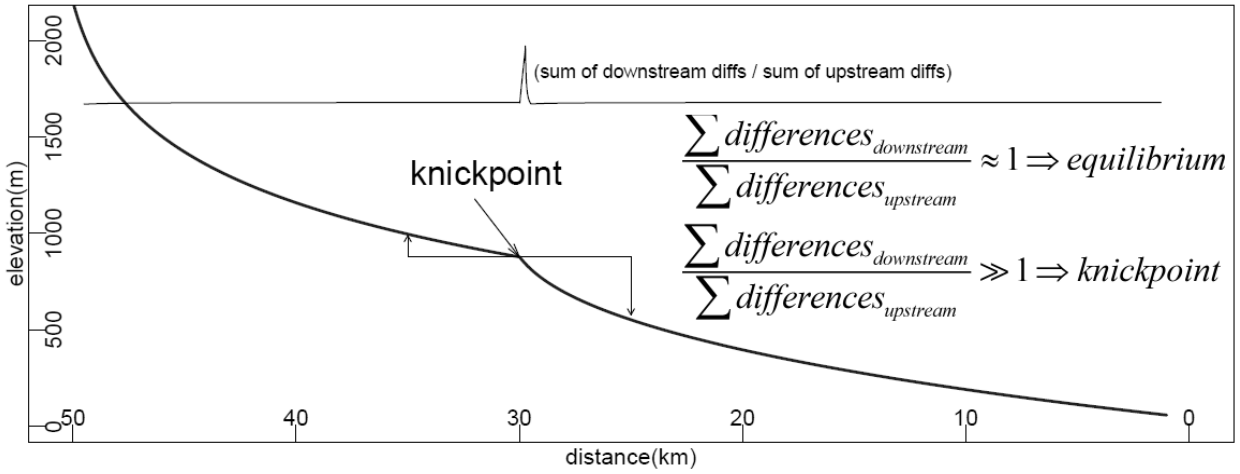

Figure 1.3: Example longitudinal profile illustrating the sum of the differences function and how it is used to find knickpoint locations. The thick line is the river profile, and the thin gray line is the sum of the differences value, which spikes at the location of the knickpoint.

We downloaded LIDAR- based digital elevation models (horizontal grid spacing of ~6m (20 ft.) and vertical resolution of ~1/3 m (<1ft)) from North Carolina's Spatial Data Download

(https://rmp.nc.gov/sdd/) as raster files that we imported into ArcMap 10. After re-projecting this raster from State Plane to UTM (Zone 17S), we used the hydrology tools in ArcMap to correct the elevation raster for hydraulic continuity, and to construct the flow direction, flow accumulation, and flow length rasters. We then used these files to find the steepest downstream paths, which we exported as *.dbf files with the sample tool. This is the last major step we take in ArcMap other than standard graphical procedures for production of figures. We based our method for extracting longitudinal profiles on techniques presented by Whipple et al. (2007).

We performed the automatic knickpoint selection and all other stream analyses with algorithms based in R, an open-source scripting language (https://www.r-project.org/); (R codes for these extraction and analysis tools are in the appendix of this paper). To eliminate repeating analyses where lower- and higher-order streams join, we reduced streams to exclusive sections, and before automatically extracting the knickpoints we smoothed the streams with a 50-meter-running-average horizontal window. As all of the streams we sampled are on the order of tens of kilometers in length, the 50-meter smoothing window allowed us to see the major features and ignore smaller ones.

To determine knickpoint locations, we combined four metrics derived from the longitudinal profile: (1) a new function called 'sum of the differences,' (2) steepness, or slope normalized for drainage area, (3) slope between each point, smoothed with another 50-m window, (4) and minimum vertical change of 6 m over 50 m of horizontal distance, (Figure 1.3). The sum of the differences function finds the ratio of the vertical change between stream pixels 50 m downstream and 50 m upstream from each point along the stream. The ratio of downstream to upstream differences will equal approximately one where the stream is at equilibrium and will be much greater than one at the location of a knickpoint, where the downstream differences are greater (Figure 1.3). The sum of the differences function will identify major knickpoints easily, but

because it yields a ratio with no units, it also picks small magnitude slope breaks that do not pertain to this study.

To improve the accuracy of our knickpoint selection, we combine the sum of the differences results with three other numerical tests to detect knickpoints. We set the parameters so liberally that each test selects many more points than actual knickpoints, and only points that pass all tests qualify as knickpoints. We could successfully pick knickpoints using only three parameters (sum of the differences, normalized steepness, and vertical change over a fixed horizontal distance) but the addition of smoothed slope allowed us to reject anthropogenic features such as dams with near-horizontal surfaces upstream. A dam occurs in our study area at Santeetlah Lake but this feature is always ignored by our automatic selection algorithm. We excluded any stream points from the lake in all analyses so our results would reflect true stream geometry and not the shortest path across a manmade lake. Out of the entire Cheoah River basin (n = 64,267 points), we removed 10,687 points from Santeetlah lake.

1.3.2 Stream Direction Calculation

To indirectly determine if the knickpoints are driven by modern tectonics or are the result of lithologic contacts, we compare the direction the stream flows with the direction of dominant bedrock fabrics in the area. To investigate patterns between knickpoints, stream directions, and bedrock fabrics, we made the following assumptions:

1) Although the dip of foliation is variable, it strikes generally northeast in our study area, consistent with the trend of the regional orogenic belt, the bedrock map patterns, and our field observations of outcrop structures;

2) material is moving downstream by meter-scale blocky failure along intersecting metamorphic fabrics and planar joint sets, not grain-by-grain weathering of the bedrock, and
3) fractures exist throughout the study area in E-W, N-S, and NW-SE sets (Figure 1.2).

If the NE-striking foliation and bedrock contacts influence erosive processes, the drainage network should be dominated by streams flowing either parallel or perpendicular to major bedrock contacts. Likewise, if these fabrics control the knickpoints, the most abundant knickpoints should occur along NW- or SE-draining streams. NW-directed streams and knickpoints could also result from a population of fractures perpendicular to the NE-SW foliation. If the streams and knickpoints occur in directions consistent with the younger fracture sets, then likely the knickpoints are not with lithologic contacts but with the fractures sets.

For the direction at each stream point, we used the azimuth of a vector connecting the nearest upstream and downstream points (Figure 1.4). By looking upstream and downstream we doubled our directional resolution, as there are 16 possible stream flow directions with our method compared to 8 from any center point. Next, we calculated the directions at the knickpoints and plotted the entire stream vs knickpoints on one rose diagram for comparison. We produced rose diagrams comparing the datasets and added them to longitudinal stream profiles (Figure 1.5-1.7).

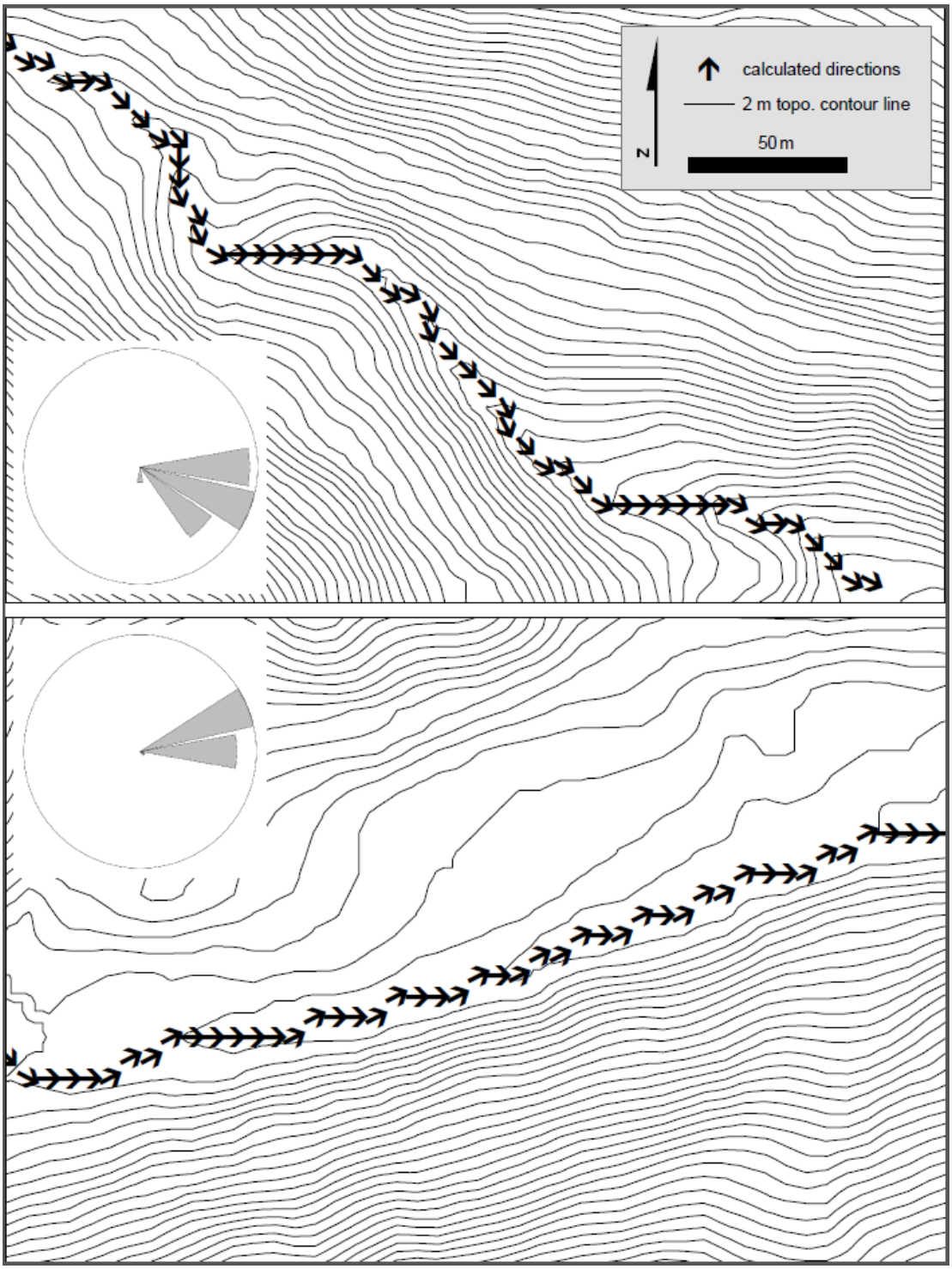

Figure 1.4: Sample streams showing calculated direction vectors (black arrows). The rose diagrams show the distribution of these segments. Note how the dominant rose petals match the general directions of the stream as indicated by the contour lines. These streams are part of Santeetlah Creek, in western Graham County, NC. The topographic contours were derived from LIDAR with ~6m horizontal resolution.

1.3.3 Knickpoint Elevation Analysis

We analyzed the elevation distributions of the knickpoints, as our previous work (Hill, 2013) and that of others (Gallen et al., 2011; Gallen et al, 2013; Miller et al., 2013) revealed clusters of high-elevation knickpoints interpreted as the result of a headwards-migrating wave of erosion moving through the southern Appalachians at ~900-1100 m elevation. We placed vertical histograms on the stream profiles to investigate how the elevations at knickpoints compare to the rest of the streams, as well as to highlight flat landscapes in the upper headwaters. We looked at the elevation distributions of overall stream points versus knickpoints by plotting the elevation data as 25-m-binned histograms on the vertical axis of each longitudinal profile (Figures 1.5-1.7). The number of stream points is always orders of magnitude greater than knickpoints, so we normalized the two elevation distributions based on their maximums and plotted them on one axis. If the knickpoints are randomly placed, the elevation distributions of the entire stream and the knickpoints should match. If the most abundant knickpoints are at elevations different than the most abundant streams, then there is either a wave of incision currently at that elevation actively dissecting the terrain, or there is an erosion-resistant layer found across the region at that elevation, which is not the case in this part of the Appalachians.

After we identified knickpoints and determined directions and elevations of all stream points, we compared the distributions of underlying bedrock at each stream point and knickpoint. We plotted the knickpoints on a geologic map to test if they are located at lithologic boundaries and to extract the bedrock lithology (Figures 1.5-1.6). To do this we used the 1:500,000 scale state wide geologic bedrock map produced in 1985 and digitized as shapefiles in 2005 (NCGS, 1985).

1.4 Results

1.4.1 Graham County – Cheoah River basin

Within the 557 km^2 Cheoah River watershed, we extracted six networks made of 102 streams represented by 64,267 pixels (Figure 1.5). Along these streams we found 152 knickpoints. The most abundant directions in the entire study area are east-flowing and north-flowing, directions parallel to two of the major lineaments and fracture sets. The knickpoints occur most frequently in similar directions to the entire stream, except the knickpoints are relatively lacking along west-flowing streams and much less abundant along north-flowing streams than the entire network. Originally, we wanted to test if there are abundant knickpoints facing NW and to determine if the NE-striking bedrock contacts and metamorphic foliation control the stream direction, and hence the regional topography. There are some NW-facing knickpoints, but they are less abundant than the E-facing or N-facing ones. Neither the streams nor the knickpoints are dominantly parallel or perpendicular to the mapped contacts or regional orogenic fabrics.

The distribution of stream-point elevations in the entire Cheoah River network differs from that of knickpoint elevations, as shown in the horizontal histograms on the side of each longitudinal profile. We found a mode for the entire stream at ~600 m, and even though the knickpoint elevations span the whole stream, they occur most often in clusters at ~500 m, ~800 m, ~1000 m, and ~1200 m. Some of the tributary networks contain knickpoints at these elevations that separate a steep landscape downstream from a flatter landscape upstream of the knickpoints (Figure 1.5). Although most evident at Santeetlah Creek, all of the Cheoah tributary networks follow a similar pattern, with the abundant knickpoints between ~1000-1200 m that separate gently sloping headwater streams upstream from steep, often incised streams below the knickpoints.

We found flat landscapes above steep ones in the digital elevation models and in our field observations. To field check some of the knickpoints, we visited Santeetlah Creek, a location with

three distinct vertical zones of topography, similar to the Cullasaja River basin. The lowest elevation zone is a low-relief, fluvial-dominated landscape with wide valleys where streams meander across broad floodplains 100's of meters wide. The second zone has steep hillslopes and deep valleys with channels containing boulders ranging from sub-meter to 10's of meters in diameter and no floodplains, similar to the Smoky Mountain streams interpreted by King (1964) and Southworth et al. (2003) as remnants of huge Pleistocene-Pliocene debris flows. To ensure that the knickpoints we detected are not the result of large boulders that have formed debris dams, we field-checked numerous knickpoints and found streams flowing over meter-scale bedrock knickpoints in the lower part of the knickzones, often accompanied by a cascade of boulder-covered knickpoints upstream and a deep pool downstream. We feel that the tendency for bedrock to be exposed most often at the toes of the knickzones justifies our separation of knickpoints from knickzones. This reduced the number of selected knickpoints by an order of magnitude, but we think it is necessary to focus only on knickpoints where the bedrock is interacting directly with the streams.

In addition to confirming knickpoint locations through field verification, we noted the quick transition into the third and highest zone of topography, where much smaller, fluvial-dominated streams once again meander across low-relief terrain above the knickpoints. Although these upper reaches of streams contain some meter-sized boulders, the general landscape of small streams and gentle hillslopes resembles the lowest first zone. The transition from the second to the third zone is at the same elevation where steep hillslopes are failing along vertical joint planes, and this transition defines the wave of incision sweeping through the drainage network. In the streams and the hillslopes, we found that sometimes the failure happens along foliation planes, but more often large, tabular, blocks bounded by vertical or sub-vertical joints move along gently dipping joints or foliation. The coupled systems of stream/hillslope erosive processes that Gallen

et al. (2011) described within the Cullasaja basin are evident at Santeetlah Creek. Although three zones of topography are well-defined, similar to the Cullasaja basin, we did not find any overhanging waterfalls similar in size to the ~20m-high Dry Falls of the Cullasaja River. However, the number of locations we could check was limited by the rugged terrain and lack of roads near the streams.

To summarize the results from Graham County, the streams and knickpoints occur most often along east-flowing streams, generally more consistent with the direction of the Swannanoa lineament than the underlying foliation or bedrock contacts. The rectangular drainage patterns along E-W and N-S streams and the outcrop-scale observations of fracture-controlled, blocky failure of bedrock at knickpoints and adjacent hillslopes (Figures 1.8-1.9) suggest knickpoint directions and locations are influenced more by lineament-parallel fractures than any other bedrock fabric.

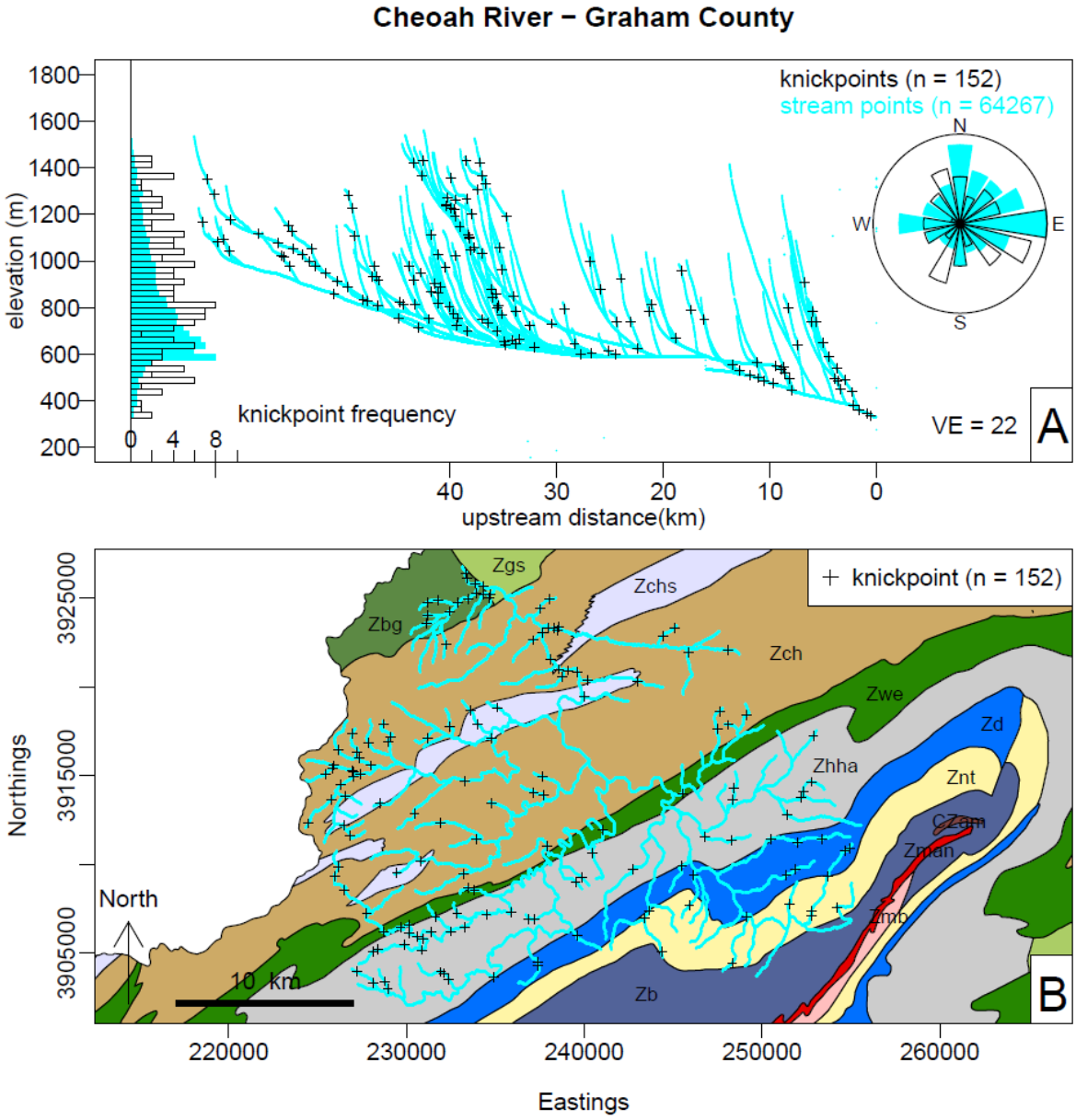

Figure 1.5 A: Longitudinal profiles for the Cheoah River basin, Graham County. The blue lines are the streams and the black crosses are the automatically selected knickpoints. The histogram and the rose diagram show the entire stream data as blue and the knickpoint data as black outline and clear bins. B: Map view of same streams shown in top figure, with the streams colored blue and the knickpoints drawn as black crosses. The bedrock map was derived from the statewide 1:500,000 geologic map that was produced in 1985 and digitized in 2005 (NCGS). Note how few knickpoints lie near bedrock contacts. This map uses a UTM zone 17S, NAD1983 projection.

1.4.2 Swain County – Smoky Mountain streams

Located in Swain County, on the opposite side of the Swannanoa lineament from the Cheoah River basin and flowing generally southward, the streams that drain from the Smoky Mountains have notably different longitudinal profiles and map-view patterns from their north-draining counterparts of Graham County. The six Smoky Mountain streams (n=68,154) range in drainage area from 76 to 346 km2, contain knickpoints (n=159), but are generally close to graded, equilibrium streams. There is a pronounced convex-up knickpoint found along the Ocanaluftee River, but it corresponds with the change from erosion-resistant meta-sandstone (Zch) to less resistant biotite gneiss (Ybgg; Figure 1.6; see appendix A1.2 for profile of this stream). The number of knickpoints is similar to Graham County, but many are less-pronounced and convex. The Swain County streams are steepest in the headwaters and do not have any flat landscapes above the upper reaches. The separate zones of topography evident in Graham County do not exist in the streams we studied in Swain County. The six Smoky Mountains streams we analyzed drain into the Swannanoa lineaments as individual networks that are only connected at the lineament and do not feed into one major stream mouth, as is the case in the Cheoah River basin to the south. The dominant stream flow direction is to the south without much variation in the directions of the entire streams from the knickpoints.

The Smoky Mountains networks do not contain the major knickpoint cluster at ~1000m found in Graham County and in other parts of the North Carolina Blue Ridge. Although some of the streams have mouths that are slightly elevated from the Cheoah River mouth, these differences are accentuated by the ~150 m high Fontana Dam, located just east of where the Cheoah meets the Swannanoa lineament. The Smoky Mountains streams are some of the steepest and straightest in all of the North Carolina Blue Ridge and house some of the highest relief landscapes in the region, with some streams dropping over 1 km in ~12 km of length (Figure 1.6).

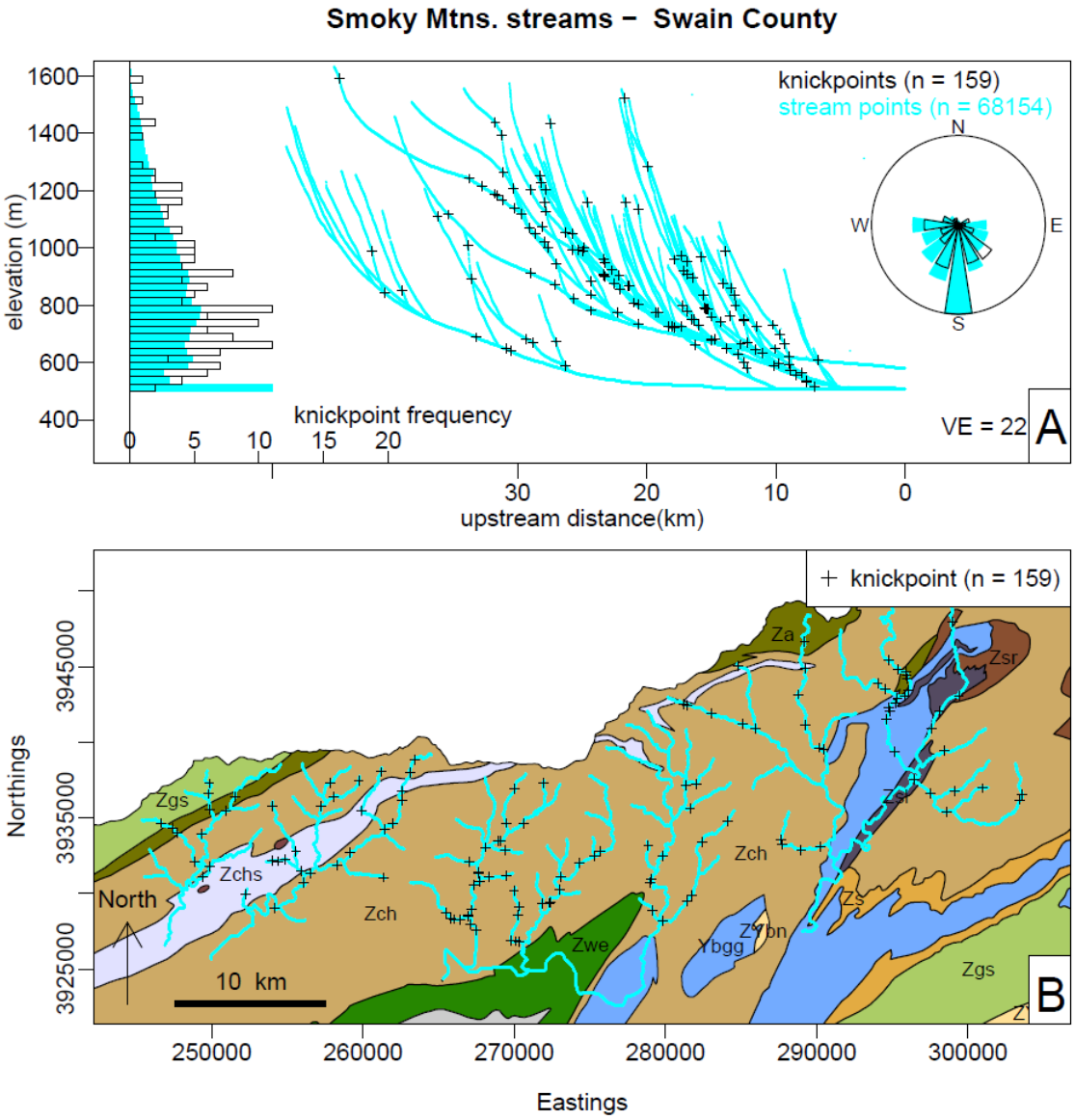

Figure 1.6: (A) Longitudinal profiles for the Smoky Mountains streams, Swain County. The blue lines are the streams and the black crosses are the automatically selected knickpoints. The histogram and the rose diagram show the entire stream data as blue and the knickpoint data as black outline and clear bins. (B) Map view of same streams shown in top figure, with the streams colored blue and the knickpoints drawn as black crosses. The bedrock map was derived from the statewide 1:250,000 geologic map that was produced in 1985 and digitized in 2005 (NCGS). Note how few knickpoints lie near bedrock contacts. This map uses a UTM zone 17S, NAD1983 projection.

1.5 Discussion

Determining the flow directions of entire stream networks allowed us to estimate internal rock fabrics influencing modern erosion, as the streams will move downhill along the path of least resistance and remove rock by whatever method is easiest. Our goal was to compare stream directions at knickpoints with known internal rock fabrics as a way to either link or separate knickpoints to known geologic events. We determined that the knickpoints do not occur most often along NW-flowing streams, parallel to the NE-striking foliation or any other internal fabrics considered to Paleozoic or older. The NE-SW striking bedrock contacts and metamorphic foliation obviously play major roles in much of the landscape, such as the deep gorge formed by the Murphy Belt syncline (Figure 1.1), but many of the streams we measured follow E-W and N-S paths independent of underlying bedrock. The most abundant knickpoints occur along these lineament-parallel streams rather than ones flowing parallel or perpendicular to NE-SW-striking fabrics. We interpret this rectangular drainage pattern as being driven by lineament-parallel faults and fractures and believe these E-W and N-S fracture sets formed during a regional-scale vertical flexure of the orogenic belt and are the main surfaces along which blocky failure is occurring (Figure 1.10). In much of our study area, new faults and fractures have greater influences on erosional processes and stream flow direction than the underlying bedrock.

The Swannanoa lineament spans over 250 km, and rather than being one feature it is a series of en echelon zones (Figure 1.1). Where the Swannanoa reaches Graham County there are a series of very prominent E-W trenches as far as 15 km to the south of the main lineament, plus there are N-S valleys that run parallel to the nearby Franklin lineament (Figure 1.1). There is a very pronounced E-W lineament along Yellow Creek, immediately south of Fontana Lake that contains minor dip slip faults and abundant vertical fractures striking parallel or sub-parallel to the lineament. Yellow Creek is a prime example of a landscape controlled by E-W lineament-parallel

fractures cutting across older NE-SW foliation. In the field, we observed outcrop-scale fractures cross cutting the foliation, as well as a transition from a flat, wide floodplain to a deeply entrenched stream with steep valley walls. We also observed fluvial deposits with cm-scale quartz cobbles ~30m above the modern floodplain, which suggests that there may have been some dip-slip motion along the Yellow Creek lineament.

Along the streams we analyzed, the underlying bedrock has little to no control on whether a knickpoint forms. As previously mentioned, although there are clear examples of bedrock-driven topography, we present here numerous examples where rugged topography is present independent of underlying bedrock. Many bedrock contacts trace across the Swannanoa lineament and exhibit little to no influence on the amount of topographic relief, indicating that there is another main driver of the landscape.

The Cheoah River's tributaries follow east-, west-, and north-flowing directions, but the knickpoints are most abundant along east-flowing streams. Although the entire Cheoah River basin contains east-, west-, and north-flowing streams, the directions of knickpoints differ for each tributary network. The knickpoints face the same general direction as the headwaters for each network (Figure 1.7). This observation is consistent with a wave of incision working its way from the Swannanoa lineament towards the headwaters. There are no flat-lying bedrock units in the highly-deformed study area, so these knickpoints are more likely transient than stationary and lithologically controlled. We interpret the abundant east-facing knickpoints as part of active processes eating away at the uplifted plateau in western Graham County. The lack of a plateau on the eastern side does not exclude this as an uplifted terrain, but more likely the ridge was lowered by erosion from both sides and the relict flat surface has been removed (Figure 1.10).

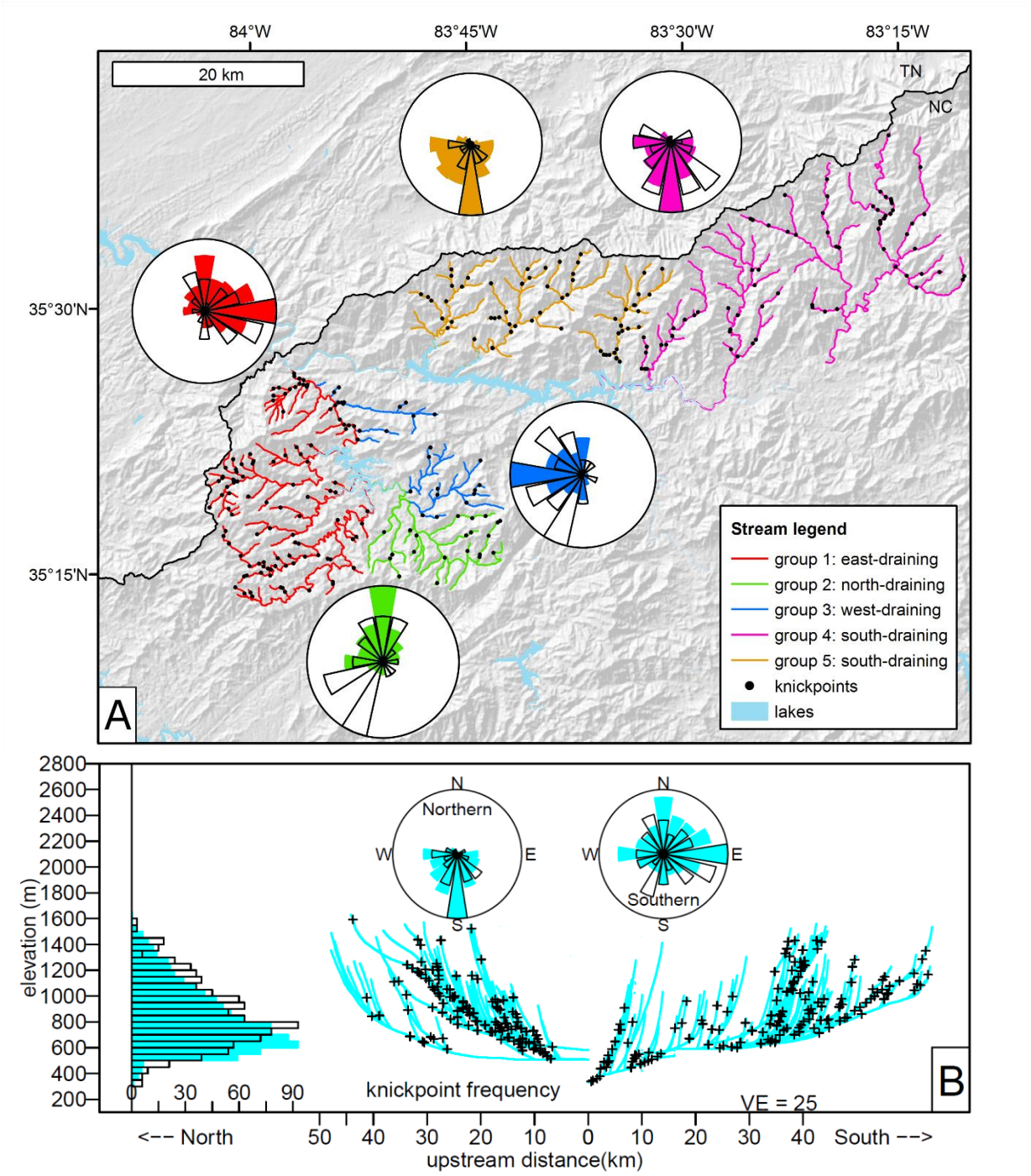

Figure 1.7: (A) Map of streams and the rose diagrams for all stream networks. The streams have been grouped and colored based on major drainage direction and relation to lineament. The colored roses are the directions of streams at the knickpoints and the white roses are the directions of all stream points. (B) Longitudinal profiles showing streams draining from either side of the topographic lineament that acts as a local base level. The blue lines are the streams and the black crosses are the automatically selected knickpoints. The two rose diagrams show the datasets from the north and south side of the lineament.

Figure 1.8: Example of typical bedrock knickpoint forming by failure of high-angle joints found along Santeetlah Creek, in Graham County. The front of the knickpoint drops ~1.5 m into a deep pool and is covered by boulders further upstream. Most of knickpoints we checked in the field had this same pattern and general morphology.

The high plateau in western Graham County is slightly less pronounced than the flat landscape upstream of the Cullasaja River basin of Macon County to the east (Figure 1.1). Gallen et al. (2013) estimated the uplift of the Cullasaja region as Mid-Miocene, but they did not give any suggestions as to where the uplift occurred. Both the Cheoah and Cullasaja rivers have relict topographic surfaces at ~1200m (Gallen et al., 2013), and both contain sinuous streams entrenched into the headwaters. Recent work by Gallen (2018) proposed that some of the knickpoints in the Cullasaja and Cheoah River systems are the result of differences in erodibility of bedrock units

that drove a drainage divide migration and ~150m of base level lowering during the Miocene. This may explain some of the knickpoints located at 500-600 m elevation but does not explain the knickpoints located at higher elevations, or the transition from an active to relict landscape above either river system. Based on our observations from nearby Graham County and the fact that both the Cheoah and Cullasaja Rivers drain into the Swannanoa lineament, we propose dip-slip faulting and intense fracturing at the lineament was the trigger for the knickpoints found in both river systems above 1000 m elevation. Blocky failure of bedrock and minor vertical motion along the Swannanoa lineament could explain the uplifted plateaus, the mechanism for knickpoint generation, and the contrasting landscapes across the lineament. If the knickpoints and the lineaments are linked, then we now have a mechanism for formation of transient knickpoints in the Blue Ridge and a potential age estimate of the lineaments as Miocene. In our previous investigations into the brittle structures crossing-cutting western North Carolina, we found many fractures and few dip-slip faults striking parallel and within lineaments. We propose that the fractures, faults, and lineaments share an origin, and the same uplift event likely sent the wave of knickpoints through Graham, Swain, and Macon counties.

Figure 1.9: Hillslope outcrop eroding by blocky failure along near-vertical E-W and N-S joint sets. This outcrop is found at ~800 m elevation and marks a transition from steep topography below to a lower-relief landscape above. Note the rock hammer and field notebook for scale.

The landscape of Swain County is steep and rugged, and there are no flat plateaus at the highest elevations, a stark contrast from Graham County. This is probably because the Smoky Mountains were never worn down all the way to a peneplain (Figure 1.10). More likely, they were at least 100's of meters above modern-day Graham county before any uplift or base level change occurred. Although there may have been minor dip-slip motion along the lineament, regional-scale doming likely caused extension and intense fracturing at the lineaments, which in turn failed quickly and caused a base level change within the fracture zone. In response to this base level change, transient knickpoints likely migrated both north and south from the Swannanoa lineament, but due to higher stream power within the steeper Smoky Mountains the rate of migration differed on either side of the lineament. This idea is consistent with numerical models that use erosion rates to estimate knickpoint migration rates (Norton et al., 2008). The knickpoints in Swain County are at higher elevations than those in Graham County, and are much less pronounced, indicating these knickpoints may have undergone knickpoint inclination and replacement, processes observed in flume models when the downward erosion rate of a knickpoint outpaces the headwards migration (Gardner, 1983). Many Smoky Mountain streams are graded with no knickpoints at all, indicating the streams have returned to equilibrium. The south-draining streams in the Smokies flow across SE-NW foliation and bedrock contacts with little to no influence by these older fabrics. On both sides of the lineaments, regardless of the presence of or lack of knickpoints, the streams are flowing most often along E-W and N-S directions, indicating any influence of NE-SW bedrock geology is minor.

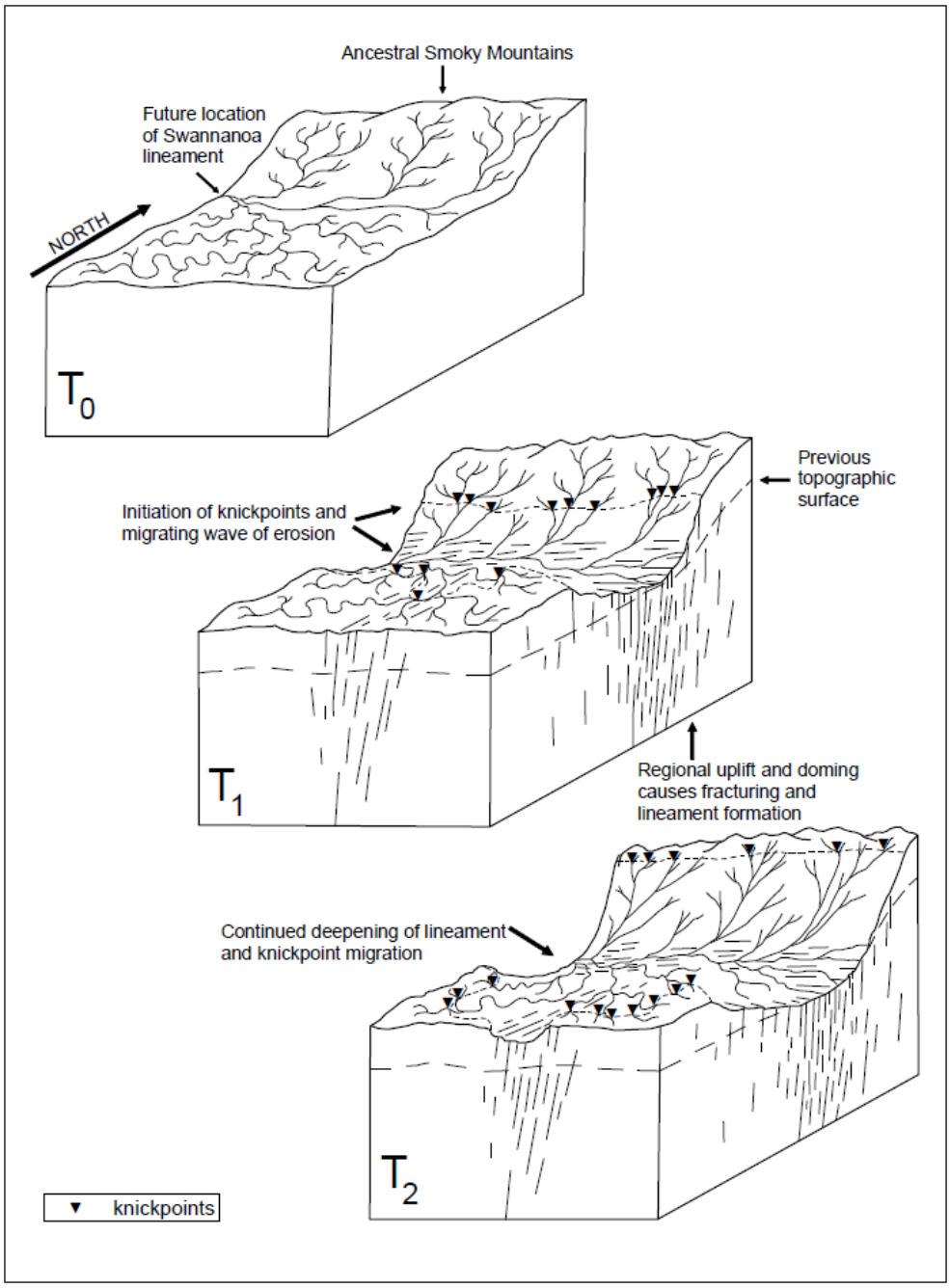

Figure 1.10: Conceptual uplift model of the study area suggesting how knickpoints might have migrated towards the to sculpt the modern topography. T_0: Prior to Cenozoic uplift, the study area likely had rugged topography in the Smoky Mountains (modern Swain County) lower-relief to the south (modern Graham County). T_1: As uplift occurred, the E-W topographic lineaments formed and the knickpoints began their ascent towards the headwaters. T_2: By the modern day, the transient knickpoints have migrated mostly through the Smoky Mountains and the streams are closer to equilibrium, compared to the knickpoints to the south that are still actively eroding the relict peneplain found in T_0.

1.6 Conclusions

With our automated knickpoint selection and direction calculations, we offer new tools for connecting geomorphic observations with neotectonic processes in areas where multiple internal heterogeneities must be considered. In the attempt to better understand knickpoint origins, we used automated methods to analyze a high-resolution elevation dataset to determine the dominant stream flow directions and the internal fabrics influencing knickpoints. Based on our results, the knickpoints are forming more often from blocky failure along E-W and N-S fractures rather than from mechanical differences across NE-SW bedrock contacts, which we interpret to mean that they are more likely transient with a neotectonic origin rather that stationary and controlled by resistance to erosion.

The southern Appalachians have a complicated past involving multiple cycles of collision and subsequent rifting, but they should not be dismissed as an old, dead mountain range. Rather, these slumbering giants experienced a rejuvenation of topography hundreds of millions of years after plate-margin-style tectonics ceased. Although differential resistance to erosion can explain some of the topographic features, here we provide evidence that underlying bedrock contacts and metamorphic foliation are not the only erosional processes currently sculpting the modern landscape. Instead, there are a family of fractures and faults we interpret to be Late Cenozoic (likely Miocene) that determine the shapes of river patterns that drain much of the North Carolina Blue Ridge. We propose that the lineament-related faults and fractures are linked to uplift of relict floodplains, formation of the transient knickpoints, and rejuvenation of rugged topography in an ancient orogen. The existence of E-W and N-S trending streams far from the lineaments suggests that even though the lineaments are confined to narrow zones, related fractures and faults may be more pervasive than previously considered.

REFERENCES

1. Beutel, E.K., 2005, Nomade, S., Fronabarger, A.K., Renne, P.R., Pangea's complex breakup: Anew rapidly changing stress field model; Earth and Planetary Science Letters, no. 235, p.471-485

2. Bishop, Paul, 2007, and Goldrick, Geoff, Morphology, processes and evolution of two waterfalls near Cowra, New South Wales, Australian Geographer v. 23, no.2, p. 116-121

3. Burton, William C., 2010, and Southworth, Scott; A model for Iapetan rifting of Laurentia based on Neoproterozoic dikes and related rocks; Geological Society of America Memoirs; v. 206, p. 455-476

4. Crosby, Benjamin T., 2006, and Whipple, Kelin X., Knickpoint initiation and distribution within fluvialnetworks: 236 waterfalls in the Waipaoa River, North Island, New Zealand, Geomorphology, v. 82, p. 16-38

5. Dennison, John M., 1997, Stewart, Kevin G., Roth, Emily A., Alcott, Allison E., Lowe, Ashley L., Vlahovic, Gordana, Post-orogenic linear fracture systems in the Great Smoky-Blue Ridge region of North Carolina, Tennessee, and Georgia; Geological Society of America Abstracts with Programs, Southeastern Section v. 29, no.3, p.13 (Dennison and Stewart, 2006).

6. Duvall, Allison, 2004, Kirby, Eric, Burbank, Douglas, Tectonic and lithologic controls on bedrock channel profiles and processes in coastal California, Journal of Geophysical Research, v. 106

7. Faill, Rodger T., 1997, A geologic history of the north-central Appalachians. Part 1. Orogenesis from the Mezoproterozoic through the Taconic orogeny; American Journal of Science; v. 297, p. 551-619

8. Gallen, Sean F., 2011, Wegmann, Karl W., Frankel, Kurt L., Hughes, Stephen, Lewis, Robert Q.,Lyons, Nathan, Paris, Paul, Ross, Kristen, Bauer, Jennifer B., Witt, Anne C., Hillslope response to knickpoint migration in the Southern Appalachians: implications for the evolution of post-orogenic landscapes; Earth Surface Processes and Landforms v. 36, no. 9

9. Gallen, Sean F., 2013, Wegmann, Karl W., and Bohnenstiehl, DelWayne R., Miocene rejuvenation of topographic relief in the southern Appalachians; GSA Today, v. 23, p. 4-10

10. Gallen, Sean F., 2018, Lithologic controls on landscape dynamics and aquatic species evolution in post-orogenic mountains; Earth and Planetary Science Letters, v. 493, p. 150-160

11. Gardner, Thomas, 1983, Experimental study of knickpoint and longitudinal profile evolution in cohesive, homogeneous material, Geological Society of America Bulletin, v. 94, p. 664-672

12. Gay, Parker S., Jr. (2000), Unmapped topographic alignments visible on 3D stereo terrain map of a 2 degrees X 2 degrees segment of the Southern Appalachians, Geological Society of America Abstracts with Programs, Southeastern Section v.32, no.2, p.19

13. Goldrick, Geoff, 1995, and Bishop, Paul, Differentiating the Roles of Lithology and Uplift in the Steepening of Bedrock River Long Profiles: An Example from Southeastern Australia; The Journal of Geology, v. 103, no.2 p. 227-231

14. Hack, John T., 1982, Physiographic divisions and differential uplift in the Piedmont and Blue Ridge; Geological Survey Professional Paper 1265

15. Hancock, Gregory S., 1998, Anderson, Robert S., Beyond Power: Bedrock River Incision Process and Form, Rivers over Rock – Geophysical Monograph 107, p. 35-60

16. Hibbard, James P., 2007, Van Stall, Cees R., Rankin, Douglas W., A comparative analysis of pre-Silurian crustal blocks of the northern and southern Appalachian orogen; American Journal of Science, v. 307, p. 23-45

17. Hibbard, James P., 2010, van Staal, Cees R., Rankin, Douglas W., Comparative analysis of the geological evolution of the northern and southern Appalachian orogen: Late Ordovician–Permian, Geological Society of America Memoirs, Memoir 206, p. 51-69

18. Hill, Jesse S., 2012, Stewart, Kevin G., Correlation of major topographic lineaments in the North Carolina Blue Ridge with regional fracture zones; Geological Society of America Abstracts withPrograms, v. 44, no. 7, p. 483

19. Hill, Jesse S., 2013, Zoned uplift of western North Carolina bounded by topographic lineaments [M.S. Thesis] Chapel Hill, University of North Carolina, 36 p.

20. Hill, Jesse.S., 2016, and Stewart, Kevin G., A newly discovered fault zone near Boone, North Carolina and Cenozoic topographic rejuvenation ofthe southern Appalachian Mountains; Geological Society of America Abstracts with Programs, v. 48, no. 7

21. Kirby, Eric, 2001, Whipple, Kelin X., Quantifying differential rock-uplift rates via stream profile analysis; Geology, v. 29, no. 5, p. 415-418

22. Korup, Oliver, 2006, Rock-slope failure and the river long profile, Geology, v. 34, no. 1. p.45-48

23. Li, Z.X., Bogdanova S.V., Collins A.S., Davidson A., De Waele B., Ernst R.E., Fitzsimons, Fuck,R.A., Gladkochub D.P., Jacobs J., Karlstrom K.E., Lul, S., Natapovm L.M., Pease V., Pisarevsky S.A., Thrane K., Vernikovsky V., 2008, Assembly, configuration, and break-up history of Rodinia: A synthesis; Precambrian research 160, no. 1, p 179-210.

24. Manspeizer, Warren, 1989, DeBoer, Jelle, Costain, John K., Froelich, Albert J., Coruh, Cahit, Olsen, Paul E., McHone, Gregory J., Puffer, John H., Prowell, David C., Post-Paleozoic activity, *in* Hatcher, R. D., Jr. Thomas, W. A., and Viele, G. W., eds, The Appalachian-Ouchita Orogen in the United States, The Geological Society of America, The Geology of North America, v. F-2, p. 319-374

25. Merschat, Arthur J., 2005, Hatcher, Robert D. Jr., Davis, Timothy L., The northern Inner Piedmont, southern Appalachians, USA: kinematics of transpression and SW-directed mid-crustal flow, Journal of Structural Geology v. 27. p. 1252-1281

26. Miller, Jerry, 1991, The Influence of Bedrock Geology on Knickpoint Development and Channel-Bed Degradation along Downcutting Streams in South-Central Indiana, The Journal of Geology, v. 99, no. 4, p. 591-605

27. Miller, Brent V. ,2006, Fetter, Allen H., Stewart, Kevin G., Plutonism in three orogenic pulses, Eastern Blue Ridge Province, southern Appalachians; GSA Bulletin, v. 118, no. ½, p. 171-184

28. Miller, Scott R., 2013, Sak, Peter B., Kirby, Eric, Bierman, Paul R., Neogene rejuvenation of central Appalachian topography: Evidence for differential rock uplift from stream profiles and erosion rates; Earth and Planetary Science Letters, 369- 370, p. 1-12

29. Norton, K.P., 2008, von Blanckenburg, F., Schlunegger, F., Schwab, M., and Kubik, P.W., Cosmogenic nuclide-based investigation of spatial erosion and hillslope channel coupling in the transient foreland of the Swiss Alps: Geomorphology, v. 95, no. 3–4, p. 474–486.

30. North Carolina Geological Survey, 1985, Geologic map of North Carolina: North Carolina Geological Survey, General Geologic Map, scale 1:500000

31. Nystrom, Paul, 1986, Late Cretaceous-Cenozoic brittle faulting beneath the western South Carolina coastal plain; reactivation of the eastern Piedmont fault system; Geological Society of America Abstracts with Programs, v. 38, no.3, p. 74

32. Pazzaglia, Frank J., 1996, and Brandon, Mark T., Macrogeomorphic evolution of the post-Triassic Appalachian Mountains determined by deconvolution of the offshore basin sedimentary record; Basin Research v. 8, no. 3, p. 255-278.

33. Pazzaglia, Frank J., 1998, Gardner, Thomas W., Merritts, Dorothy J., Bedrock incision and longitudinal profile development over geologic timescales determined by fluvial terraces, Rivers over Rock Geophysical Monograph 107, p. 35-60

34. Poag, Wylie C., 1989, Sevon, William D., A record of Appalachian denudation in postrift Mesozoic and Cenozoic sedimentary deposits of the U.S. middle Atlantic continental margin; Geomorphology, v.2, p. 119-157

35. Queiroz, G.L, 2014, Salamuni, E., Nascimento, E.R., Knickpoint Finder: A software tool that improves neotectonic analysis; Computers and Geosciences, v. 76, p.80-87

36. Sklar, Leonard S., 2004, Dietrich, William E., A mechanistic model for river incision into bedrock by saltating bed load; Water Resources Research, v. 40, W06301

37. Stock, Jonathan D., 2006, and Dietrich, William, Erosion of steepland valleys by debris flows, Geological Society of America Bulletin, v. 118, no. 9-10, p. 1125-1148

38. Snyder, Noah P., 2000, Whipple, Kelin X., Tucker, Gregory E., Merritts, Dorothy J., Landscape response to tectonic forcing: Digital elevation model analysis of stream profiles in the Mendocino triple junction region, northern California, Geological Society of America Bulletin, v. 112, no. 8, p. 1250-1263

39. Stewart, Kevin G., 2006, Dennison, John M., Tertiary-to recent arching and the age and origin of fracture-controlled lineaments in the southern Appalachians; Geological Society of America Abstracts with Programs, Southeastern Section Vol. 38, No. 3, p. 27

40. Stewart, Kevin G., 2015, Estimates on the magnitude and timing of postorogenic topographic rejuvenation of the southern Appalachians using isostasy and deformed coastal plain rocks; Geological Society of America Abstracts with Programs, Southeastern Section Vol. 47, No. 2, p. 82

41. Southworth, Scott, 2003, Schultz, Art, Denenny, Danielle, and Triplett, James, Surficial Geologic Map of the Great Smoky Mountains National Park Region, Tennessee and North Carolina, U. S. Geological Survey, open file report 03-381

42. Southworth, Scott, 2012, Schultz, Art, Aleinkoff, John N., Merschat, Arthur J., Geologic Map of the Great Smoky Mountains National Park region, Tennessee and North Carolina, United States Geological Survey Scientific Investigations Map 2997

43. Thomas, William. A., 2006, Tectonic inheritance at a continental margin; GSA Today, v 16, no. 2

44. Tollo, Richard P., 1996, Hutson, Frederick E., 700 Ma rift event in the Blue Ridge province of Virginia: A unique time constraint on pre-Iapetan rifting of Laurentia; Geology, v. 24, no.1, p.59-62

45. Tull, James, F., 2010, Allison, David T., Whiting, Stephen E., John, Nick L., Southern Appalachian Laurentian margin initial drift-facies sequences: Implications for margin evolution; Geological Society of America Memoir 206, p. 935-956

46. Wobus, Cameron, 2006, Whipple, Kelin X., Kirby, Eric, Snyder, Noah, Johnson, Joel, Spyropolou, Katerina, Crosby, Benjamin, Sheehan, Daniel, Tectonics from topography: Procedures, promise, and pitfalls, Geological Society of America Special Paper no. 398, p. 55-74

47. Whipple, Kelin, 2007, Wobus, Cameron, Crosby, Ben, Kirby, Eric, Sheehan, Daniel, New Tools for Quantitative Geomorphology: Extraction and Interpretation of Stream Profiles from DigitalTopographic Data; GSA Annual Meeting

CHAPTER 2: THE BOONE FAULT AND ITS IMPLICATIONS FOR CENOZOIC TOPOGRAPHIC REJUVENATION OF THE SOUTHERN APPALACHIAN MOUNTAINS

2.1 Introduction

In this paper we document the first mappable fault associated with Cenozoic uplift of the southern Appalachians. Near Boone, North Carolina, at the northern edge of the Grandfather Mountain window we mapped a brittle fault zone along what was previously called the Linville Falls thrust fault. The minor faults associated with this zone, which we are calling the Boone fault, typically dip steeply and strike WNW. There are normal (north-dipping) and reverse (south-dipping) faults and both show south-side-up motion. Based on how this high-angle fault zone corresponds with a sharp topographic scarp separating the Linville Falls shear zone from the Grandfather Mountain formation, we suspect it may be younger than the Paleozoic faults bounding the rest of the window. To test if it is a late, post-orogenic structure, we performed a paleostress inversion of 165 minor faults. The inversion yields stress tensors with SSW-plunging maximum compression directions, which do not match stresses that drove Paleozoic SE-NW shortening or Mesozoic E-W rifting, but likely represent Cenozoic NNE-SSW extension associated with doming and blocky uplift of the southern Appalachians. We interpret these faults to mean the Grandfather Mountain window is not entirely framed by a Paleozoic fault, but rather is bounded in part by a high-angle Cenozoic fault zone. We mapped ~10 km of the Boone fault along the northeastern edge of the Grandfather Mountain window, but we think it could be part of the ~180 km long and 20 km wide regional-scale topographic lineament swarm spanning from the Valley and Ridge in Tennessee to the Piedmont in North Carolina.

We also present geomorphic and seismic data consistent with a landscape currently responding to uplift. We analyzed the longitudinal profiles of dozens of streams draining into the fault zone and found numerous knickpoints hundreds of meters above the valley floor. In addition to these disequilibrium profiles, some of the streams contain map-view evidence of drainage capture consistent with south-side-up motion along the Boone fault. Based on the abundance of knickpoints and the existence of perched floodplains in the headwaters, the disequilibrium streams are likely associated with the Boone fault. A cluster of shallow earthquakes occurred in 2013 and 2014 about 4 km south of the Boone fault and damaged sidewalks, roads, and building foundations in an area with abundant evidence of active slope creep. Modern earthquakes and active landslides indicate that the Boone fault is likely still jostling and is the cause of many of the unstable slopes and land-use hazards that threaten the town of Boone. Our work offers a solution to the long-standing issue of why the Appalachians are still so high and documents a seismically active fault that is accommodating uplift of the North Carolina Blue Ridge.

The Appalachians have a well-documented tectonic history spanning the Neoproterozoic to the late Paleozoic (e.g. Hatcher et al., 2005; Hibbard et al., 2010). However, a family of well-developed topographic lineaments crossing the southern Appalachians appear to be younger than the main orogenic belt (Hack, 1982). Recent workers have shown that the southern Appalachians underwent hundreds of meters of uplift in the Neogene (Gallen et al, 2013; Miller et al., 2013; Hill and Stewart, 2018) and others have suggested that these lineaments represent fracture and fault zones that accommodated this uplift (Dennison and Stewart, 2001; Stewart and Dennison, 2006; Hill, 2013). Although there is an abundance of evidence for late Cenozoic uplift of the Appalachians, no faults in the Blue Ridge have been associated with the rejuvenation of topography.

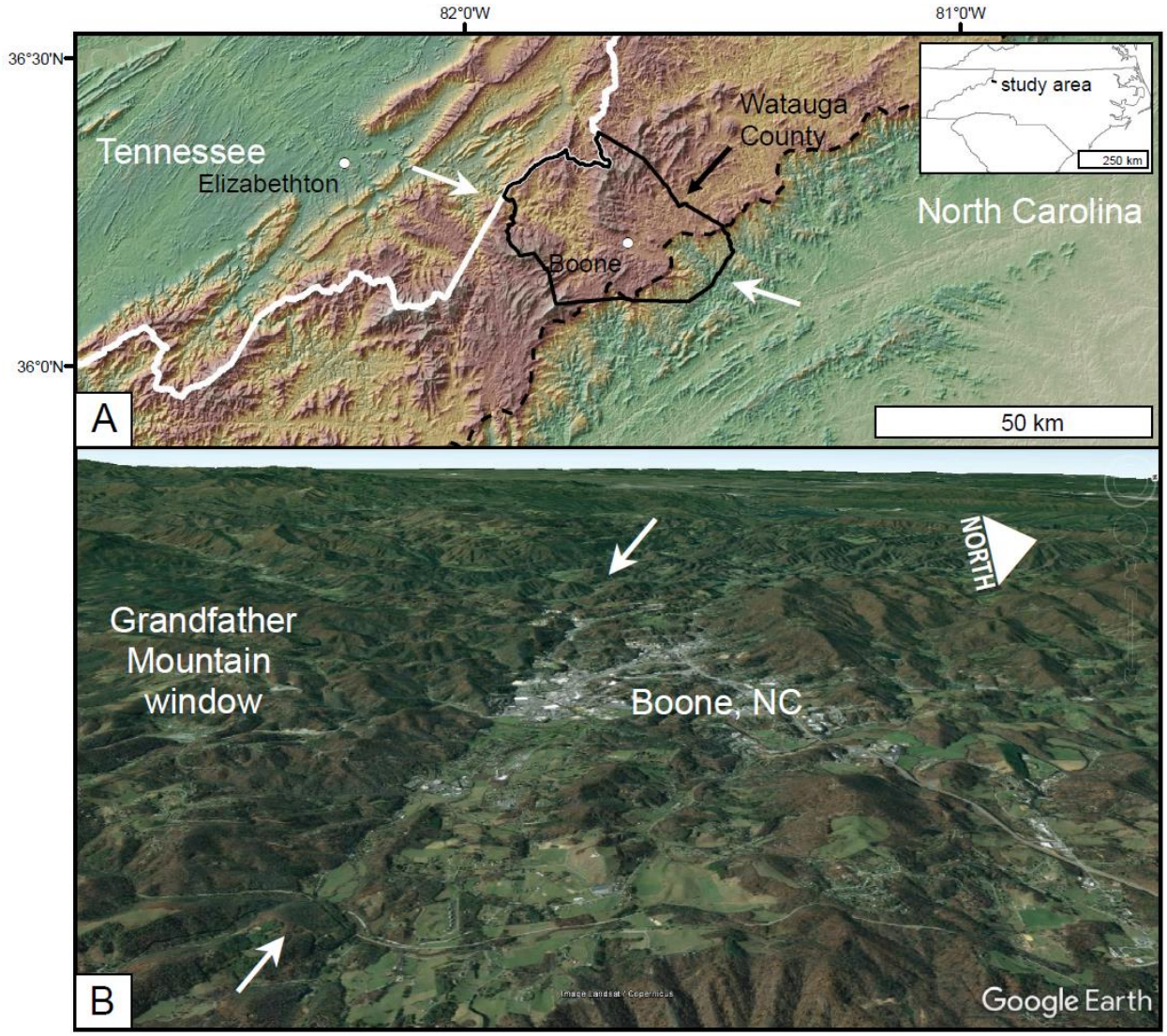

Figure 2.1: (A) Digital elevation model of western North Carolina and eastern Tennessee showing the Boone lineament swarm striking WNW across the NE-trending mountain belt. The dashed line is the Blue Ridge Escarpment and the white arrows correspond with those in figure part B. (B) Oblique view in Google Earth looking WNW along the topographic escarpment corresponding to the Boone fault that crosses through the town of Boone, North Carolina.

In this study, we focus on clarifying the structural evolution of WNW-trending lineaments (Figure 2.1) in an area of Watauga County near Boone, North Carolina (USGS 7.5" quadrangles included: Boone, Deep Gap, Sherwood, Valle Crucis, and Zionville; all in North Carolina) where they are abundant and crosscut many Paleozoic contacts and fault zones. We mapped an 80 km^2 area, measured brittle faults for paleostress analysis, and produced a 1:12,000 scale geologic map

(Figure 2.2). The mapping resulted in several significant changes to the existing geologic maps (Bryant and Reed, 1970; Gillon et al., 2009) and identified a previously unmapped brittle fault zone, here named the Boone fault, which post-dates the documented Paleozoic structures in the area. In addition, our study area has an exceptionally high number of modern landslides near or within the lineaments, likely because the rocks are highly fractured and faulted (Gillon et al., 2009).

To understand the driving mechanism behind the Boone fault zone, we performed a paleostress inversion of minor faults along its length. To estimate the timing and magnitude of fault motion, we used 6m horizontal, sub-meter vertical resolution LIDAR data from North Carolina's Spatial Data Download site (https://sdd.nc.gov/sdd/DataDownload.aspx) to analyze dozens of longitudinal profiles of streams draining into the fault zone. We looked for knickpoints along profiles and for map-view evidence of drainage capture to investigate whether recent vertical motion on the Boone fault was recorded as a geomorphic signature. In this paper, we highlight the importance of Cenozoic structures in understanding Appalachian landscape evolution and slope-failure related hazards in an area classically considered to be an inactive mountain belt.

2.2 Geologic Setting and Background

The rocks of the Blue Ridge geologic province of western North Carolina have a complex record of deformation, sedimentation, magmatism, and metamorphism. The oldest significant tectonic event was the Mesoproterozoic Grenville orogeny during the assembly of Rodinia (Faill, 1997, Hibbard et al., 2006; Li et al., 2008). The Grenville was followed by Neoproterozic failed rifting of Rodinia and the deposition of sedimentary rocks that would become the metasedimentary rocks of the Grandfather Mountain window, followed by opening of the Iapetus Ocean (Tull et al., 2010; Burton and Southworth, 2010). The Taconic orogeny in the Ordovician preceded an episode of localized magmatism and transpressional tectonics during the Devonian (e.g. Miller et al., 2006). The late Paleozoic Alleghanian orogeny resulted in assembly of Pangea and is generally thought to have been responsible for the mostly greenschist-grade metamorphism and mylonitic faults that are pervasive throughout the study area (e.g. Merschat et al., 2005).

The bedrock of the study area is a mix of greenschist-to-amphibolite-grade metamorphosed sedimentary and igneous rocks cut by a major Alleghanian thrust, the Linville Falls fault (Figure 2.2). The Linville Falls fault frames the Grandfather Mountain window and is marked by a mylonite zone locally more than a kilometer thick (Trupe et al., 2004) that separates Mesoproterozoic gneisses and Neoproterozoic metamorphosed Iapetan rift sediments in the footwall from overlying Neoproterozoic to Paleozoic schists, gneisses, and amphibolites in the hanging wall (Bryant and Reed, 1970; NCGS, 1985). The rocks are typically strongly foliated and locally lineated, especially in proximity to Paleozoic fault zones (e.g. Linville Falls fault). Alleghanian duplexing and doming of the Grandfather Mountain window tilted the foliation north of the window towards the northeast (Bryant and Reed, 1970; Boyer and Elliot, 1982). Mesozoic rifting followed the Alleghanian, and although there are no documented Mesozoic deformation

structures in our field area, Spotila et al. (2004) proposed that the Blue Ridge escarpment began as a Mesozoic rift-flank uplift and has migrated westward to its present position (Figure 2.1).

Despite the lack of an active plate boundary in this area since the Late Triassic, there is a growing body of stratigraphic, structural, and geomorphic evidence that the southern Appalachians have undergone a period of uplift in the Neogene. Miocene conglomerates in the coastal plain of South Carolina contain large metamorphic clasts (Nystrom, 1986). Offshore sedimentation increased in the Atlantic and the Gulf of Mexico during the Middle Miocene (Poag and Savon, 1989; Galloway et al., 2011). Dennison and Stewart (2001) proposed that the sudden influx of coarse clastics into the coastal plain in the Early Neogene was a result of uplift of the southern Appalachian Blue Ridge. There are folded Paleogene rocks overlain by flat Neogene rocks along the Selma arch at the southern terminus of the Blue Ridge province (Stewart, 2015). Gallen et al. (2013) showed that knickpoints along streams in the Cullasaja basin of western North Carolina likely formed as a response to Neogene uplift. Similar knickpoints exist along the Susquehanna River in Pennsylvania, and likely were also triggered by Neogene uplift (Miller et al., 2013). The evidence for a Neogene uplift event in the Appalachians is increasing, yet there are no previously documented faults associated with this event.

In strong contrast to the Paleozoic fabrics in western North Carolina are the well-developed topographic lineaments that trend WNW-ESE, E-W, and N-S, which commonly correspond to deep linear valleys. Although some of these lineaments were recognized decades ago (Hack, 1982; Gay, 2000) many more have become apparent after the recent release of LIDAR-based digital elevation models that now cover the entire state of North Carolina (available at https://rmp.nc.gov/sdd/). The topographic lineaments cross from the

Piedmont to the Valley and Ridge for over 250 km and are clearly post-Alleghanian structures (Figure 2.1). Hack (1982) identified and named several of the larger lineaments in the southern Appalachians and described them as trench valleys that affected the geomorphology by a combination of minor offsets and enhanced erosion due to fracturing. Stewart and Dennison (2006) speculated that the lineaments are fault or fracture zones associated with Neogene doming of the southern Appalachians. Working further south from our study area, we found that average strikes of joint surfaces and minor faults within the zone of lineaments are parallel to the lineaments while similar structures outside the lineaments are oblique to the lineament trends (Hill, 2013).

Gillon et al. (2009) identified hundreds of lineaments near Boone, NC and found that intersecting lineaments and metamorphic foliation create unstable blocks that contribute to the high concentration of landslides in this area. In their study, they interpreted the lineaments to be part of a regional network of fractures and faults and were able to show that some had normal, dip-slip motion. They proposed a zone of existing and potential rock slope instability that corresponds strongly with what we have mapped as the Boone fault. A strong correlation between lineaments and slope movement exists at the east end of our study area where the lineaments intersect the Blue Ridge escarpment (Figure 2.1). The deep reentrant of the escarpment at this location is likely due to the presence of abundant fractures and faults associated with lineaments. The Blue Ridge escarpment has moved westward by stream capture of previously westward-draining headwaters (Prince et al, 2011), a process likely intensified in this area due to the intersection of the escarpment and the fracture-controlled lineaments.

2.3 Geologic Bedrock Mapping and Paleostress Analysis of the Boone Fault

2.3.1 Methods

We mapped the Boone fault at the northern edge of the Grandfather Mountain window along a section of what was previously mapped as the Linville Falls thrust fault (Figure 2.2). We mapped an 80 km^2 area using 560 outcrops as control points. At each location, we made detailed bedrock descriptions and measured the orientation of any metamorphic foliation, joint sets, or faults present. We divided the Cranberry Gneiss north of the window into five subunits, consisting of a quartz monzonite, chloritic felsic gneiss, a granitic gneiss, a biotite gneiss, and a biotite-amphibolite gneiss (see appendix for a detailed description of map units). We drew many of our contacts by walking parallel to the strike of foliation and were able to add detail to the existing maps that contained the Cranberry Gneiss (Bryant and Reed, 1970; Gillon et al., 2009). In the Grandfather Mountain formation, within the window, we divided the rocks into a meta-basalt, a meta-siltstone, and a meta-sandstone. We directed much of our attention to the area where the Cranberry Gneiss is in contact with the Grandfather Mountain formation along what was previously mapped as the Linville Falls thrust fault.

When a fault moves, the slip direction is assumed to be the maximum shear stress direction within the fault plane and is recorded as a fault slickenline (e.g. Twiss and Moores, 2007). One way to simplify the description of the stresses that drive faulting is with principal stress tensors, which describe only normal stresses and no shear stresses. We used a program called WinTensor (Delvaux and Sperner, 2003) to calculate the best-fit principal stress tensors using measured fault planes and slickenlines. Knowing the best-fit principal stresses that drove outcrop-scale faults lets us approximate the mechanism that caused the Boone fault to move. We performed a paleostress inversion of 165 minor brittle faults at four outcrops along its length (Figures 2.3-2.4) and compared the resultant stress tensors with stress directions known to have caused shortening and

rifting events in the study area in an attempt to understand the timing of Boone fault motion. If it formed during NW-directed Paleozoic shortening, the expected stress tensor would show SE-NW maximum- and vertical minimum-compressional stress. Examples of NW-directed shortening structures exist throughout the orogenic belt (e.g. Hibbard et al, 2006). If the fault zone formed during Mesozoic E-W rifting, the stress tensor should have vertical maximum and horizontal E-W minimum compressional stress directions. We hypothesize that the Boone fault may be associated with a regional uplift event that drove upper crustal faulting along the lineaments. In some of our previous work on topographic lineaments cutting across the Appalachians (Hill and Stewart, 2016), we hypothesized that the lineaments accommodated Cenozoic regional doming and blocky uplift by fracturing and minor dip-slip faulting along high-angle surfaces. If the Boone fault is associated with vertical motion along the lineament that contains it, the maximum and minimum principal stresses should obliquely plunge into the fault, and the intermediate principal stress direction should lie within the fault plane.

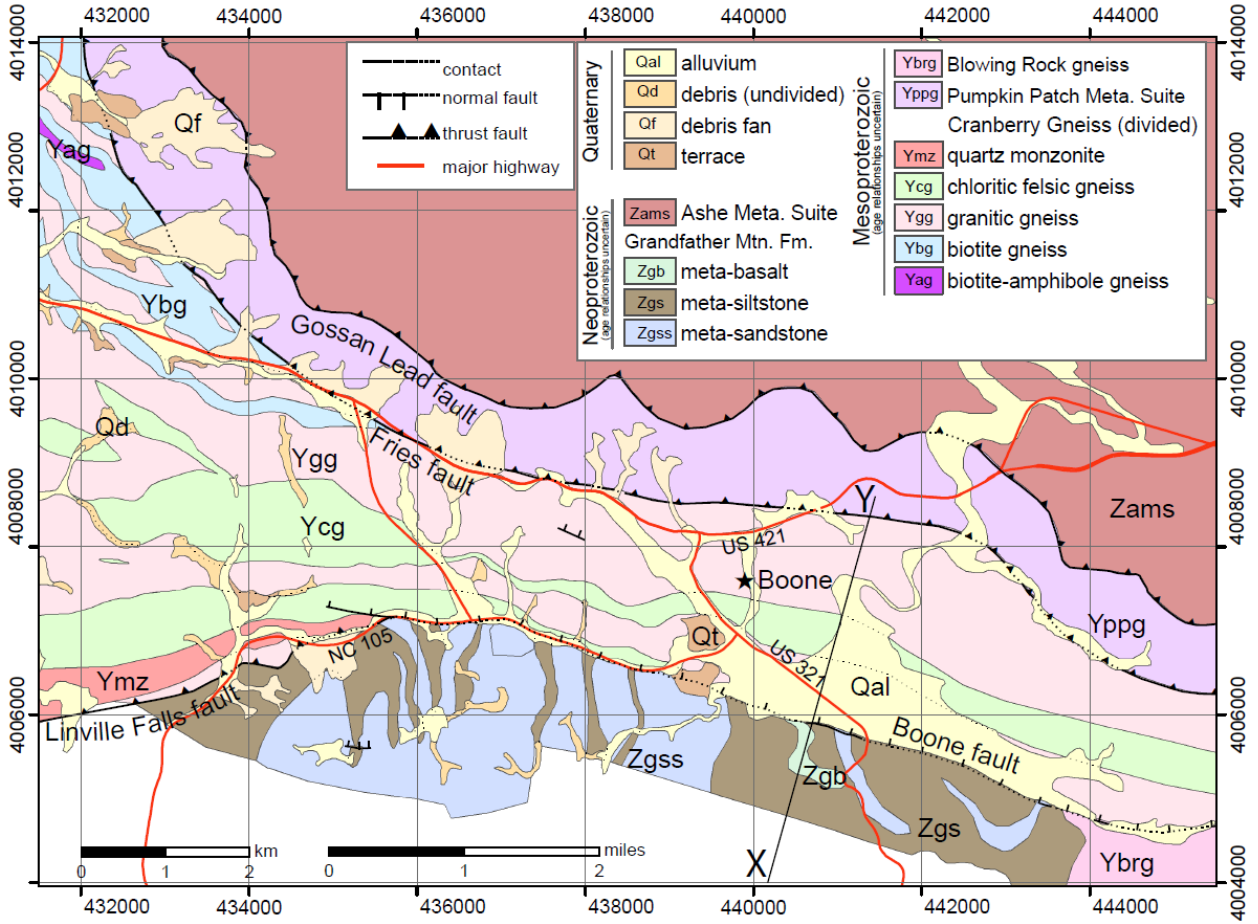

Figure 2.2: Simplified version of 1:12,000 scale bedrock map, centered on the town of Boone, North Carolina (modified from Hill and Stewart, 2015). The WNW-striking Boone fault separates the basement rocks of the Cranberry Gneiss from the metasedimentary rocks of the Grandfather Mountain formation along what has been previously mapped as the Linville Falls thrust fault. X and Y indicate the cross section line shown in Figure 2.8.

2.3.2 Results

The brittle fault zone is most evident along a ~10 km topographic scarp south of Boone, NC (Figure 2.1). Brittle faults within this zone typically dip steeply and strike WNW, and although most occur along the fault scarp that separates the Grandfather Mountain metasedimentary rocks in the south from the Cranberry Gneiss basement rock to the north, some exist several kilometers to the north and south of the main fault zone. There are normal (north-dipping) and reverse (south-dipping) faults and both show south-side-up motion (Figure 2.3). The majority of the faults we measured had slickenlines indicating dip-slip motion, although some fault surfaces show oblique or strike-slip senses of shear. Some of the high-angle faults strike N-S, but the majority are parallel to the main topographic scarp (Figure 2.4).

Faults typically form at ~30° to the maximum compressional direction, where the shear stress is high but the normal stress is low enough for the rocks to fail (Twiss and Moores, 2007). The inversions we performed on the Boone fault yield principal stress tensors with oblique, SSW-plunging maximum and NNE-plunging minimum compression directions. The intermediate principal stress direction is near horizontal and trends parallel to the Boone fault in 3 of the 4 outcrops at which we ran the inversion. This geometry does not fit Paleozoic SE-NW shortening or Mesozoic E-W rifting but is compatible with the south-side-up motion of the Grandfather Mountain window along high-angle, WNW-striking, normal and reverse faults (Figure 2.5). Based on the inversion results, we can eliminate Paleozoic or Mesozoic as the age of faulting that was recorded by the Boone fault.

Along the Boone fault, there is no mixing of the Cranberry Gneiss and Grandfather Mountain formation, which is different from the Linville Falls fault that bounds the rest of the window (Bryant and Reed, 1970). The Boone fault and related fractures crosscut the mylonitic fabric associated with older Linville Falls fault-related foliation, which we interpret to mean the

Boone fault moved along new failure surfaces rather than those of the Linville Falls fault. Adams and Su (1996) noted how the Cranberry Gneiss is separated from the Grandfather Mountain metasedimentary rocks by a structural discordance and noted the abrupt lithologic change between the two packages of rocks. Based on the brittle fault contact and the paleostress tensors that are consistent with vertical motion along WNW-striking faults, we interpret the Boone fault as a high-angle fault zone that has cut the southern edge of the Linville Falls shear zone and uplifted the northern edge of the Grandfather Mountain window.

Figure 2.3: Photo looking WNW along strike of the Boone fault, where high angle faults visibly cut metamorphic foliation associated with the Linville Falls fault. These high angle faults show south-side-up motion consistent with uplift of the Grandfather Mountain window along the Boone fault.

At one outcrop along the Boone fault (Figure 2.4, stop 156), there are abundant dip-slip brittle faults that strike predominantly N-S, but the resultant stress tensor is very similar to the best-fit tensors found at the outcrops containing WNW- and W-striking faults (Figure 2.4, stops 001, 003, and 379). We interpret the faults at stop 156 to have formed within the same stress field as the rest of our other Boone fault sites did, and possibly pre-existing planes of weakness influenced the orientation of faulting.

We propose that the ~10 km of the Boone fault we mapped along the northeastern edge of the Grandfather Mountain window is part of the ~180 km long and 20 km wide regional-scale topographic lineament swarm spanning from the Valley and Ridge in Tennessee to the Piedmont in North Carolina (Figure 2.1). The topographic scarp along the Boone fault is one of many en echelon segments of the Boone lineament swarm, which may include stretches of the Long Ridge thrust fault to the west of our main study area (Figure 2.6). Other WNW-trending faults and bedrock contacts are parallel and along strike of the Boone fault in many parts of the lineament swarm, such as where the Stone Mountain fault offsets the Beech Granite (Bryant and Reed, 1970). This regional fracture and fault zone likely accommodated uplift of the southern Appalachians along many vertical and near-vertical surfaces, some of which have been previously interpreted as brittle Alleghanian faults that moved during alternating ductile and brittle deformation stages during Pangean assembly (Adams and Su, 1996; Stewart et al., 1997).

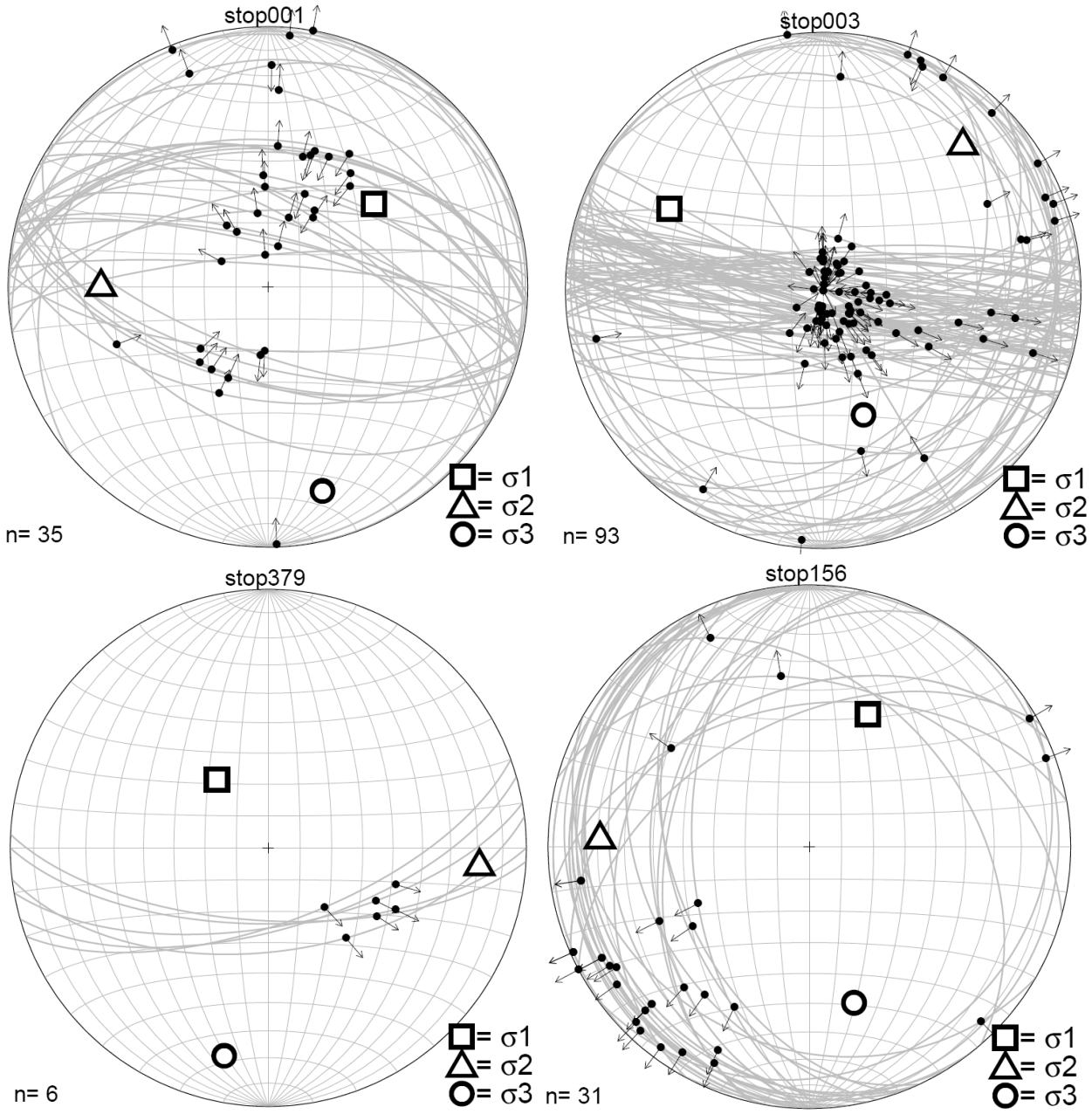

Figure 2.4: Equal-area, lower-hemisphere plots showing brittle faults (gray lines) with slickenlines (black dots) found along the Boone fault zone. The paleostress inversions yielded the best-fit maximum, intermediate, and minimum (circles, triangles, squares, respectively) compressive stress directions that formed the faults. Arrows on normal faults point towards center and on reverse faults they point away. We are using the engineering convention, where σ3 = maximum compression and σ1 = minimum.

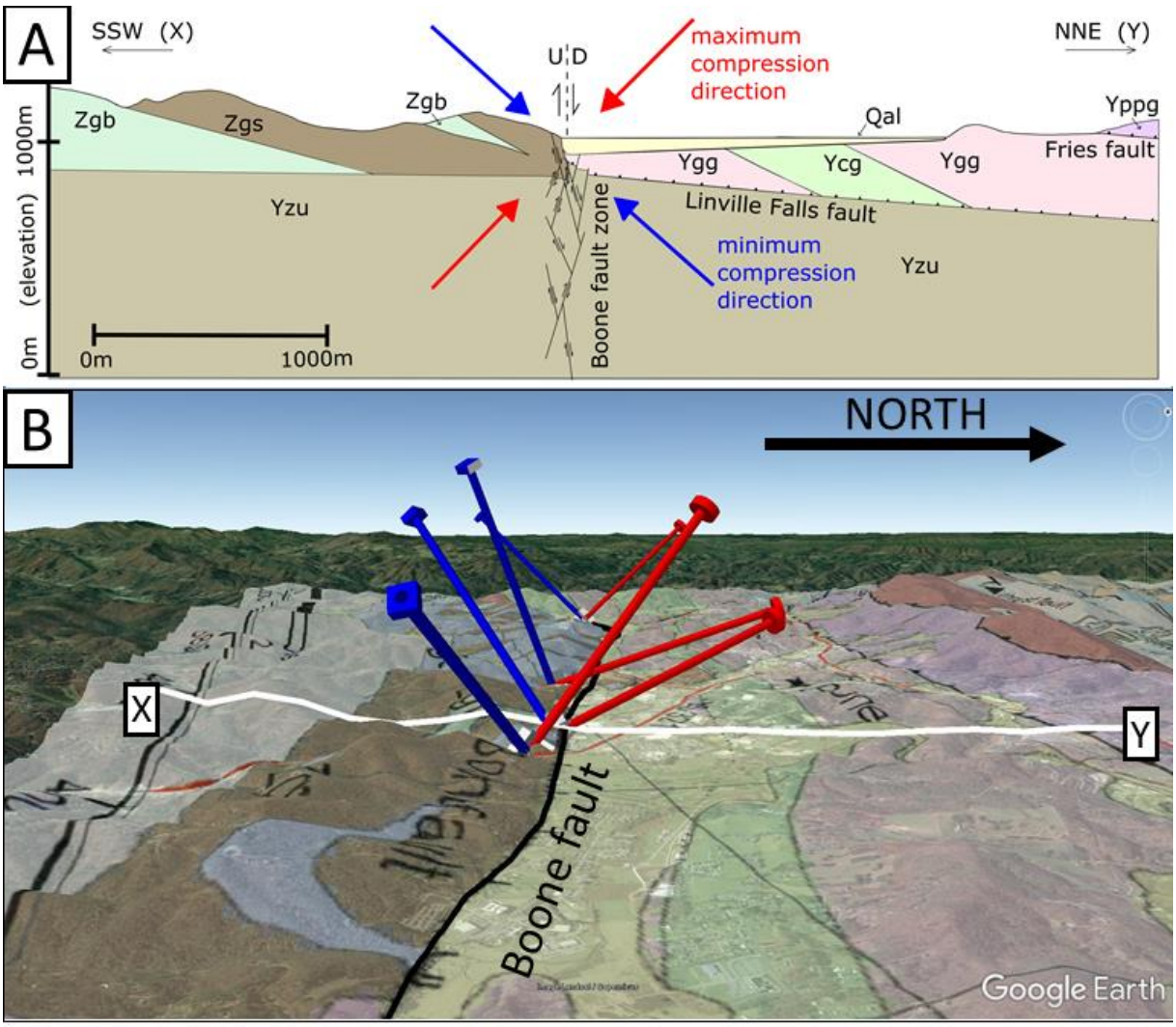

Figure 2.5: (A) Schematic SSW-NNE bedrock cross section showing best-fit paleostress tensors for high-angle, WNW-striking brittle faults with south-side-up motion along the Boone fault. Although there is some variation in the resultant stress directions at the four outcrops displayed in figure 2.6, the stress tensors are generally consistent with vertical motion. (B) Google Earth image looking westward along strike of the Boone fault (traced as the green line). The 3-D models show the paleostress inversion results as three orthogonal axes. The red (circles) and blue (squares) represent the maximum and minimum compressive stress directions, respectively.

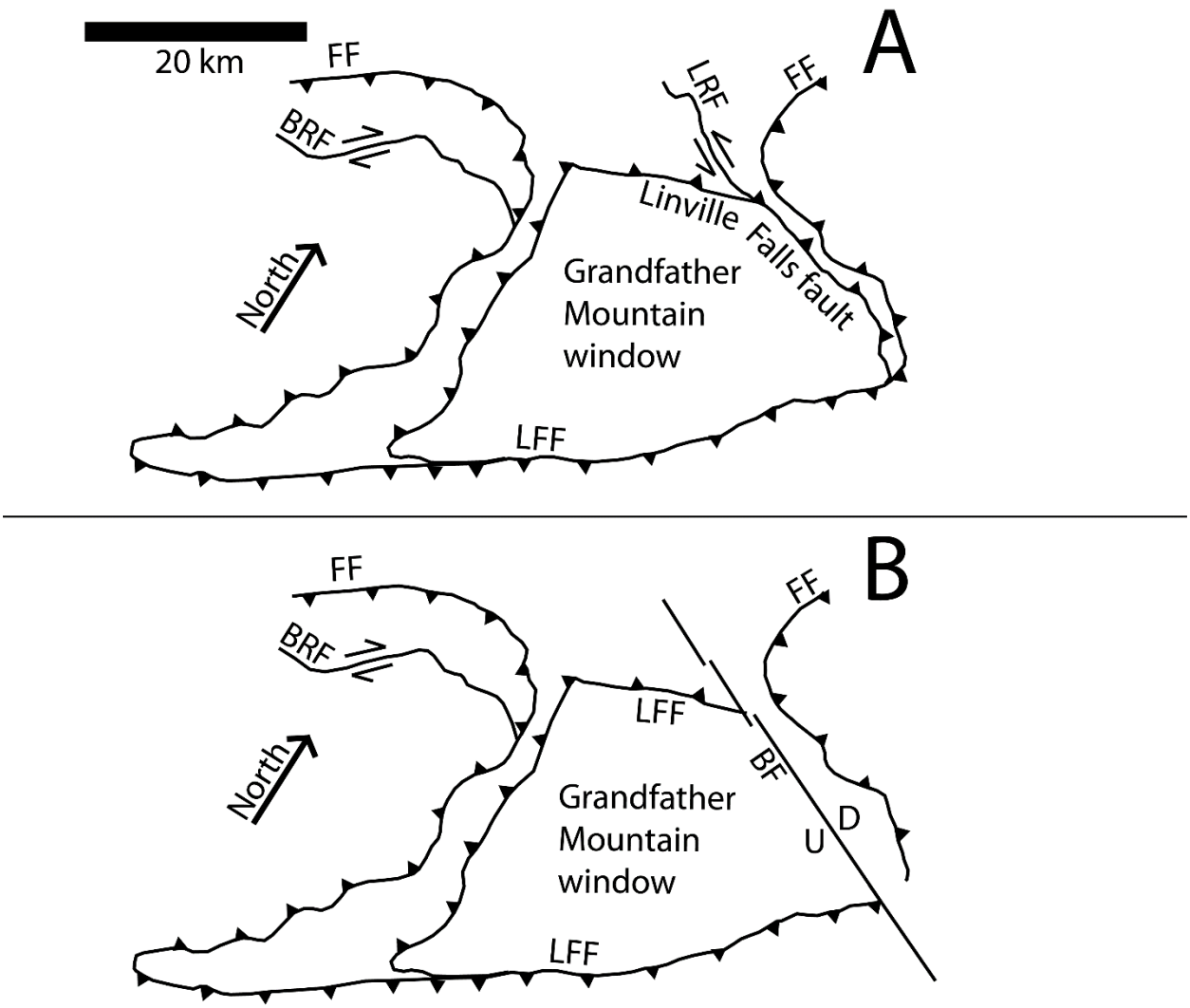

Figure 2.6: (A) Simplified map of the Grandfather Mountain window and surrounding faults (LFF = Linville Falls fault, FF = Fries fault, LRF = Long Ridge fault; BRF = Burnsville fault). The window was previously interpreted to be bounded on all sides by the Linville Falls fault. These contacts were modified from Hibbard et al. (2006). (B) Map of study area showing the Boone fault (BF) with south-side-up motion of along what was previously mapped as a section of the Linville Falls and the Long Ridge faults.

2.4 Geomorphic evidence for Cenozoic motion along the Boone fault

2.4.1 Methods

In addition to bedrock mapping, we assessed the geomorphology around the Boone fault for any evidence of recent motion. To do this, we mapped slope-movements deposits as either undivided debris flows or debris fans, as well as any alluvium and terrace deposits present (Figure 2.2). We also obtained LIDAR from the North Carolina Spatial Data Download (https://rmp.nc.gov/sdd/) to analyze the longitudinal profiles of dozens of streams draining into the fault zone (Figure 2.7). Using an automated knickpoint selection process (detailed methods available in Ch. 1 of this dissertation), we searched for knickpoints along dozens of streams that drain into the Boone fault zone. We investigated the map view patterns of the streams surrounding the Boone fault for evidence of drainage capture (Figure 2.8). We hypothesized that the high alluvial valleys we mapped in the Grandfather Mountain window are relict landscapes that were likely part of ancient river system (Figure 2.9). To test this idea, we produced an elevation histogram of the streams in Watauga County (Figure 2.10), assuming that in mountainous terrain, flat areas such as river valleys would show a high frequency of points at the elevation of the valley. We compared the stream elevation distribution with the knickpoint elevation

2.4.2 Results

Many of the surficial deposits we mapped are consistent with a landscape responding to recent uplift. There are abundant debris deposits (Qd) throughout the study area with patches of young trees above noticeable lobes of debris toes. There are also many "pistol butt" shaped trees, an indication that the hillslopes are experiencing active creep (Ven Den Eeckhaut et al., 2009). We found numerous knickpoints (n=178) hundreds of meters above the valley floor (Figure 2.7), suggesting that the Boone fault accommodated ~ 200 m of uplift since the streams were in equilibrium. There is no trend between the location of the knickpoints and lithologic contacts, but

they appear in two main modes of elevation. In addition to the disequilibrium longitudinal profiles, some of the headwater streams that drain into the Boone fault have hook-shaped patterns (Figure 2.8), indicative of drainage capture events.

There are two main river systems draining away from the Boone fault zone, the South New River to the east and the Watauga River to the west (Figure 2.10). These two river systems contain much of the flat topography of Watauga county and are the locations of the majority of human development around Boone. These two active rivers have flat valleys in Watauga County at ~950 m and ~800 m, accordingly, as evident in the histogram of stream elevations (Figure 2.10). There is a third mode of stream elevation points at ~1100 m that does not correspond with any known river valley but is immediately above the highest group of knickpoints (Figure 2.10).

Gillon et al. (2009) documented hundreds of slope-movement events in Watauga County, and many of these are concentrated in a zone of rock slope instability that corresponds with the Boone fault on our map. A few kilometers north of our map, Mills and Granger (2002) used cosmogenic isotopic burial age dating techniques to estimate major debris fans (Qf) on the west slopes of Rich Mountain to be as young as 1.45 Ma. The abundance of modern debris deposits suggests that the landscape is still adjusting to uplift, and the proximity to the Boone fault suggests that unstable slopes may be a result of young faulting. Terrace deposits near the Boone fault may also be remnants of floodplains abandoned due to recent uplift.

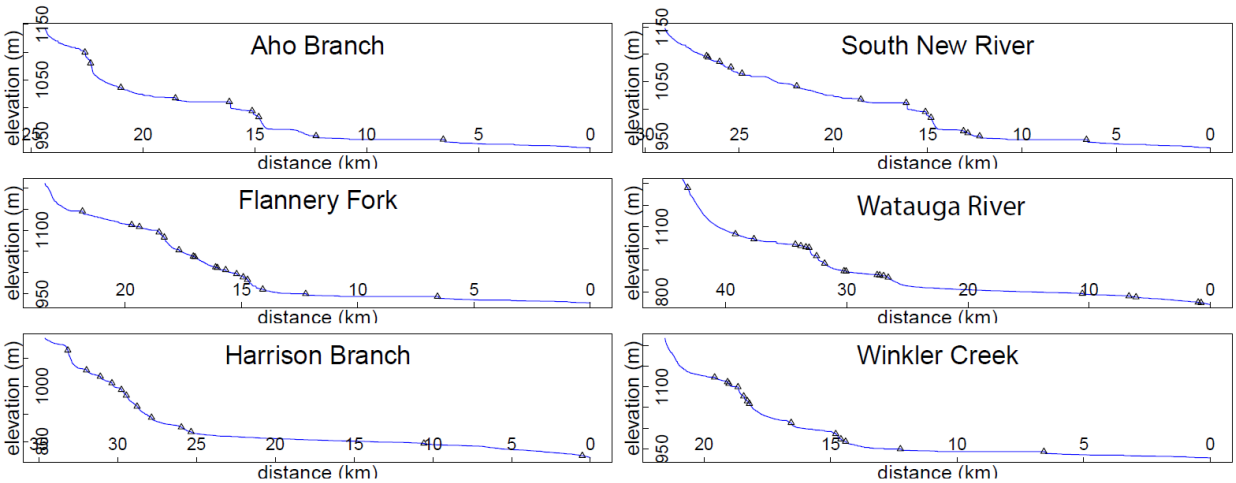

Figure 2.7: Six longitudinal profiles from streams that drain into the Boone fault and contain a similar pattern of knickpoints, likely from recent vertical motion on the fault. The major slope break on these profiles is between 200-400 m above the valley floor, indicating there has likely been that amount of uplift since the streams were at equilibrium. We analyzed dozens of other river profiles with similar geometries, shown on the map in figure 2.8.

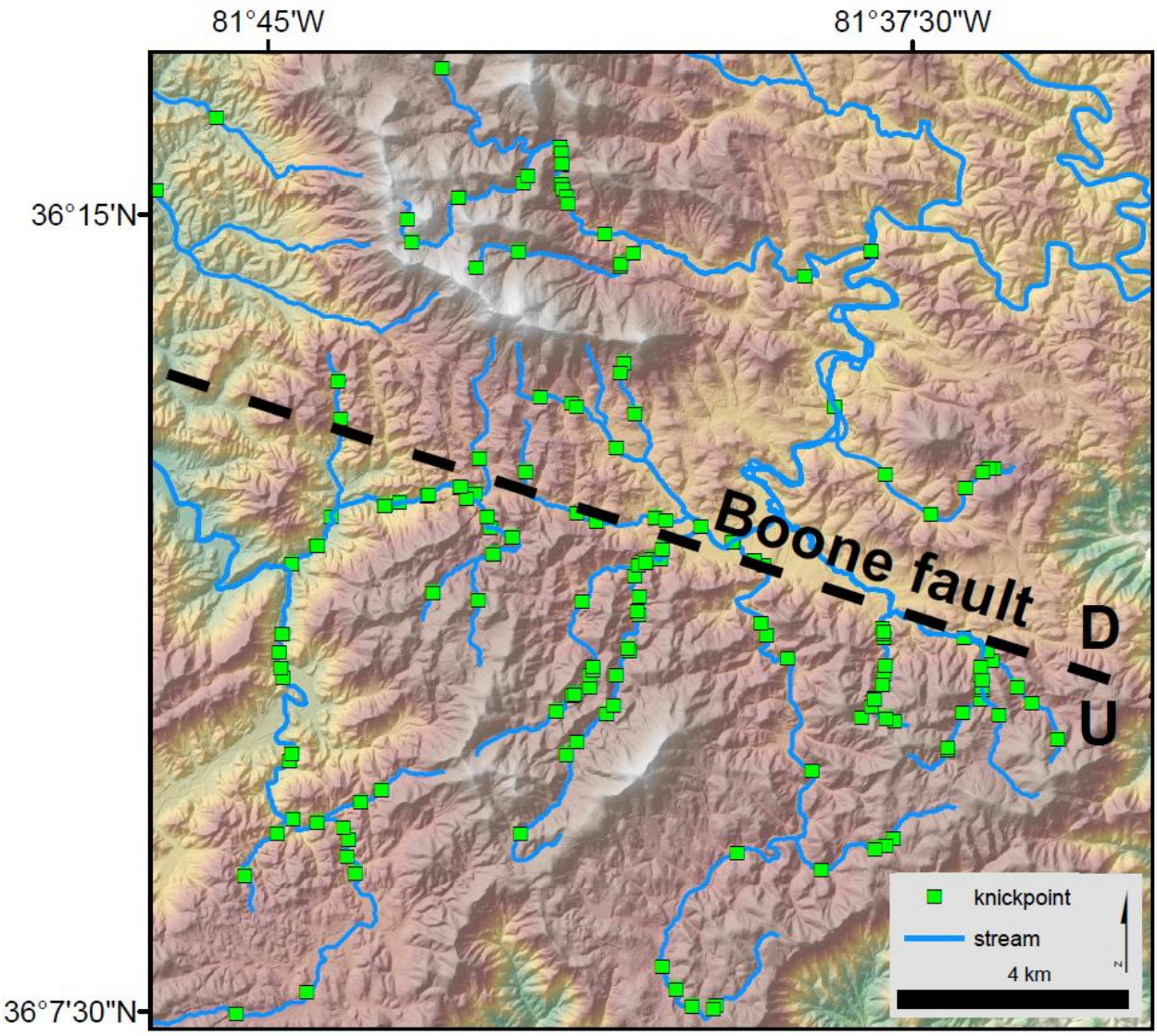

Figure 2.8: Digital elevation model showing streams with knickpoints that drain from the high plateau above the Boone fault. Note the hook-shaped headwaters of the streams in the southern part of the map, which we interpret as a result of stream capture related to south-side-up motion along the Boone fault.

The South New River forms a large alluvial valley whose southern edge is defined by the topographic escarpment along the Boone fault, but many smaller floodplains exist to the south of the Boone fault within the Grandfather Mountain window. We interpret these to be uplifted ancient floodplains raised during the south-side-up motion of the Boone fault. There is a pattern of alternating steep-flat-steep-flat topography in the proposed uplifted landscape to the south of the

Boone fault. The histogram of stream elevation has modes that correspond to the South New and Watauga Rivers, as well as a third mode that we think is related to the relict landscape above the Boone fault (Figure 2.10). The streams draining away from this uplifted surface are actively dissecting it by migration of the knickpoints along north-draining streams. This idea is supported by the histogram of knickpoint elevations, which shows knickpoints in two clusters between the South New River valley and the uplifted valley at 1000 m and 1100 m (Figure 2.10). This distribution of knickpoint elevations could represent multiple pulses of uplift along the Boone fault, where each event caused a base level change and sent a new series of knickpoints upstream. Similar stream profiles have been described in the Sierra Nevada of California, where multiple phases of uplift resulted in a relict landscape in the highest reaches of the streams and an intermediate landscape between the headwaters and the mouth (Clark et al., 2005).

We interpret the hook-shaped streams as evidence of drainage capture related to uplift of the landscape to the south of the fault (Figure 2.9). We think the hook-shaped headwaters in our study area imply that the high plateau to south of the Boone fault may still be in flux, and the presence of the hooks suggests that there may be other faults to the south that allowed the plateau to move upward. Similar hook-shaped map-view stream patterns exist where headwater streams have been captured by the migration of the eastern continental divide along the Blue Ridge Escarpment (Prince et al., 2011).

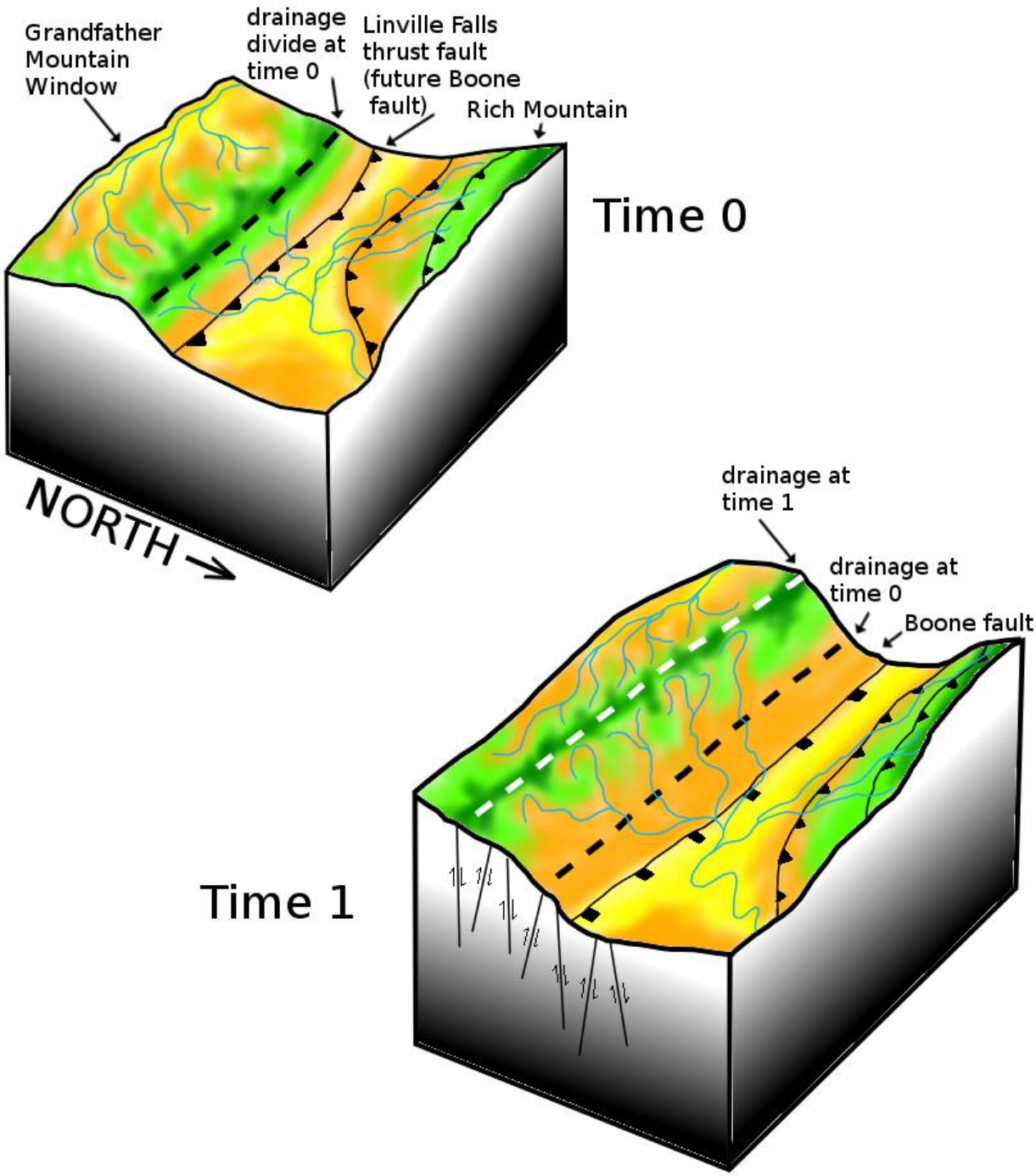

Figure 2.9: Block diagram illustrating how uplift on the Boone fault could have driven drainage divide migration and led to the formation of the hook-shaped drainage patterns observed in the headwaters above the fault zone.

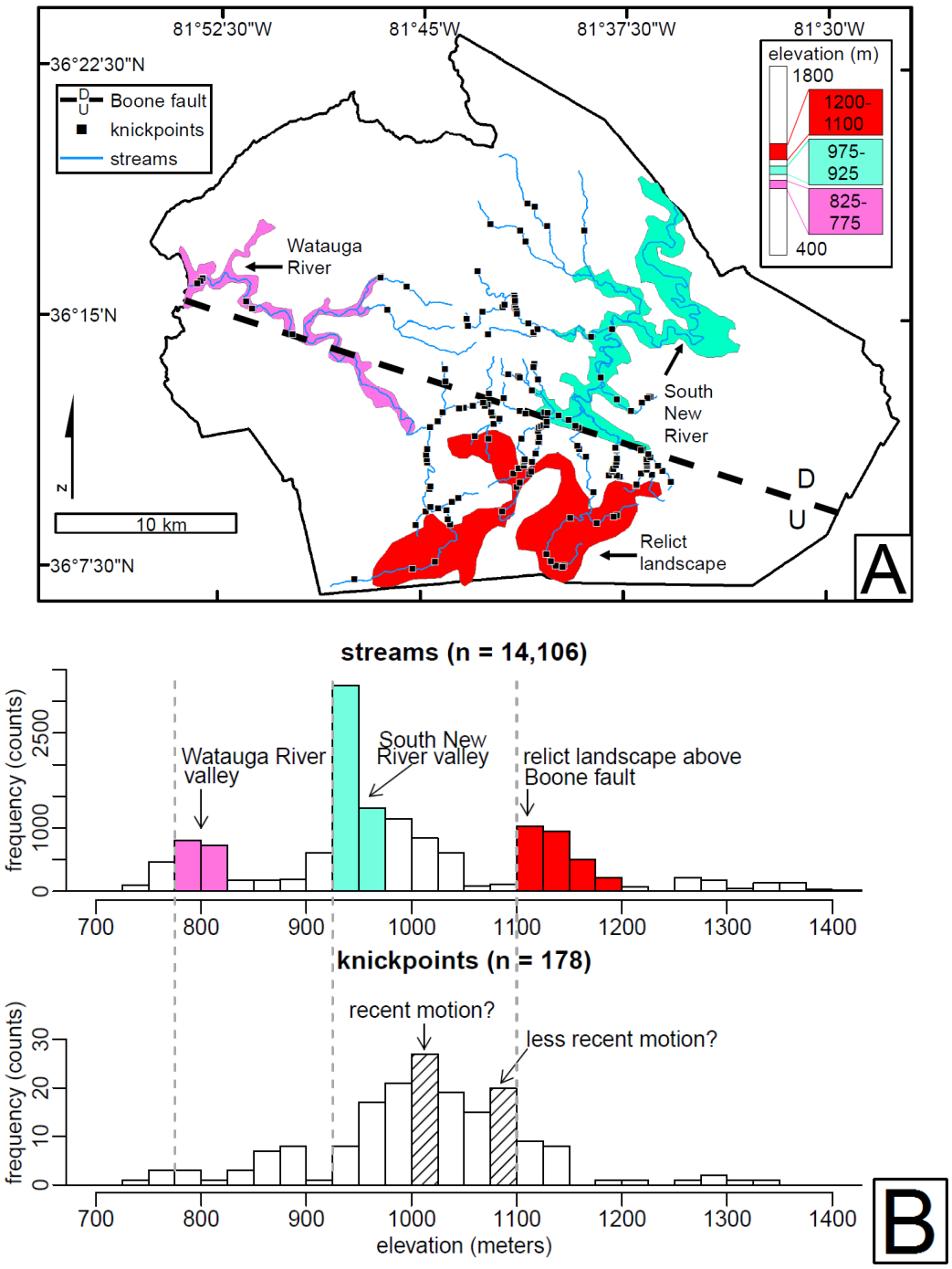

Figure 2.10: (A) Map of Watauga County showing three zones of flat topography: the Watauga River valley (pink), the South New River valley (cyan), and what we interpret as a relict river valley uplifted as a result of motion along the Boone fault (red). (B) Elevation histogram of the streams we analyzed, which are in three modes corresponding to the three valleys. The knickpoints are at two elevation modes between the South New River and the relict valley above the Boone fault, suggesting multiple pulses of motion on the Boone fault.

2.5 Modern seismicity and surface deformation near the Boone fault

There have been minor earthquakes within and near the study area in recent years (NEIC, 2018). These events ranged from 2.3 to 3.1 in magnitude and from 1.0 to 12.7 km in depth (Figure 2.11). Forming a cluster near the newly mapped Boone fault, four events from 2013 and 2014 have hypocenters that align in an E-W direction, sub-parallel to the main Boone fault zone. Three of the four hypocenters lie on a plane at different depths, which is consistent with the possibility of a vertical fault plane. During the June 2014 event (M = 2.5 and depth = 6.7 km), shaking at depth led to slope movement and deformation at the surface. Although the seismicity was too small and too deep to produce a surface rupture, motion on the fault at depth triggered shaking and deformation at the surface in the form of a cracked building foundation, sidewalk, and retaining wall. At the same location, a tree was split in two, a loud sound was heard and interpreted as a truck hitting the building, a fissure formed in the hillslope, and a crack propagated across US hwy. 321 (Randy McCoy, oral communication, 2016). During the August 2014 event (M = 2.9 and depth = 9.4 km), shaking caused a foundation to crack on a house located ~8km to the WNW of the epicenter, near one of the smaller normal fault segments we mapped to the south of the main fault zone (Doug Harker, oral communication, 2017). These events mean the Boone fault is a post-orogenic fault zone that may be still active.

2.6 Discussion of the age of the Boone fault

The high-angle Boone fault cuts the NW-dipping foliation of the Linville Falls shear zone, and the orientations of the best-fit principal stress tensors do not match the stresses that drove Paleozoic NW-directed shortening, thus the Boone fault is younger than the Linville falls shear zone. The resultant paleostress directions are also inconsistent from those that formed the generally N-S and NNE-SWW-striking Triassic normal faults or NNE-SSW-trending Jurassic diabase swarms found in the North Carolina Piedmont and Blue Ridge, which means the Boone fault must be post-Jurassic. While the stress inversions alone are not enough to eliminate the Late Mesozoic or Early Cenozoic as possible ages of the Boone fault, our geomorphic and seismic analyses support a Late Cenozoic age.

The rivers draining into the Boone fault zone contain longitudinal profiles similar to streams Gallen et al. (2013) interpreted to have recorded 100s of meters of Neogene uplift of the North Carolina Blue Ridge. The streams analyzed by Gallen et al. (2013) drain into topographic lineaments and contain knickpoints at elevations between 900 m and 1200 m that separate active and relict landscapes hundreds of meters above the stream mouths. The similarities in the knickpoint locations and longitudinal geometries to the streams around Boone allow us to speculate that the vertical motion on the Boone fault likely began in the Neogene and has been recorded by a series of transient knickpoints currently located in the headwaters. This timing of fault initiation matches the increase in offshore sedimentation (Poag and Savon, 1989) and folding of Coastal plain sediments during the Neogene (Stewart, 2015), and we interpret the Boone fault as having helped accommodate Late Cenozoic doming and blocky uplift of the southern Appalachians.

Based on modern seismicity, the Boone fault may be active (NEIC, 1973-2018). We propose that it is the driving mechanism for the unstable landscapes around the Town of Boone.

To our knowledge, the Boone fault is the first seismically active fault documented in the western North Carolina Blue Ridge.

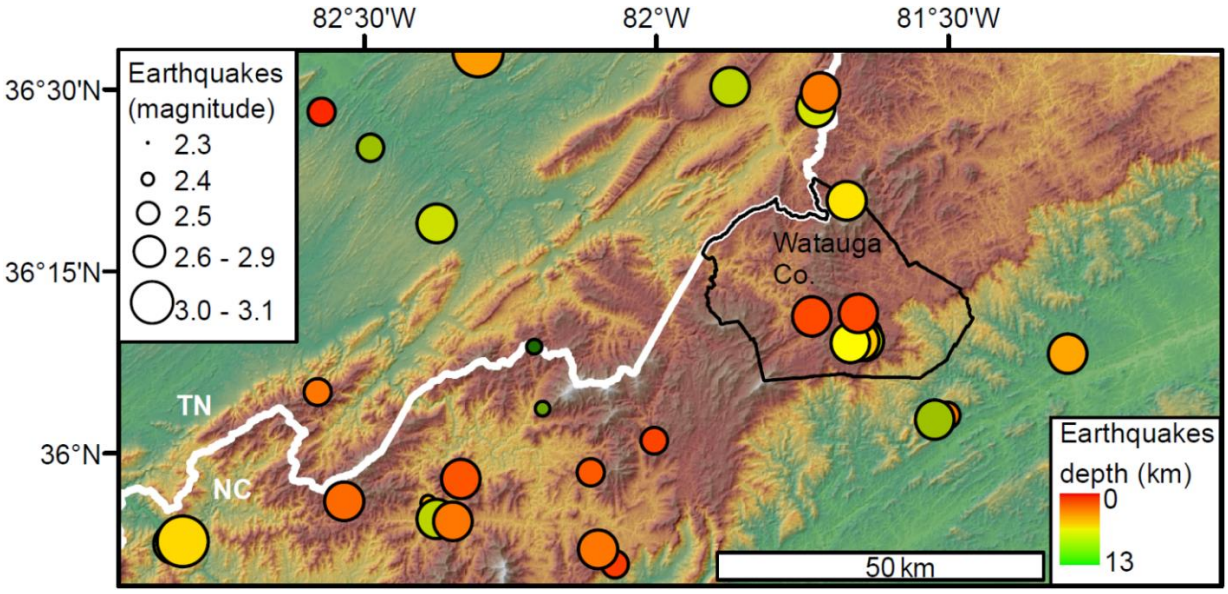

Figure 2.11: HydroSHEDS digital elevation model of eastern Tennessee and western North Carolina showing the WNW-trending Boone lineament that stretches over 180 km from the Valley and Ridge eastward to the Piedmont province. The circles represent earthquake epicenters (NEIC, 1973-2018), many of which are along the Boone lineament or the E-W Laurel Creek lineament in the southern part of the image.

2.7 Conclusions

In this paper, we present data consistent with a landscape responding to recent uplift, not one that has been steadily eroding since the Paleozoic. The Boone fault is a steeply dipping fault zone that accommodated south-side-up motion of the northern edge of the Grandfather Mountain window. We interpret the 10-km long Boone fault as a minor part of the ~180 km-long and ~20 km-wide Boone lineament swarm. The young faults and disequilibrium landscape suggest the Grandfather Mountain window is not entirely framed by a Paleozoic fault, but rather is bounded in part by a Neogene fault zone. There is abundant evidence that the southern Appalachians were uplifted in the Neogene, and to our knowledge, the Boone fault zone is the first mappable Blue Ridge structure attributed to late Cenozoic topographic rejuvenation. The evidence for young topography and Cenozoic tectonics related to the Boone fault we present is four-fold: (1) the WNW-brittle faults do not fit known tectonic events based on stress inversions; (2) the streams draining into the Boone fault contain abundant knickpoints and are similar to other Neogene knickpoints; (3) the hook-shaped headwaters south of the Boone fault are consistent with major drainage reorganization; and (4) the active seismicity associated with surface deformation near the fault zone implies that the Boone fault is potentially still active. We propose that the Boone lineament and other lineaments of similar size and orientation formed during blocky, Late Cenozoic uplift of the orogen associated with delamination of the lithospheric root (See Ch. 3 for a detailed discussion of this mechanism). Based on our work, the rapidly-growing mountain community of Boone should regard the Boone fault zone as potentially active when making future land use plans.

REFERENCES

1. Adams, Mark G., 1996, and Su, Qi, The nature and timing of deformation in the Beech Mountain thrust sheet between the Grandfather Mountain and Mountain City windows in the Blue Ridge of Northwestern North Carolina, The Journal of Geology, v. 104, p. 197-213

2. Boyer, Steven E., 1982, and Elliot, David, Thrust Systems, The American Association of Petroleum Geologists Bulletin, v. 66, no. 9, p. 1196-1230

3. Bryant, B., 1970, and Reed, J.C., Geology of the Grandfather Mountain window and vicinity, North Carolina and Tennessee: U.S. Geological Survey, Professional Paper 615, scale 1:62,500

4. Burton, William C., 2010, and Southworth, Scott; A model for Iapetan rifting of Laurentia basedon Neoproterozoic dikes and related rocks; Geological Society of America Memoirs; v. 206, p.455- 476

5. Clark, Marin K., 2005, Maheo, Gweltaz, Saleeby, Jason, and Farley, Kenneth A., The non-equilibrium landscape of the southern Sierra Nevada, California; GSA Today, v. 15, no. 9, p. 4-10

6. Delvaux, D., 2003, and Sperner, B., New aspects of tectonic stress inversion with reference to the TENSOR program. In: New Insights into Structural Interpretation and Modelling (D. Nieuwland Ed.). Geological Society, London, Special Publications, 212: 75-100.

7. Dennison, John M., 2001, and K. G. Stewart, Regional structural and stratigraphic evidence for dating Cenozoic uplift of Southern Appalachian highlands; Geological Society of America, Southeastern Section Meeting, Abstracts with Programs. Vol. 33. No. 6.

8. Gallen, Sean F., 2013, Wegmann, Karl W., and Bohnenstiehl, DelWayne R., Neogene rejuvenation of topographic relief in the southern Appalachians; GSA Today, v. 23, no.2, p.4- 10

9. Galloway, William E., 2011, Whiteaker, Timothy L., and Ganey-Curry, Patricia, History of Cenozoic North American drainage basin evolution, sediment yield, and accumulation in the Gulf of Mexico basin; Geosphere, v. 7; no. 4; p. 938–973

10. Gay, Parker S., Jr., 2000, Unmapped topographic alignments visible on 3D stereo terrain map of a 2 degrees X 2 degrees segment of the Southern Appalachians, Geological Society of America Abstracts with Programs, Southeastern Section v.32, no.2, p.19

11. Gillon, K.A., 2009, Wooten, R.M., Latham R.L, Witt A.W. Douglas, T.J., Bauer, J.B., and Fuemmeler, S.J, Integrating GIS-Based Geologic Mapping, LiDAR-Based Lineament Analysis and Site Specific Rock Slope Data to Delineate a Zone of Existing and Potential Rock Slope Instability Located Along the Grandfather Mountain Window-Linville Falls Shear Zone Contact, Southern Appalachian Mountains, Watauga County, North Carolina, American Rock Mechanics Association ARMA 09-181

12. Faill, Rodger T., 1997, A geologic history of the north-central Appalachians. Part 1. Orogenesis from the Mezoproterozoic through the Taconic orogeny; American Journal of Science; v. 297, p. 551-619

13. Hack, John T., 1982, Physiographic divisions and differential uplift in the Piedmont and Blue Ridge; Geological Survey Professional Paper 1265

14. Hatcher, Robert D. Jr., 2005, Merschat, Arthur J., and Thigpen, J. Ryan, Blue Ridge Primer, in Blue Ridge Geology Geotraverse East of the Great Smoky Mountains National Park, Western North Carolina (eds. Hatcher, Robert D., Jr., and Merschat, Arthur J.); Carolina Geological Society Annual Field Trip Guidebook

15. Hibbard, J. P., 2006, van Staal, C.R., Rankin, D.W., and Williams, H., Lithotectonic map of the Appalachian Orogen, Canada-United States of America, Geological Survey of Canada, Map 2096A, scale 1:500,000

16. Hibbard, James. P., 2010, van Staal, Cees R., and Rankin, Douglas W., Comparative analysis ofthe geological evolution of the northern and southern Appalachian orogen: Late Ordovician-Permian; Memoir of the Geological Society of America, v. 206, p. 51-69

17. Hill, Jesse S., 2013, Zoned uplift of western North Carolina bounded by topographic lineaments: M.S. Thesis, University of North Carolina at Chapel Hill, 51 p.

18. Hill, Jesse S., 2016, and Stewart, Kevin G., A newly discovered fault zone near Boone, North Carolina and Cenozoic topographic rejuvenation of the southern Appalachian Mountains, Geological Society of America Abstracts with Programs, v. 48, no. 7

19. Hill, Jesse S., 2018, and Stewart, Kevin G., Young topography, new faults, and mantle reorganization in an ancient mountain range: A case study from the Appalachians, Geological Society of America Abstracts with Programs, v. 50, no. 3

20. Li, Z.X., 2008, Bogdanova S.V., Collins A.S., Davidson A., De Waele B., Ernst R.E., Fitzsimons, Fuck, R.A., Gladkochub D.P., Jacobs J., Karlstrom K.E., Lul, S., Natapovm L.M.,

Pease, V., Pisarevsky S.A., Thrane K., Vernikovsky V., Assembly, configuration, and break-up history of Rodinia: A synthesis; Precambrian research 160, no. 1, p 179-210.

21. Merschat, Arthur J., 2005, Hatcher, Robert D. Jr., and Davis, Timothy L., The northern Inner Piedmont, southern Appalachians, USA: kinematics of transpression and SW-directed mid-crustal flow, Journal of Structural Geology v. 27. p. 1252-1281

22. Miller, Brent V. ,2006, Fetter, Allen H., and Stewart, Kevin G., Plutonism in three orogenic pulses,Eastern Blue Ridge Province, southern Appalachians; GSA Bulletin, v. 118, no. ½, p.171-184

23. Miller, Scott R., 2013, Sak, Peter B., Kirby, Eric, and Bierman, Paul R., Neogene rejuvenation of central Appalachian topography: Evidence for differential rock uplift from stream profiles and erosion rates; Earth and Planetary Science Letters, 369- 370, p. 1-12

24. Mills, Hugh H., 2002, and Granger, Daryl E., Cosmogenic isotope burial dating reveals 1.5 million-year-old fan deposit in Blue Ridge Mountains of North Carolina; Geological Society of America Abstracts with Programs.

25. National Earthquake Information Center (2018): http://earthquake.usgs.gov/regional/neic/

26. Nystrom, Paul, 1986, Late Cretaceous-Cenozoic brittle faulting beneath the western South Carolina coastal plain; reactivation of the eastern Piedmont fault system; Geological Society of America Abstracts with Programs, v. 38, no.3, p. 74

27. North Carolina Geological Survey, 1985, Statewide Bedrock Map, 1:500,000 scale

28. Poag, Wylie C., 1989, Sevon, William D., A record of Appalachian denudation in postrift Mesozoic and Cenozoic sedimentary deposits of the U.S. middle Atlantic continental margin; Geomorphology, v.2, p. 119-157

29. Prince, Philip S., 2011, Spotila, James A., and Henika, William S., Stream capture as a driver oftransient landscape evolution in a tectonically quiescent setting, Geology, v. 39, no. 9, p.823-826

30. Spotila, James A., 2004, Bank, Greg C., Reiners, Peter W., Naeser, Charles W., Naeser, Nancy D., and Henika, Bill S., Origin of the Blue Ridge escarpment along the passive margin of Eastern North America, Basin Research, v. 16, p. 41-63
31. Stewart, Kevin G., 1997, Adams, Mark G., Trupe, Charles H., Paleozoic structure, metamorphism, and tectonics of the Blue Ridge of western North Carolina, Carolina Geological Society, 1997 Field Trip Guidebook, p. 16-17

32. Stewart, Kevin G., 2006, Dennison, John M., Tertiary-to-recent arching and the age and origin of fracture-controlled lineaments in the southern Appalachians. Geological Society of America Abstracts with Programs, v. 38. no. 3.

33. Stewart, Kevin G., 2015, Estimates on the magnitude and timing of post-orogenic topographic rejuvenation of the southern Appalachians using isostasy and deformed Coastal Plain rocks, Geological Society of America Abstracts with Programs, v. 47., no. 2., p. 82

34. Trupe, Charles H, 2004, Stewart, Kevin G., Adams, Mark G., and Foudy, John P., Deciphering the Grenville of the southern Appalachians through evaluation of the post-Grenville tectonic history in northwestern North Carolina, Geological Society of America Memoir 197, p. 679-695

35. Tull, James, F., 2010, Allison, David T., Whiting, Stephen E., John, Nick L., Southern Appalachian Laurentian margin initial drift-facies sequences: Implications for margin evolution; Geological Society of America Memoir 206, p. 935-956

36. Twiss, Robert J., 2007, and Moores, Eldridge, M., Structural Geology, second edition; W. H. Freeman and Company, New York

37. Van Den Eeckhaut, M., 2009, Muys, B., Van Loy, K., Poesen, J., and Beeckman, H., Evidence for repeated re-activation of old landslides under forest; Earth Surface Processes and Landforms, v. 34, p. 352-365

CHAPTER 3: MANTLE MOTION AND TOPOGRAPHIC REJUVENATION IN THE SOUTHERN AND CENTRAL APPALACHIANS

3.1 Introduction

The high topography of the southern and central Appalachians does not coincide with the physiographic provinces but instead cuts across them. This band of rugged topography correlates to areas of high slope and local relief in the Appalachian Plateau of Pennsylvania, the Valley and Ridge of Virginia and West Virginia, and in the Blue Ridge of North Carolina. We present geomorphic maps to show that the surface of the Appalachians does not always match the underlying bedrock geology and believe that although currently located at a passive margin, this ancient orogen has undergone uplift likely associated with a delaminating lithosphere. To support our claim that the topography is partly controlled by rearrangement of the mantle, we compare our surface maps to tomographic maps ranging from 36 to 915 km depth. There is a reasonably good fit between the swath of high topography and a seismic anomaly that was recently interpreted as a piece of lithosphere descending into the mantle (Biryol et al., 2016). It is our interpretation that upper mantle reorganization has driven a Cenozoic rejuvenation of topography and caused many of the structures and landforms that would not exist if the ancient orogenic belt has been eroding steadily since the Paleozoic. If mantle motion is the main driver of the current landscape, it may also be responsible for the formation of the anomalous topographic lineaments that cross the mountain belt and correspond to young faults and align with clusters of earthquake epicenters. We support our claim that mantle reorganization is the cause of topographic rejuvenation by showing that removal of an eclogitic root 15-25 km thick would uplift the lithosphere between 450-750m, which is consistent with uplift estimates previously derived from geomorphic studies.

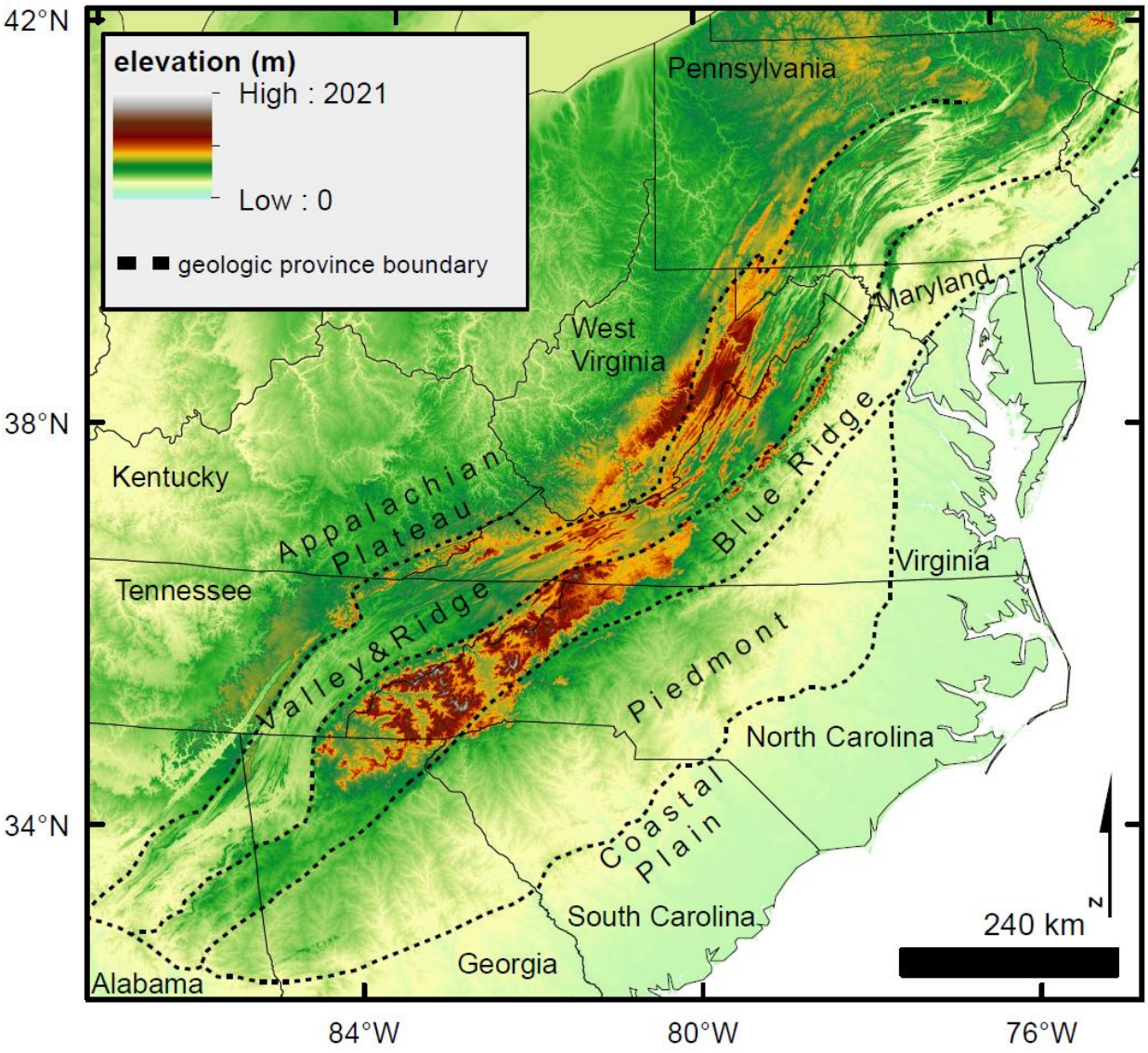

Figure 3.1: Digital elevation model of the southern and central Appalachians derived from HydroSHEDS data with ~90m horizontal resolution. The dashed black lines separate major geologic provinces (modified from Hibbard et al., 2006). Note the swath of high topography that starts in the Blue Ridge of North Carolina, crosses into the Valley and Ridge of Virginia, then ends in the Appalachian Plateau of West Virginia and Pennsylvania.

Ideas of how landscapes respond to orogenesis have evolved over time (e.g. Davis, 1899; Penck, 1953; Hack, 1975). When mountains form through the interaction of tectonic plates, they grow in elevation until they collapse due to their own weight, or are eroded away after tectonic

processes cease (e.g. Teng, 1996). Burbank and Anderson (2012) described an unrelenting competition between tectonic and erosional processes that build up and break down the crust. Although much of the mountain topography forms either at the plate margins or when plates rift, intraplate relief can be generated in ways that are not fully clear. To better understand how intraplate mountains can exist long after orogenesis, we focused on the southern and central Appalachians, an ancient mountain range with a long history of both uplift and erosion.

The Appalachians have experienced multiple Wilson cycles over the past billion years and although currently located at a passive margin, this ancient orogen has rugged, high topography. While many landscape features can be attributed to the underlying local lithology, the topography and relief in each of the major physiographic provinces varies by up to a kilometer along the orogen (e.g. McKeon, et al, 2014). The Blue Ridge is much higher and has far greater relief in North Carolina than in Virginia, Maryland, or Pennsylvania (Figure 3.1). The Valley and Ridge is mountainous in Virginia but forms rolling hills in Tennessee and Pennsylvania. Likewise, the Appalachian Plateau in West Virginia and southern Pennsylvania is much higher than its southern counterparts. The mismatch between elevation and lithology along the mountain belt offers an excellent opportunity to improve our understanding of post-orogenic landscapes.

The main focus of this paper is to understand what mechanisms could generate the topography of the modern Appalachians. We compared maps of slope, local relief, and topography with lithologic boundaries and to test for a connection between our surficial observations and mantle dynamics, we overlaid elevation contours onto seismic tomography slices showing P-wave perturbations ranging from 36 km to 915 km depth (Biryol et al., 2016). We performed isostacy calculations to test for a causal link between mantle motion and the topography and to compare the amount of Neogene uplift estimated by Hill (2013), Gallen et al., (2013), and Miller et al.,

(2013) with the predicted uplift magnitude that would result from delamination of an eclogitic crustal root.

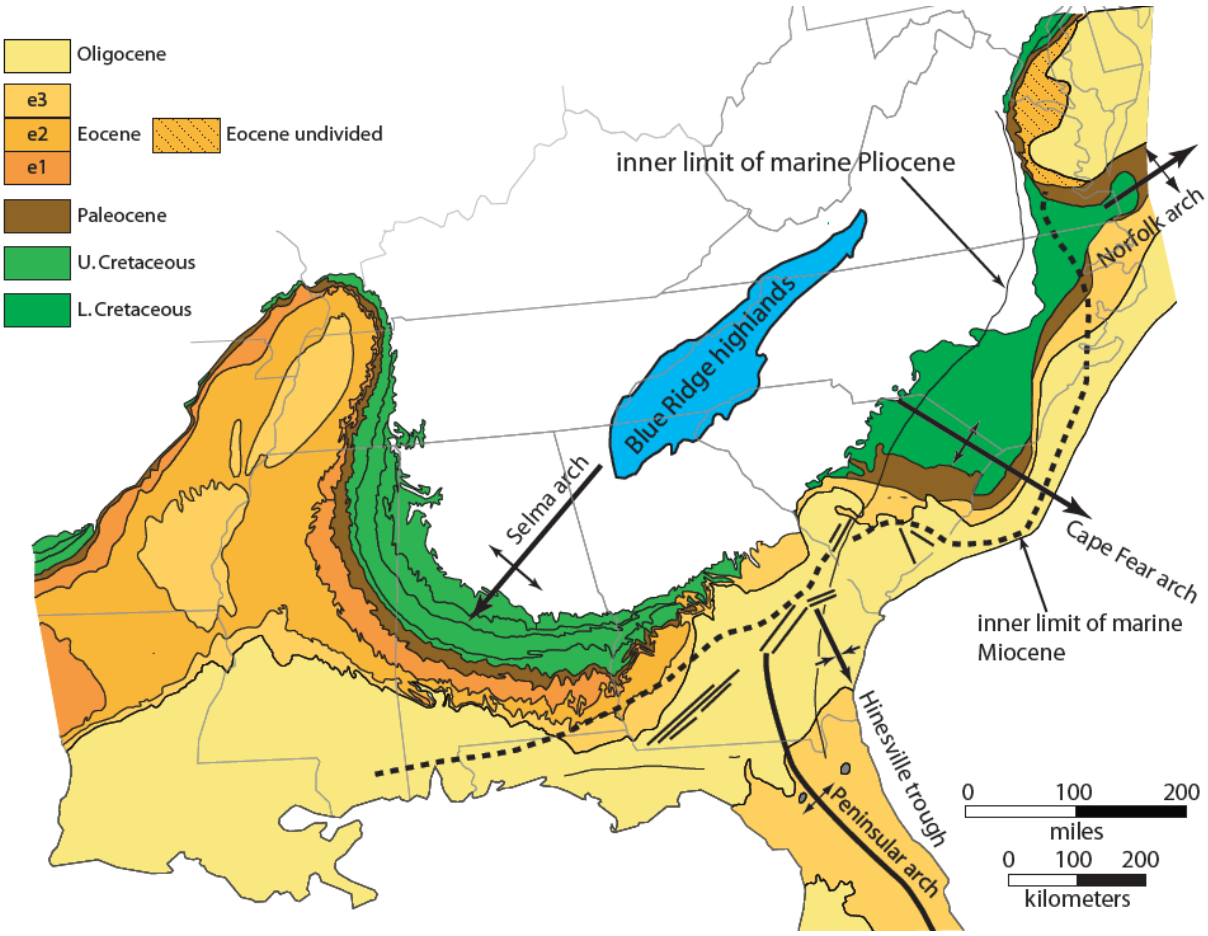

Figure 3.2: Map of structural arches across the southeastern US likely associated with Cenozoic uplift. Note the folded Cretaceous rocks unconformably overlain by Paleocene strata. There are also pinching out of the folded Oligocene and Eocene rocks, suggesting multiple phases of Cenozoic uplift (Stewart, 2015).

3.2 Background

3.2.1 Sedimentological evidence for Post-Paleozoic uplift

Along the eastern seaboard of North America, there is offshore-sedimentological evidence that the mountain range has experienced multiple episodes of Mesozoic and Cenozoic topographic rejuvenation (e.g. Poag and Savon, 1989; Pazzaglia and Brandon, 1996). Although the Appalachians likely had 3.5-4.5 km of average relief by the end of the Alleghanian orogeny (Slingerland and Furlong, 1989), the post-Paleozoic story is not simply erosion wearing down the orogen to its current form. Poag and Savon (1989) showed that increased Atlantic sedimentation occurred in five pulses during the Middle Jurassic, the Early and Late Cretaceous, the Middle Miocene, and in the Quaternary. The grain sizes of sediments deposited in the Gulf of Mexico increased during the Middle Miocene (Galloway et al., 2011). Increased sedimentation and grain size in the Middle Miocene is likely the result of regional uplift that contributed material to streams draining to both the east and west of the continental divide (Gallen et al., 2013). There is also evidence of late Cenozoic uplift of the mountain belt found in continental sedimentary records. In the Coastal Plain of South Carolina, Miocene coarse-grained conglomerates contain clasts from the Blue Ridge and Piedmont provinces (Nystrom, 1986). In southern Florida, coarse-grained Miocene rocks contain metamorphic clasts up to 5cm that likely traveled over 700 km from their source (Missimer et al., 2014).

3.2.2 Stratigraphic evidence for Post-Paleozoic arching

Multiple phases of Cenozoic deformation have been recorded in the stratigraphy of the Coastal Plain. Stewart (2015) presented evidence for uplift in the Paleocene and the Miocene at the southern terminus of the mountains as the Selma arch, where Eocene rocks lie unconformably above folded Cretaceous and Paleocene units, and flat-lying Miocene rocks are above folded

Oligocene sedimentary layers (Figure 3.2). In southern Florida, Maliva et al. (2006) used drill-core records to show up to 100m of arching of Middle Miocene rocks covered by Late Miocene and Early Pliocene rocks. Near the fall line of eastern North Carolina and southern Virginia, faults offset Miocene and older strata but are crossed by late Miocene rocks, indicating vertical motion around 8 Ma (Weems et al., 2009). Rowley et al. (2013) interpreted folded topographic scarps in the Coastal Plain as previously horizontal Atlantic shorelines that warped around 3.5 Ma and now have at least 60 m of elevation variation. The Cape Fear arch is a prominent feature with stratigraphic evidence of uplift ranging from the late Mesozoic through the late Cenozoic (e.g. Popenoe, 1985; Soller, 1988; Gardner, 1989; Ward et al, 1991) including into the modern day (Van de Plassche et al, 2014).

3.2.3 Geomorphic evidence for a landscape out of equilibrium

When a landscape is uplifted, the streams draining away from it preserve a record of base level change in the form of knickpoints, or slope breaks along the river profiles (e.g. Whipple and Tucker, 1999). These geomorphic indicators can be used to estimate the timing and magnitude of uplift. These estimates are derived from reconstructed longitudinal river profiles that contain knickpoints and separate active landscapes downstream from relict, uplifted surfaces upstream. In the southern and central Appalachians, many streams with knickpoints are actively eroding high and flat surfaces interpreted as uplifted floodplains by Hack (1982). In western North Carolina, Gallen et al. (2013) used knickpoint locations above the stream mouth and erosion rates to calculate that the knickpoints along the Cullasaja River and its tributaries initiated ~8.5 Ma in response to ~480m of base level change associated with epeirogenic uplift of the Appalachians. In our previous work (Hill, 2013), we studied the Santeetlah Creek basin, which is close to the Cullasaja River and also contains a series of knickpoints separating a high plateau upstream from steep rivers

downstream. We estimated that the Santeetlah Creek knickpoints are migrating upstream in response to as much as 750 m of uplift, and based on similarities in geometry, general proximity, and a common local base level to the Cullasaja, we interpreted these knickpoints to also have initiated in the Miocene (see Ch. 1 of this dissertation for a detailed discussion of these knickpoints). In a study of the Susquehanna River in Pennsylvania, Miller et al. (2013) showed that a series of knickpoints are migrating upstream in response to ~150m of uplift that began between 3.5-15 Ma. They also used cosmogenic isotopes to calculate erosion rates upstream and downstream of knickpoints and found that erosion is much greater downstream. The fore-mentioned knickpoints in North Carolina are along streams draining to the Gulf of Mexico from high surfaces in the Blue Ridge province, while those in Pennsylvania are draining from the Appalachian Plateau towards the Atlantic Ocean, suggesting that landscapes on both sides of the continental divide are out of equilibrium.

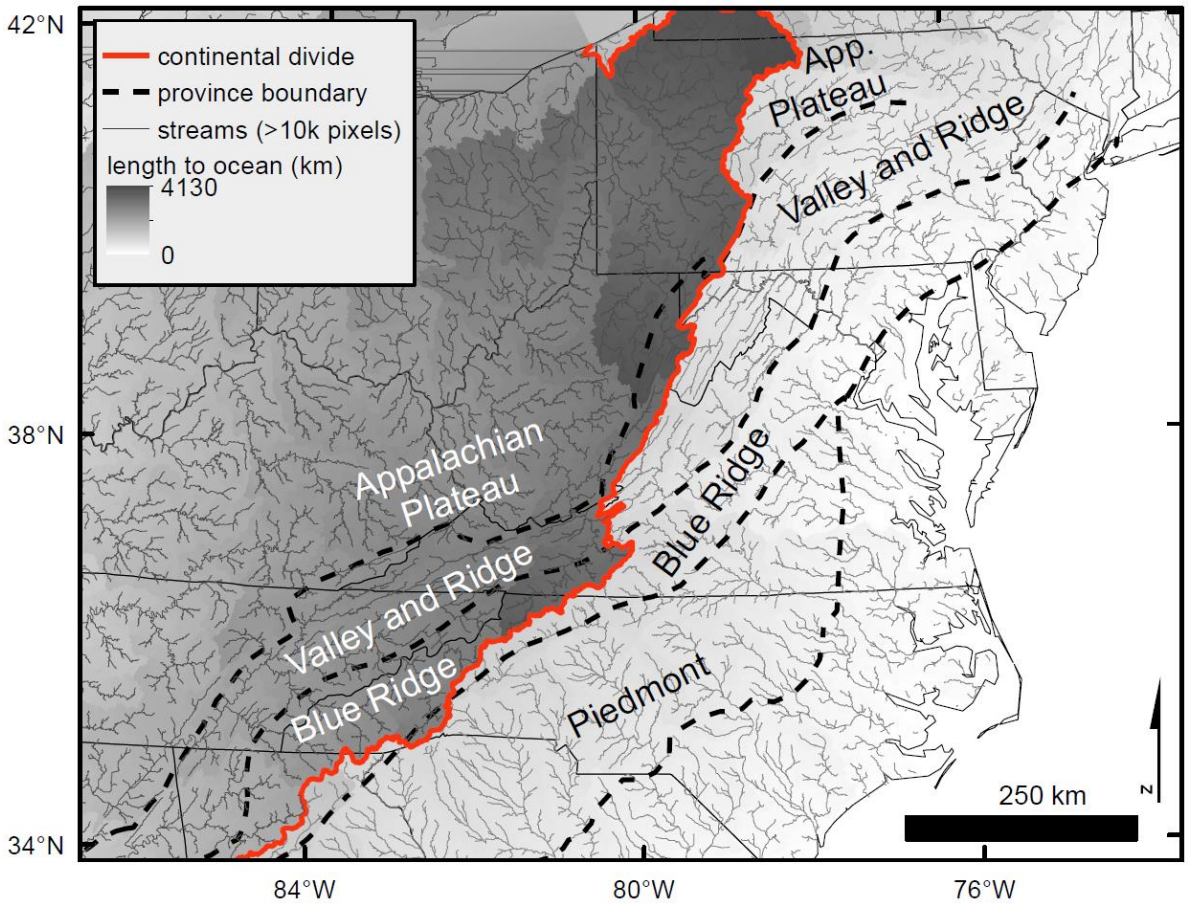

Figure 3.3: Stream length map showing the eastern continental divide (red line) crossing the geologic province boundaries (black dashes). The grey lines are streams with drainage areas greater than 10,000 pixels (84.6 km^2).

Low-temperature geochronology can be used to estimate the timing and rates of exhumation based on (U-Th)/He ratios and annealing of fission tracks in apatite grains (e.g. Green et al., 1986; Boettcher and Milliken, 1994; Flowers et al., 2007). In a low-temperature geochronology study of the southern and central Appalachians, McKeon et al. (2014) analyzed samples from hilltops and valleys, and postulated that relief was increased during the Cretaceous, when valleys were eroded at nearly twice the rate of the surrounding hilltops. In their study, they found no record of Miocene uplift but recognized a mismatch between their results and the increase in offshore sedimentation during the Miocene (Poag and Savon, 1989). They also noted that the magnitude of Cenozoic erosion may have not been great enough to leave a cooling record in the

low-temperature geochronology. Work by Naeser et al. (2004) in the Smoky Mountains used zircon and apatite fission-track thermochronology to show that denudation rates have been slow and steady since the Late Cretaceous. The lack of agreement between these low-temperature studies and the abundance of sedimentological and stratigraphic evidence for Miocene uplift may indicate the amount exhumation was less than 1 km, which is the approximate minimum required to expose the partial annealing zone and expose rocks that contain a low-temperature record (McKeon et al., 2014). However, in an earlier apatite fission track study of Pennsylvanian sandstones from the central Appalachian Valley and Ridge, Boettcher and Milliken (1994) estimated erosional unroofing of 2.3 km from 140-80 Ma, 0.4 km from 80-20 Ma, and 1.5 km from 20 Ma to the present.

Relief can be enhanced when drainage divides migrate and capture the headwaters of adjacent watersheds, which some authors have attributed as a driver of topography in the Appalachians. Previous authors proposed that the eastern continental divide has migrated westward due to capture of the previously westward-draining streams by the headwaters of those currently feeding into the Atlantic (Pazzaglia and Brandon, 1996; Spotila et al., 2004). This process may have happened as punctuated events rather than a steady retreat of the divide (Prince et al., 2010; Prince et al., 2011). Streams that once flowed to the Atlantic may also have been captured by westward-draining ones during a rearrangement of headwaters due to variability of bedrock strength, a process recently attributed the generation of up to 150 m of incision in southwestern North Carolina (Gallen, 2018). It appears that stream capture is a process that can affect river systems and landscapes on both sides of the continental divide.

3.2.4 Young faults and other brittle structures in the Southern and Central Appalachians

The Appalachians generally trend NE-SW, but there are topographic lineaments that cross the orogen and are clearly post-Alleghanian. These features were described by Hack (1982) as what he called 'trench valleys' with minor offsets due to faults and intense fracturing. There are three main families of lineaments that trend E-W, WNW-ESE, and N-S (Gay, 2000), and they have been interpreted to be the result of upper crustal extension due to regional doming (Dennison and Stewart, 2001; Stewart and Dennison, 2006). The orientation of fractures and minor faults is parallel to the general trend of these features, indicating that these post-Alleghanian structures are fracture controlled, and contain dip-slip faults and hot springs (Hill, 2013). There have been numerous earthquake swarms within the lineaments of North Carolina, and it appears that there may be modern motion along some of these features (see Ch. 2 of this dissertation for a more detailed discussion). In northwestern North Carolina and eastern Tennessee, there is a WNW-trending lineament that spans over 250 km. There is a WNW-striking, high-angle fault zone we are calling the Boone fault that contains minor dip-slip faults associated with south-side-up motion of the Grandfather Mountain window (see Ch. 2 for a detailed discussion). Based on a paleostress inversion of these faults, the shapes of streams draining into the fault zone, and modern seismicity, we interpret the Boone fault as a Cenozoic fault zone.

In the Pennsylvania Blue Ridge, there is a 120 km long E-W lineament at 40° N that contains a series of steeply-dipping, E-W normal faults in a 15 km wide zone called the Transylvania fault (Root and Hoskins, 1977). The strike of the fault zone changes from 270° to 290° as it crosses into the Valley and Ridge and into the Appalachian Plateau. Although there is no mapped surface expression in the Appalachian Plateau, the WNW lineament is evident in the topography and has been mapped in the subsurface where a vertical structural discontinuity truncates aeromagnetic signals and correlates with the boundary of oil and gas deposits (Wagner

and Lytle, 1976). Some workers interpreted this feature as an Alleghanian lateral thrust ramp (Dodson and Thomas, 2008). However, Root and Hoskins (1977) noted that the Transylvanian fault offsets the bounding faults of the Triassic Gettysburg Basin, but gave no evidence for age of faulting other than post-Triassic.

3.2.5 Previous interpretations of a delamination underneath a passive margin

In seismic studies of the lower crust and upper mantle of the eastern United States, some workers have postulated that lithospheric delamination may have influenced the vertical position of the crust. Wagner et al. (2012) deployed seismic stations aligned in a WNW trend across the Blue Ridge and Piedmont and used receiver functions to build an image of the lithosphere underneath northwestern North Carolina. They found abrupt changes in seismic velocities at ~45 and ~60 km depth underneath the Piedmont, which they interpreted as a doubled Moho as a result of tectonic wedging underneath the Laurentian lithosphere. They proposed that the doubled Moho under the Piedmont could contribute to low topography, and the lack of this feature under the higher-elevation Blue Ridge could be evidence of delamination that drove uplift. Wagner et al. (2012) proposed that the Piedmont may being held down by a dense root and the adjacent Blue Ridge may owe its higher elevation to uplift associated with the loss of the crustal root. They also imaged a seismic discontinuity at ~100 km depth, which they interpreted as the boundary of a possible accreted fossil slab. In a more regionally extensive study, Biryol et al. (2016) used earthquake data collected by the EarthScope transportable array and the SESAME project to build a tomographic model of p-wave perturbations in the lithosphere and upper mantle ranging from 36 to 915 km depth. They showed numerous seismic anomalies in the tomographic model and found seismically fast, dense pieces of lithospheric material that appear to be foundering. As the pieces of continental lithosphere descend, they are being replaced by hot, seismically slow material.

Biryol et al. (2016) proposed that delamination of the crustal root and replacement by more buoyant mantle material may be the cause of intraplate seismicity, volcanism, and uplift.

Moucha et al. (2008) produced mantle flow simulations to show that vertical movement of mantle material could have driven up to 100 m of dynamic topography in the past 30 million years and that the Coastal Plain of the eastern United States should not be considered a stable continental platform. In a different numerical uplift simulation of dynamic topography from the mid-continent to the coast, Liu (2014) presented a model based on subsidence of the Mississippi River valley and the Atlantic shelf that could have driven uplift of the mountain range. Liu speculated that subsidence-driven vertical flexure of the lithosphere caused differential erosion, which in turn could have generated up to 400 m of relief and 200 m of elevation change of the southern Appalachians during the Miocene.

3.3 Methods

3.3.1 Topographic and geomorphic maps

To build a regional digital elevation model (DEM), we downloaded 3-arc-second HydroSHEDS (~92 m resolution) void-filled elevation data tiles (https://hydrosheds.cr.usgs.gov/dataavail.php) and merged them together in ArcMap 10.5 with the mosaic tool (Figure 3.1). We traced the boundaries between the four major geologic provinces from a regional lithotectonic map (Hibbard et al., 2006). We used this DEM and the hydrology tools in ArcMap to produce flow direction, flow accumulation, and flow length raster files. We used the hydrology raster files to determine the watersheds and to delineate the eastern continental divide (Figure 3.3). With the HydroSHEDS mosaic DEM, we produced geomorphic maps to compare with the major geologic provinces along the orogen, using the standard toolbox in ArcMap 10.5 and the geomorphic metrics as described at http://gis4geomorphology.com/basin-basics-i/. Before making these maps, we smoothed the DEM with the filter tool, found in the spatial analyst toolbox, using a low-pass filter, which traverses a 3x3 moving window over the DEM and reassigns the average value of the window to each center pixel. With the filtered DEM, we made a map of local relief (Figure 3.4), which differs from relief in that the size of the sampled area to determine the highest and lowest elevation is smaller (our sampling window was 1,390 m x 1,390 m). High local relief values can indicate areas that are responding to uplift and/or incision (Anhert, 1984), especially in a passive margin setting (Summerfield, 1991). To calculate local relief, we used the ArcMap focal statistics tool with a 15x15 pixel rectangular window and a range operator. The local relief map allowed us to qualitatively look for patterns along strike of the major geologic provinces, and to quantify the shape of the topography with increasing latitude. To assess any changes along strike of the orogen, we separated the map into five bands of ~1.5°

latitude, and then split each band by geologic province. This analysis yielded 19 zones, because the Piedmont province is not present on the continent at the highest latitudes of our study area.

There are some areas of the southern and central Appalachians that are steepest at the highest elevation, but other high-elevation areas that are relatively flat and have been interpreted as relict low-elevation landscapes that have been uplifted to their current position (Hack, 1982; Gallen et al, 2013; Hill, 2013). To distinguish between these two end-members of high topography, we produced a map that incorporates both elevation and slope into a single image and are calling it a binary-slope map (Figure 3.5). To construct this map, we first used the HydroSHEDS mosaic DEM to produce a slope map, in degrees. We then used the raster calculator tool to select all pixels that are above 750 m elevation and separate them into those greater than or less than 10 degrees slope. This process separated high peaks from high plateaus in order to determine the locations of any previously unrecognized relict topography.

3.3.2 Comparison of topography with structures in the lower crust and upper mantle

To test if the Appalachian high topography can be linked to delamination of the continental lithosphere, we compared the topographic, local relief, and binary slope-maps to results from seismic studies of the lower crust and upper mantle (Wagner et al., 2012; Biryol et al., 2016). To do this, we input the latitude, longitude, and depth values from the Biryol et al. model into ArcMap and interpolated 20 tomographic slices ranging from 36 to 915 km depth with the kriging tool in the spatial analyst toolbox. Our aim is to test whether the F5 anomaly presented in the Biryol et al. (2016) paper is spatially correlated to the swath of high topography crossing from the Blue Ridge to the Appalachian Plateau with increasing latitude. The F5 anomaly is present at 130 km depth in the North Carolina Blue Ridge, at 165km depth in the North Carolina Blue Ridge and Virginia Valley and Ridge, evident at 200 km depth under the Virginia Valley and Ridge, and

fairly continuous at 240 km depth. At 280 km depth, it is present only under the Appalachian Plateau of West Virginia. The center of the fast-seismic anomaly at question is most evident at ~240 km depth, so we overlaid topographic contours corresponding with elevations higher than 750 m (at 300 m intervals) extracted from the smoothed HydroSHEDS DEM onto a tomographic slice at that depth (Figure 3.6A). Next, we produced a cross-section from the tomographic model along the line Y-Y'-Y", which follows the high topography and makes a slight bend near the middle of the section line (Figure 3.6B).

The comparison of the topography and the tomography allowed us to test for a spatial correlation but did not allow investigation for a causal link. Wagner et al. (2012) interpreted seismic discontinuities at ~45 and 60 km depth as a doubled Moho under the Piedmont of western North Carolina and the result of underplating of a Grenville eclogitic root due to wedging of an accreted terrane during the assembly of Pangea. This piece of high-density material is present under the Piedmont but missing from the high-elevation Blue Ridge. To test the hypothesis that delamination of this ~15 km block of lithospheric root could have driven uplift we estimated the magnitude of uplift expected if it were replaced by less-dense, more buoyant mantle material. We replaced a 15 km thick block with a density of 3.4 g/cm³ (approximate density of eclogite) with material with a density of 3.3 g/cm³ (approximate estimate of upper mantle) and calculated the expected change in elevation. We estimated a 50 km thick crust with a density of 2.77 g/cm³. We then compared this change in elevation with the amounts of uplift proposed in previous geomorphic studies (~480m from Gallen et al., 2013; ~750 m from Hill, 2013) where knickpoints were used to project the relict landscapes above current river mouths as estimates of base level change.

The study by Wagner et al. (2012) was limited to one section line across high topography of western North Carolina, but we were curious how the crustal thickness compared to the

topography across our entire study area. To do this, we used a crustal thickness model that was compiled from multiple seismic studies (Cook et al., 1979; Cook and Vasudevan, 2006; Hawman, 2008; French et al., 2009; Abt et al., 2010; Moidaki et al., 2010; Hawman et al., 2012; Wagner et al., 2012; and Parker et al., 2013) and presented in the supplemental material of Biryol et al. (2016). We added the latitude, longitude, and depth to Moho from this model into ArcMap and made an interpolation with the kriging tool, then added topographic contours from the HydroSHEDS DEM (Figure 3.7). We then split the crustal thickness map into the same 5 latitudinal zones separated by geological province from which we extracted the geomorphic data. For each zone we determined the maximum and mean crustal thickness and compared those values to the elevation for each zone (Figures 3.8 and 3.9).

Lastly, we wanted to investigate whether our study area is at isostatic equilibrium, based on the crustal thickness model and the current topography. We calculated the predicted elevation for a crust with a density of 2.77 g/cm^3 and anchored our model at the thinnest crust and lowest elevation of our study area, which is at the coast where the mean crustal thickness = ~34 km and elevation = 0 m (Figure 3.8). We then calculated the predicated elevation of each zone and compared these estimates to the observed data to test for isostatic equilibrium (Figure 3.9).

3.4 Results

3.4.1 Topographic and geomorphic maps

The elevation, binary slope, and local relief maps we produced show a lack of consistency along the orogen in all of the major geologic provinces (Figures 3.1, 3.4, & 3.5; table 1 in the appendix). The local relief map (Figure 3.4) has high values in the same zones that have high elevation (Figure 3.1), but also shows high local relief in the Appalachian Plateau of Kentucky and West Virginia (zones AP3 & AP4) and in the Piedmont of NC (PI2). It appears that even though the streams draining from these areas have a long path to the Gulf of Mexico (Figure 3.3), they are experiencing incision and a roughening of the topography. The binary slope map highlights contrasting topographic styles of the high elevation areas (Figure 3.5). There are flat highlands in southern North Carolina where previous studies have shown flights of knickpoints separating active landscapes from relict ones upstream (Gallen et al.; Hill, 2013; Ch. 1 of this dissertation). There are steep highlands in central North Carolina that transition back to flat areas for the remainder of the Blue Ridge province along strike to the north until southwestern Virginia, where the elevation of the Blue Ridge drops quickly. As the high elevation crosses into Virginia and West Virginia, the topographic style is mixed as far as northern West Virginia, where there is a stark change to a uniformly flat highland landscape, even though the underlying lithology is constant.

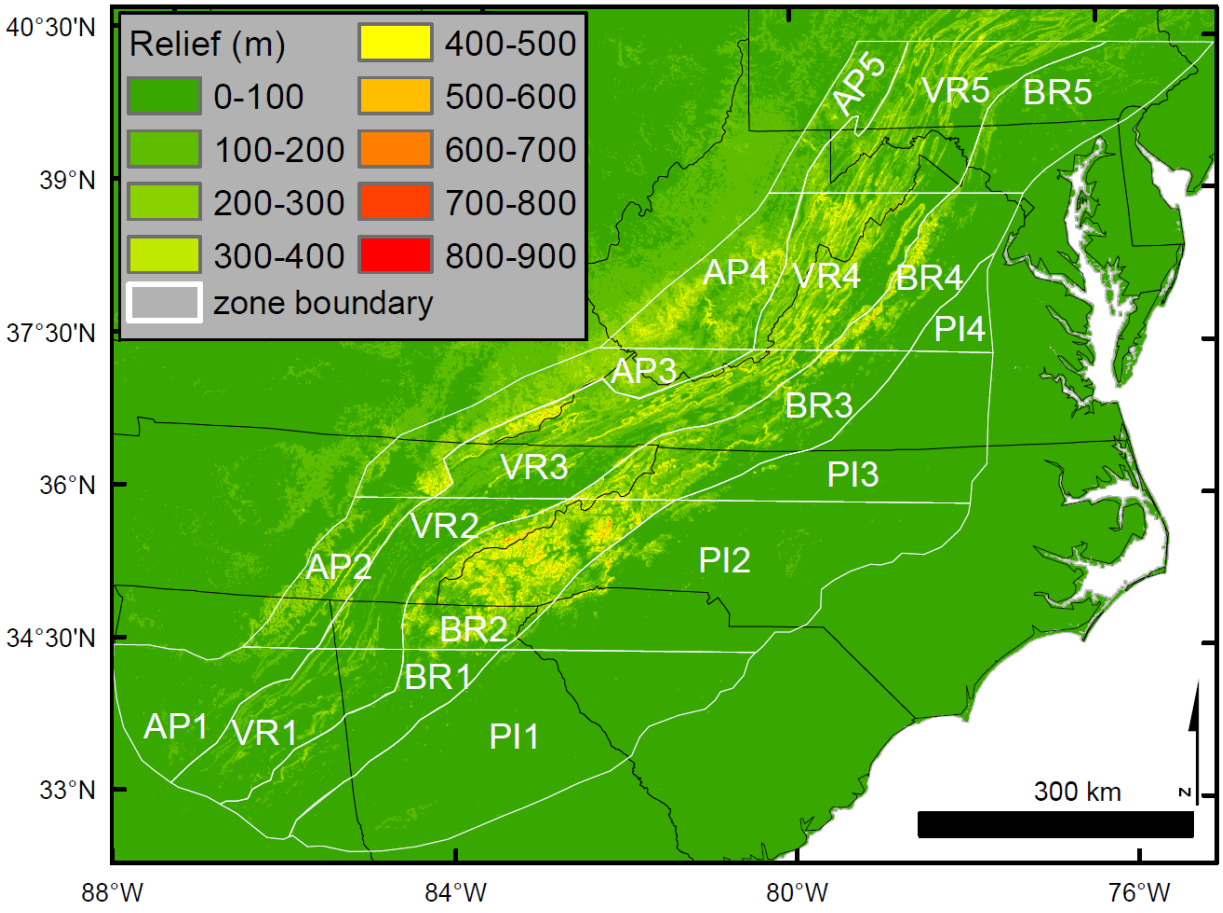

Figure 3.4: Local relief map calculated with a 15x15-pixel moving window (1,390 m x 1,390 m) that finds the range and reassigns the relief to each point. Note how the areas of high local relief do not match the geologic provinces but do fit reasonably well with the swath of high topography and the slow-seismic anomaly. The Appalachian Plateau of Virginia and West Virginia has high local relief that extends further west than the high topography.

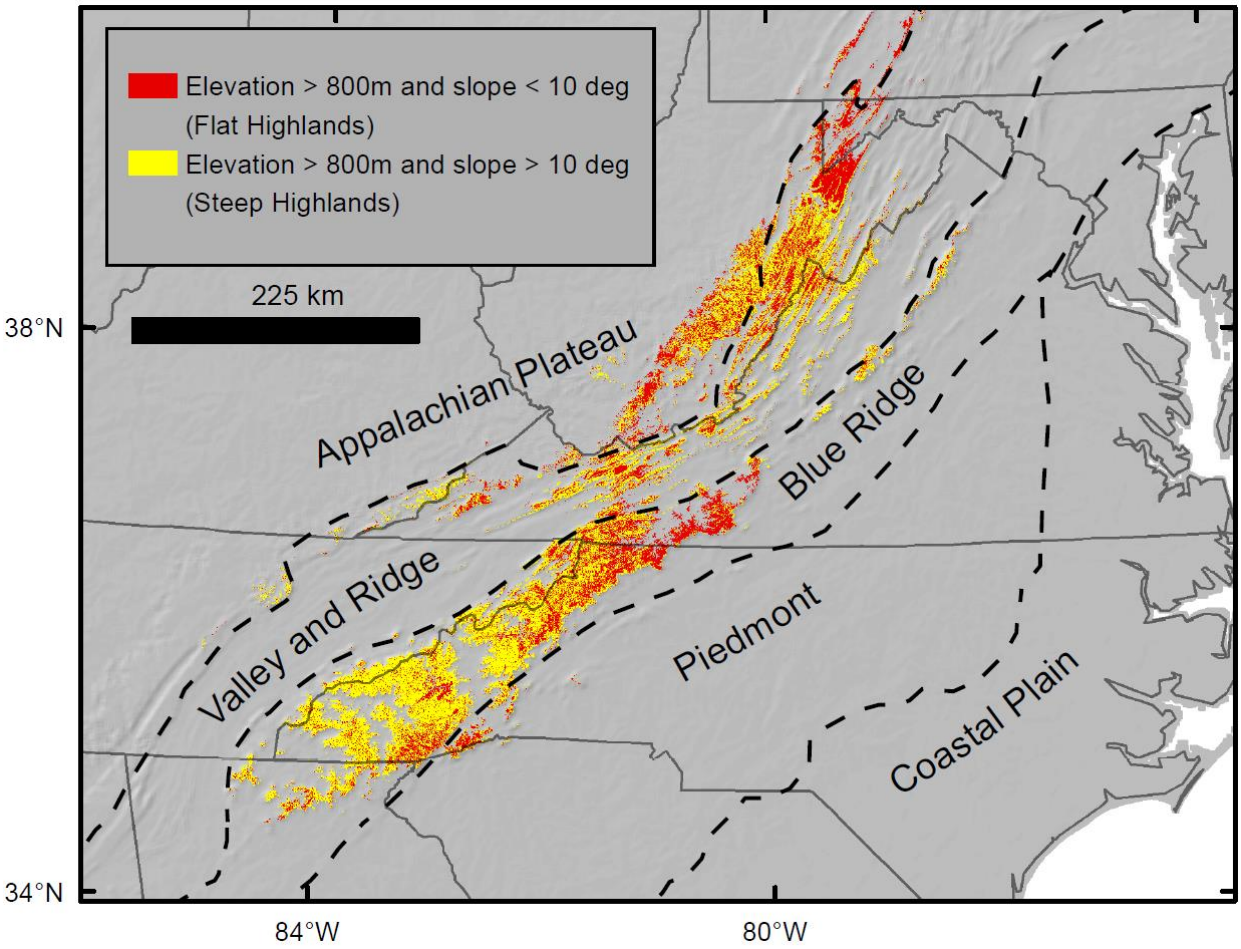

Figure 3.5: Binary-slope map emphasizing high peaks and high plateaus. It shows all pixels above 800 m separated by slope greater than 10° (yellow) and less than 10° (red). Note how the topographic style changes from dominantly high peaks in the south to mostly high plateaus in the north.

3.4.2 Seismic tomography, crustal thickness map, and isostacy calculations

The topographic contours from the HydroSHEDS DEM have a strong positive spatial correlation to the fast anomaly in the seismic tomography slice at 240 km depth (Figure 3.6A). Although the topography and the tomography appear to match, neither follow any of the major geologic provinces. The tomographic cross section Y-Y'-Y", which follows the high topography, shows a fast anomaly underneath a slow section of upper mantle and crust (Figure 3.6B). The top of the fast anomaly starts at ~100 km depth, which is consistent with the lowest seismic discontinuity imaged in the profiles of Wagner et al. (2012). Based on the distance between the doubled Moho discontinuities they presented, we calculated the expected uplift for delamination of 15 km and 25 km thick eclogitic layers, which resulted in 450 m and 750 m, accordingly.

When we combined the elevation contours with the crustal thickness map (Figure 3.7), only one zone of high topography overlies thick crust. With the exception of zone BR2, there are discrepancies between the amount of elevation and the thickness of crust in most of the study area. Surprisingly, the thickest crust is in the lowest latitude zone, where the topography is relatively low. As evident in Figures 3.8 and 3.9, all of the zones in our study area have lower mean elevations than expected for the amount of crustal thickness if there was isostatic equilibrium. Crustal thickness decreases from zone 2 to zone 4, then increases again in zone 5. This increase coincides with the edge of the fast-seismic anomaly evident in the tomography cross section Y-Y'-Y" (Figure 3.6) and is close to the 40° N latitude Transylvania fault zone (Root and Hoskins, 1977).

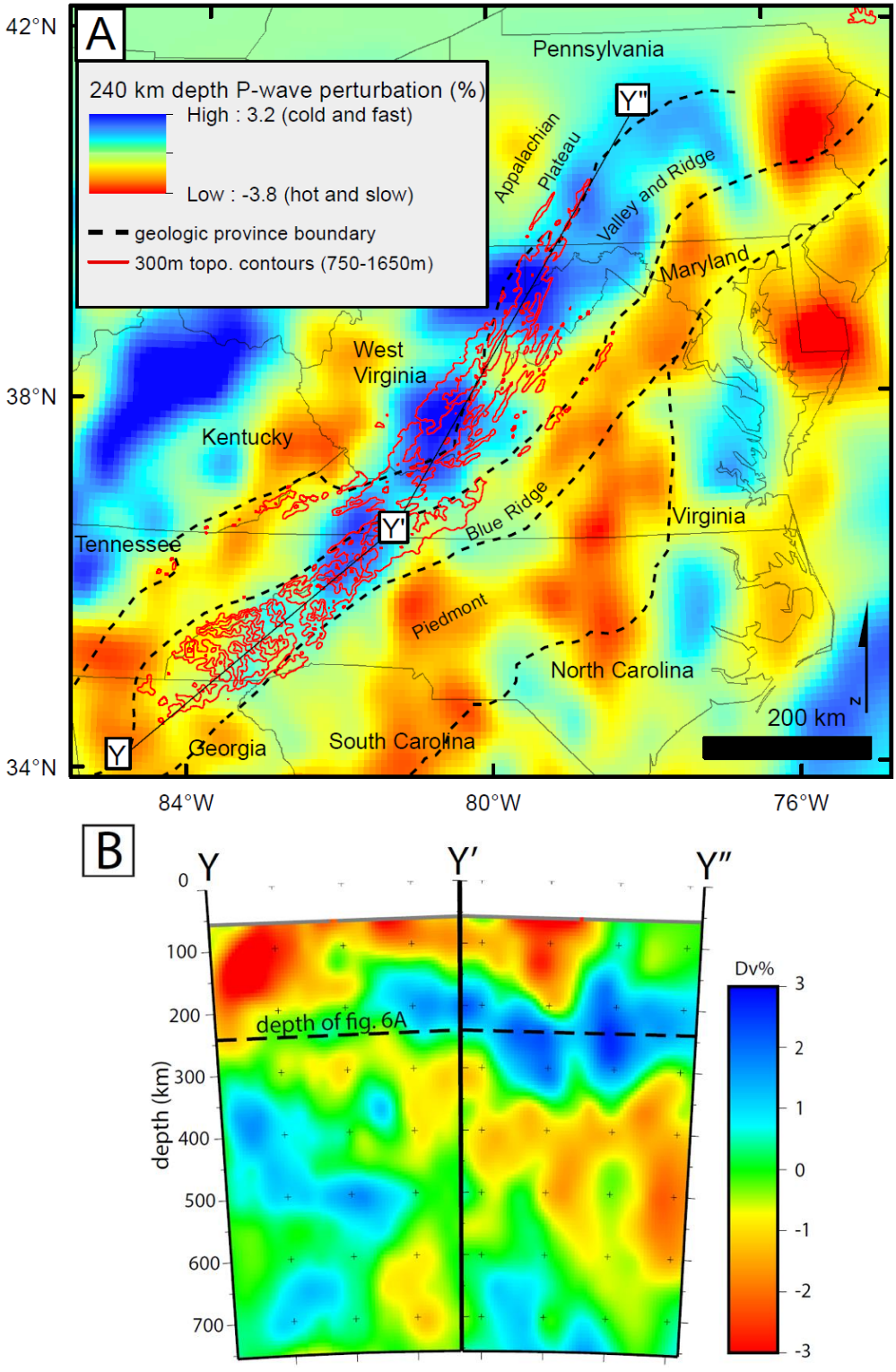

Figure 3.6: (A)Tomographic model showing p-wave perturbations at 240 km depth. The blue zones are cold rocks that speed up the p-waves and the red zones are hot rocks that slow down the waves. Note the large fast anomaly that matches the swath of high topography but does not fit the geologic provinces or the mountain belt as a whole, likely a drip structure associated with

lithospheric delamination (Data from Biryol et al., 2016). (B) Cross section through the large fast-seismic anomaly (Y-Y'-Y"). Dashed line is the depth of the slice shown in part A.

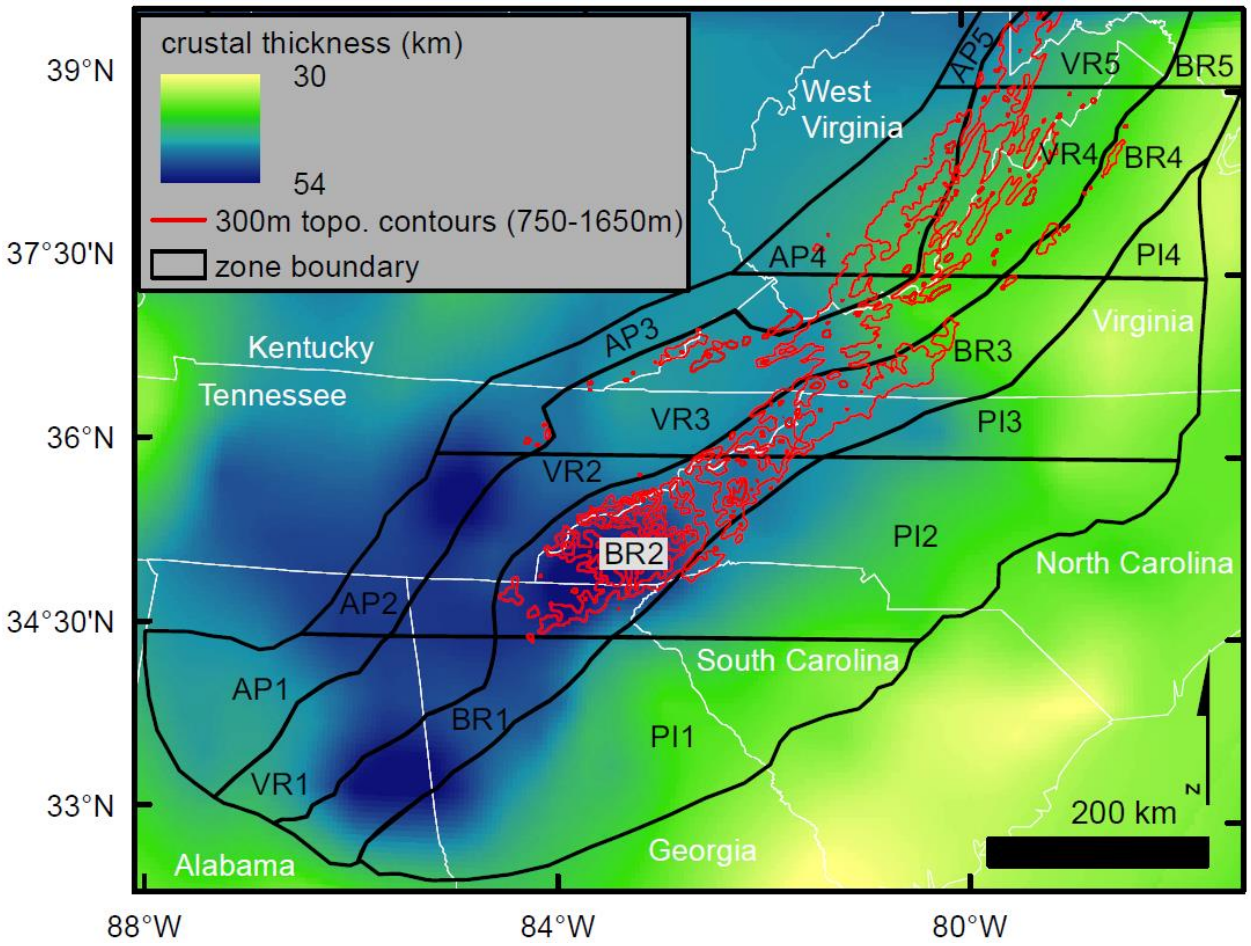

Figure 3.7: Map of crustal thickness with topographic contours overlain as red lines (Data from Biryol et al., 2016). There is not a strong correlation between thick crust and high elevation, except for in zone BR2. Note the thickened crust in BR1 and AP2 in the southern part of the image, where there is no topography above 750 m. The crustal thickness values were extracted from each zone and shown in Figures 3.8 and 3.9.

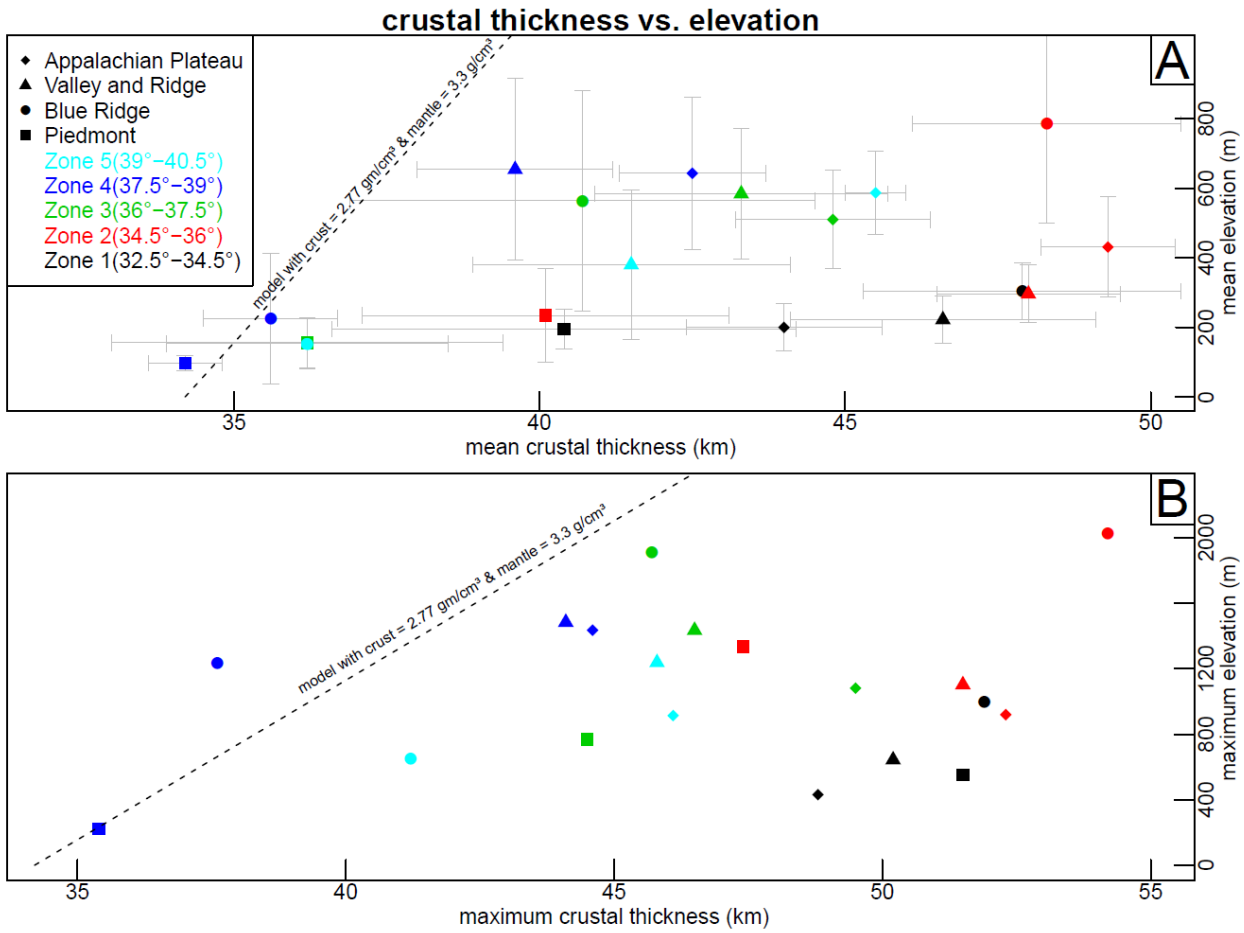

Figure 3.8: (A) Mean crustal thickness in km vs. mean elevation in m. The gray bars show one standard deviation from the mean. Each zone is indicated by color and each geologic province by symbol shape. The dashed line indicates the expected elevation at isostatic equilibrium, based on the thinnest crust at sea level. With the exception of the Piedmont in zone 4, all zones are overcompensated isostatically. (B) Maximum crustal thickness in km vs. maximum elevation in m for each zone. All zones except the Blue Ridge of zone 4 are overcompensated.

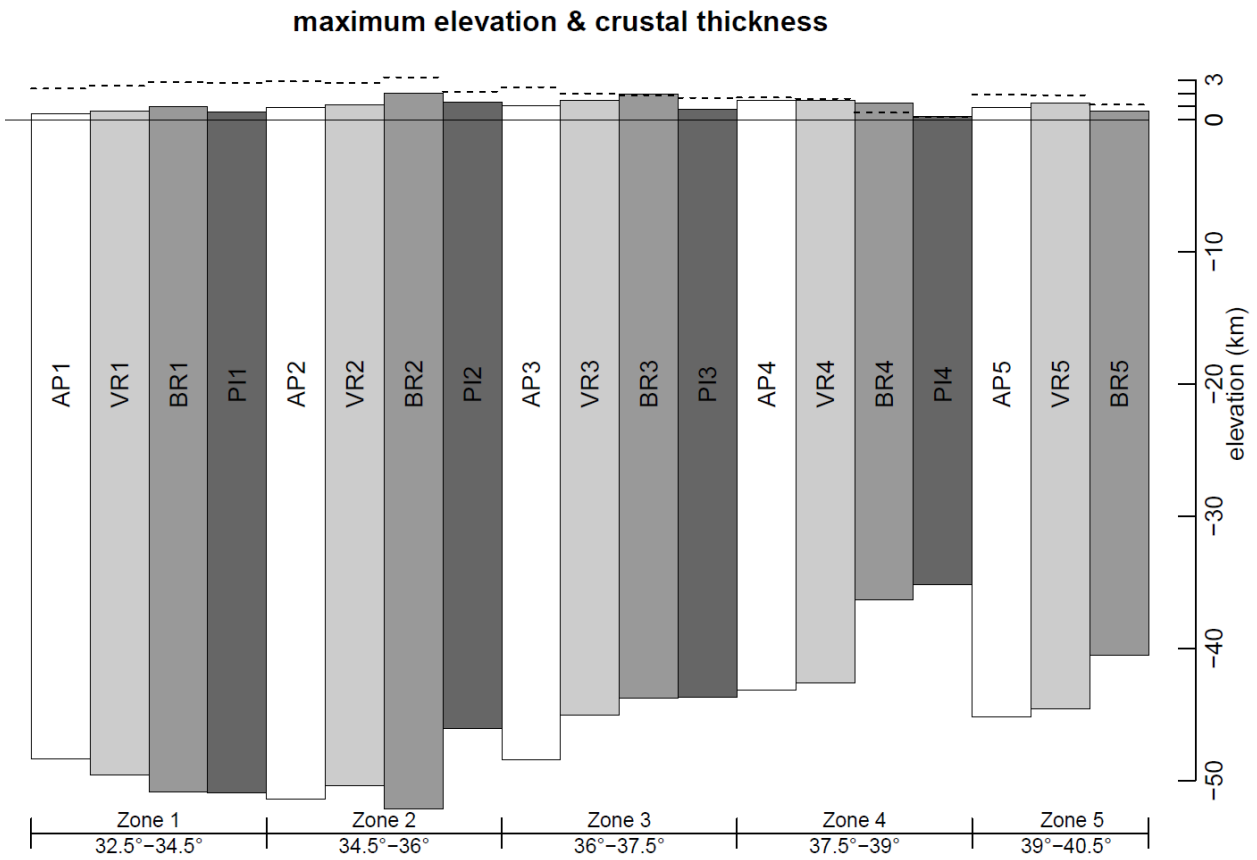

Figure 3.9: Model showing observed crustal thicknesses from each zone in Figure 3.7 with elevation data extracted from the HydroSHEDS DEM. The dashed lines show the expected elevation for each crustal thickness at a state of isostatic equilibrium. Note the decreasing crustal thickness from zone 2 to zone 4, then the sudden increase at zone 5. This increase coincides with the northern edge of the fast-seismic anomaly in Figure 3.6.

3.5 Discussion

It is evident that the topography of the southern and central Appalachians cannot be explained simply as a product of the underlying crustal geology, as there are major discrepancies in elevation, local relief, and type of highlands along the length of all the major geologic provinces. We have shown here that there is a much stronger spatial correlation between the high topography and the proposed delamination structure seen at 240 km depth in the seismic tomography model than between the topography and lithology. Our estimates of 450 -750m of uplift that would result from delamination of a dense lithospheric root are consistent with the amounts of uplift proposed by previous geomorphic studies by us and others (Gallen et al., 2013; Hill, 2013). Although stream capture may have contributed to some relief generation in the Appalachians, it is our interpretation that delamination and the subsequent replacement by more buoyant, less dense mantle material has driven regional-scale uplift. Rather than a broad and uniform arching along strike of the orogen, the uplift was more likely blocky and accommodated by vertical movement along the topographic lineaments. This interpretation could explain the existence of the lineaments, as well as the dip-slip, high angle fault zones we have mapped within them, and the contrasting highland topography seen in the binary-slope map. Many of the knickpoints that have been observed in the southern Appalachians are along streams that drain into lineaments, and in many places there are stark contrasts of topographic style across these linear features (Hack, 1982; Hill, 2013).

The crustal thickness compared to the topography across our study area indicates that the southern and central Appalachians are isostatically overcompensated and need to continue to move upwards to approach equilibrium (Figures 3.8 and 3.9). This observation argues against the idea that this passive margin is simply a result erosion of the mountains after the Paleozoic collisional events and supports our claim that the rejuvenation of topography is attributed to Late Cenozoic mantle dynamics. Other authors have proposed a heterogeneous crustal root with varying

mechanical properties along strike of the Appalachians, which is consistent with our findings (e.g. Stewart and Watts, 1997).

Delamination of lithospheric roots has been attributed to uplift in other mountain ranges at margins that are no longer active (e.g. Ducea, 2011), such as the Sierra Nevada in California (e.g. Zandt et al., 2004), the European Alpine Belt (De Boorder et al., 1998), or the Carpathian Mountains of Romania (Girbacea and Frisch, 1998; Fillerup et al., 2010). One obvious difference between these locations and the Appalachians is the greater amount of time that has passed between when subduction was active and when the delamination occurred. To resolve this temporal issue, we propose that the delamination of the lithospheric root that we are attributing to Miocene Appalachian rejuvenation was likely not the first foundering event since the Paleozoic. It is possible that the Cretaceous uplift event that is evident in sedimentary records and low-temperature studies was also driven by delamination of the lithosphere. If the crustal root was assembled during multiple events, it is plausible that it may have fallen apart in a piecemeal fashion.

3.6 Conclusions

Although the bedrock in the Appalachians is undoubtedly very old, we propose that the topography of the mountain range is much younger. There is a clear mismatch between lithology and elevation on a regional scale, but a strong spatial correlation exists between the high elevation and the location of a foundering lithospheric root currently between 100 and 280 km depth. Our calculations of the uplift expected by removal of a 15-25 km thick, dense root are consistent with observed geomorphic estimates and support a causal link between the dynamic mantle and Cenozoic rejuvenation of topography. By comparing the thickness of crust and topography across 19 zones in our study area, we have shown that the Appalachians are overcompensated isostatically and are still responding to a vertical readjustment due to lithospheric foundering.

REFERENCES

1. Abt, D. L., 2010, Fischer, K. M., French, S. W., Ford, H. A., Yuan H. Y., and Romanowicz, B., North American lithospheric discontinuity structure imaged by Ps and Sp receiver functions; Journal of Geophysical Research, v. 115

2. Anhert, Frank, 1984, Local relief and the height limit of mountain ranges; American Journal of Science, v. 284, p. 1035-1055

3. Bryant, B, 1970, and Reed, J.C., Geology of the Grandfather Mountain window and vicinity, North Carolina and Tennessee; United States Geological Survey Professional Paper 15, scale 1:62,500

4. Biryol, Berk C., 2016, Wagner, Lara S., Fischer, Karen M., Hawman, Robert B., Relationship between observed upper mantle structures and recent tectonic activity across the Southeastern United States; Journal of Geophysical Research Solid Earth, 121

5. Boettcher, Stefan S., 1994, and Milliken, Kitty L., Mesozoic-Cenozoic unroofing of the southern Appalachian basin: apatite fission track evidence from Middle Pennsylvanian sandstones; The Journal of Geology, v. 102, no. 6, p. 655-668

6. Burbank, Douglas W., 2012, and Anderson, Robert S., Tectonic Geomorphology – 2nd edition, Wiley-Blackwell, West Sussex, UK

7. Cook, F. A., 1979, Albaugh, D. S., Brown, L. D., Kaufman, S., Oliver, J. E., and Hatcher, R. D., Thin-skinned tectonics in the crystalline southern Appalachians: COCORP seismic-reflection profiling of the Blue Ridge and Piedmont; Geology, 7, 563–567.

8. Cook, F. A., 2006, and Vasudevan, K., Reprocessing and enhanced interpretation of the initial COCORP Southern Appalachians traverse; Tectonophysics, 420, 161–174

9. Davis, William M., 1899, The geographical cycle; Geographical Journal, v.14, no. 5, p. 481-504

10. De Boorder, H., 1998, Spakman, W., White, S.H., and Wortel, M.J.R., Late Cenozoic mineralization, orogenic collapse and slab detachment in the European Alpine Belt; Earth and Planetary Science Letters, v. 164, p. 569-575

11. Dennison, John M., 2001, and K. G. Stewart, Regional structural and stratigraphic evidence for dating Cenozoic uplift of Southern Appalachian highlands; Geological Society of America, Southeastern Section Meeting, Abstracts with Programs. Vol. 33. No. 6.

12. Dodson, Elizabeth L., 2008, and Thomas, William A., Structural geology of the Transylvania fault zone in the Appalachian thrust belt, Bedford County, Pennsylvania; Geological Society of America, Southeastern Section Meeting, Abstracts with Programs. Vol. 40. No. 2., p. 27

13. Ducea, Mihai N., 2011, Fingerprinting orogenic delamination; Geology, v. 39, no. 2, p. 191-192

14. Flowers, R.M., 2007, Schuster, D.L., Wernicke, B.P., and Farley, K.A., Radiation damage control on apatite (U-Th)/He dates from the Grand Canyon region, Colorado Plateau; Geology, v. 35, no. 5, p. 447-450

15. French, S., 2009, Fischer, K., Syracuse, E., and Wysession, M., Crustal structure beneath the Florida-to-Edmonton broadband seismometer array; Geophysical Research Letters, v 36

16. Fillerup, Melvin A., 2010, Knapp, James A., Knapp, Camelia C., and Raileanu, Victor, Mantle earthquakes in the absence of subduction? Continental delamination in the Romanian Carpathians; Lithosphere, v. 2, no. 5, p. 333-340

17. Gallen, Sean F., 2013, Wegmann, Karl W., Bohnenstiehl, DelWayne R., Miocene rejuvenation of topographic relief in the southern Appalachians; GSA Today, v. 23, no.2, p.4- 10

18. Gallen, Sean F., 2018, Lithologic controls on landscape dynamics and aquatic species evolution inpost-orogenic mountains; Earth and Planetary Science Letters, v. 493, p. 150-160

19. Galloway, William E., 2011, Whiteaker, Timothy L., and Ganey-Curry, Patricia, History of Cenozoic North American drainage basin evolution, sediment yield, and accumulation in the Gulf of Mexico basin; Geosphere, v.7, no.4, p. 938-973

20. Gardner, Thomas W., 1989, Neotectonism along the Atlantic passive continental margin: a review; Geomorphology, v. 2, p. 71-97

21. Gay, Parker S., Jr., 2000, Unmapped topographic alignments visible on 3D stereo terrain map of a 2 degrees X 2 degrees segment of the Southern Appalachians; Geological Society of America Abstracts with Programs, Southeastern Section v.32, no.2, p.19

22. Girbacea, Radu, 1998, and Frisch, Wolfgang, Slab in the wrong place: Lower lithospheric mantle delamination in the last stage of the Eastern Carpathian subduction retreat, Geology, v. 26, no. 7, p. 611-614

23. Green, P.F., 1986, Duddy, I.R., Gleadow, A.J.W., Tingate, P.R., and Laslett, G.M., Thermal annealing of fission tracks in apatite; Chemical Geology, v. 59, p. 237-253

24. Hack, John T., 1975, Dynamic equilibrium and landscape evolution, In Melhorn, W.N, and Flemal, R.C. (eds), Theories of Landform Evolution, p. 87-102

25. Hack, John T., 1982, Physiographic divisions and differential uplift in the Piedmont and Blue Ridge; United States Geological Survey Professional Paper 1265, p. 49

26. Hawman, R. B., 2008, Crustal thickness variations across the Blue Ridge Mountains, southern Appalachians: An alternative procedure for migrating wide-angle reflection data; Bulletin of the Seismological Society of America, 98, 469–475

27. Hawman, R. B., 2012, Khalifa, M. O., and Baker, M. S., Isostatic compensation for a portion of theSouthern Appalachians: Evidence from a reconnaissance study using wide-angle, three component seismic soundings, Geological Society of America Bulletin, v. 124, p. 291–317

28. Hibbard, J. P., 2006, van Staal, C.R., Rankin, D.W., and Williams, H., Lithotectonic map of theAppalachian Orogen, Canada-United States of America; Geological Survey of Canada, Map2096A, scale 1:500,000

29. Hill, Jesse S., 2013, Zoned uplift of western North Carolina bounded by topographic lineaments: M.S. Thesis, University of North Carolina at Chapel Hill, 51 p.

30. Lehner, B., 2008, Verdin, K., and Jarvis, A., New global hydrography derived from spaceborne elevation data. Eos, Transactions, American Geophysical Union, v. 89, no. 10, p 93-94.

31. Liu, Lijun, 2014, Rejuvenation of Appalachian topography caused by subsidence-induced differential erosion, Nature Geoscience, v. 7, p. 518- 523

32. Maliva, Robert G., 2006, Missimer, Thomas M., and Guo, Weixing, Structural deformation of thesouthern Florida peninsula during the Late Miocene to Early Pliocene: geophysical log evidence; Gulf Coast Association of Geological Societies Transactions, v. 56, p. 527-538.

33. McKeon, Ryan E., 2014, Zeitler, Peter K., Pazzaglia, Frank J., Idleman, Bruce D., and Enkelmann, Eva, Decay of an old orogen: Inferences about Appalachian landscape evolution from low-temperature thermochronology; Geological Society of America Bulletin, v. 126, no. 1/2, p. 31-46

34. Miller, Scott, R., 2013, Sak, Peter B., Kirby, Eric, and Bierman, Paul R., Neogene rejuvenation ofcentral Appalachian topography: Evidence for differential rock uplift from stream profiles and erosion rates; Earth and Planetary Science Letters, v. 369-370, p. 1-12

35. Missimer, Thomas M., 2014, and Maliva, Robert G., Miocene rejuvenation of the southern Appalachian Mountains and fluvial transport of coarse siliciclastics to southern Florida; Geological Society of America Abstracts with Programs, v. 46, no. 6, p. 379

36. Moidaki, M., 2010, Gao, S. S., Liu, K. H., Abdelsalam, M. G., Hogan, J. P., and Atekwana, E.,Converted P-to-S phase and Moho quality beneath the New Madrid seismic zone from receiver function studies, Geoscience Research, v. 1 no. 1, p 7–21

37. Nystrom, Paul, 1986, Late Cretaceous-Cenozoic brittle faulting beneath the western South Carolina coastal plain; reactivation of the eastern Piedmont fault system; Geological Society of America Abstracts with Programs, v. 38, no.3, p. 74

38. Pazzaglia, Frank J., 1996, and Brandon, Mark T., Macrogeomorphic evolution of the post-Triassic Appalachian Mountains determined by deconvolution of the offshore basin sedimentary record; Basin Research, v. 8, p. 255-278

39. Parker, E. H., 2013, Hawman, R. B., Fischer, K. M., and Wagner, L. S., Crustal evolution across thesouthern Appalachians: Initial results from the SESAME broadband array; Geophysical Research Letters, v. 40, p. 3853–3857,

40. Penck, W, 1953, Morphological Analysis of Landforms, St. Martin's Press, New York

41. Poag, Wylie C., 1989, and Savon, William D., A record of Appalachian denudation in postrift Mesozoic and Cenozoic sedimentary deposits of the U.S. middle Atlantic continental margin; Geomorphology, v. 2, p. 119-157

42. Popenoe, P., 1985, Cenozoic depositional and structural history of the North Carolina margin fromseismic-stratigraphic analyses, *in* Poag, C. W., ed., Geologic evolution of the United States, Atlantic margin: New York, Van Nostrand Reinhold, p. 125-187

43. Prince, Philip S., 2010, Spotila, James A., and Henika, William S., New physical evidence of the role of stream capture in active retreat of the Blue Ridge escarpment, southern Appalachians; Geomorphology, v. 123, p. 305-319

44. Prince, Philip S., 2011, Spotila, James A., and Henika, William S., Stream capture as driver of transient landscape evolution in a tectonically quiescent setting; Geology, v. 39, no. 9, p. 823-826

45. Root, Samuel I., 1977, and Hoskins, Donald M., Lat 40° N fault zone, Pennsylvania: A new interpretation; Geology, v. 5, p. 719-723

46. Rowley, David B., 2013, Forte, Alessandro M., Moucha, Robert, Mitrovica, Jerry X., Simmons, Nathan A., and Grand, Stephen P., Dynamic topography change of the eastern United States since 3 million years ago; Science, v. 340, p. 1560-1563

47. Slingerland, Rudy, 1989, and Furlong, Kevin P., Geodynamic and Geomorphic Evolution of the Permo-Triassic Appalachian Mountains; Geomorphology, v. 2, p. 23-37

48. Soller, David R., 1988, Geology and tectonic history of the lower Cape Fear river valley, southeastern North Carolina; United States Geological Survey Professional Paper 1466-A, 65 p.

49. Spotila, James A., 2004, Bank, Greg C., Reiners, Peter W., Naeser, Charles W., Naeser, Nancy D., and Henika, Bill S., Origin of the Blue Ridge escarpment along the passive margin of Eastern North America; Basin Research, v. 16, p. 41-63

50. Stewart, J., 1997, and Watts, A.B., Gravity anomalies and spatial variations of flexural rigidity at mountain ranges; Journal of Geophysical Research, v. 102, no. B3, p. 5327-5352

51. Stewart, Kevin G., 2006, Dennison, John M., Tertiary-to-recent arching and the age and origin of fracture-controlled lineaments in the southern Appalachians; Geological Society of America Abstracts with Programs, v. 38. no. 3.

52. Stewart, Kevin G., 2015, Estimates on the magnitude and timing of post-orogenic topographic rejuvenation of the southern Appalachians using isostasy and deformed Coastal Plain rocks; Geological Society of America Abstracts with Programs, v. 47., no. 2., p. 82

53. Summerfield, M.A, 1991, Sub-aerial denudation of passive margins: regional elevation versus local relief models; Earth and Planetary Science Letters, v. 102, p. 460-469

54. Teng, Louis S., 1996, Extensional collapse of the northern Taiwan mountain belt; Geology, v. 24, no. 10, p. 949-952

55. Van De Plassche, Orson, 2014, Wright, Alex J., Horton, Benjamin P., Engelhart, Simon E., Kemp, Andrew C., Mallinson, David, and Kopp, Robert E., Estimating tectonic uplift of the Cape Fear arch (south-eastern United States) using reconstructions of relative sea level; Journal of Quaternary Science, v. 28, no 8, p. 749-759

56. Wagner, Lara, S., 2012, Stewart, Kevin, and Metcalf, Kathryn, Crustal-scale shortening structures beneath the Blue Ridge Mountains, North Carolina, USA; Lithosphere, v. 4, no. 3, p. 242-256

57. Wagner, Walter R., 1976, and Lytle, William S., Greater Pittsburgh region revised surface structure and its relation to oil and gas fields; Pennsylvania Geological Survey, 4th Series, Information Circular 80, 20 p.

58. Ward, Lauck W., 1991, Bailey, Richard H., and Carter, Joseph G., Pliocene and Early Pleistocene stratigraphy, depositional history, and molluscan paleobiogeography of the Coastal Plain, *in* Horton, J. Wright and Zullo, Victor A., ed., The geology of the Carolinas, Carolina Geological Society fiftieth anniversary volume: Knoxville, The University of Tennessee Press, p. 274-289

59. Weems, Robert E., 2009, Lewis, William C., and Aleman-Gonzalez, Wilma B., Surficial geologic map of the Roanoke rapids 30' x 60' Quadrangle, North Carolina, United States Geological Survey Open File Report 1149, scale 1:100,000

60. Whipple, Kelin X., 1999, and Tucker, Gregory E., Dynamics of the stream-power river incision model: Implication for height limits of mountain ranges, response timescales, and research needs; Journal of Geophysical Research, v. 104, no. B8, p. 17,661-17,674

61. Zandt, George, 2004, Gilbert, Hersh, Owens, Thomas J., Ducea, Mihai, Saleeby, Jason, and Jones, Craig H., Active foundering of a continental arc root beneath the southern Sierra Nevada in California; Nature, v. 431, p. 41-46

APPENDIX 1: LONGITUDINAL PROFILES AND R CODE

A1.1 Graham County Streams

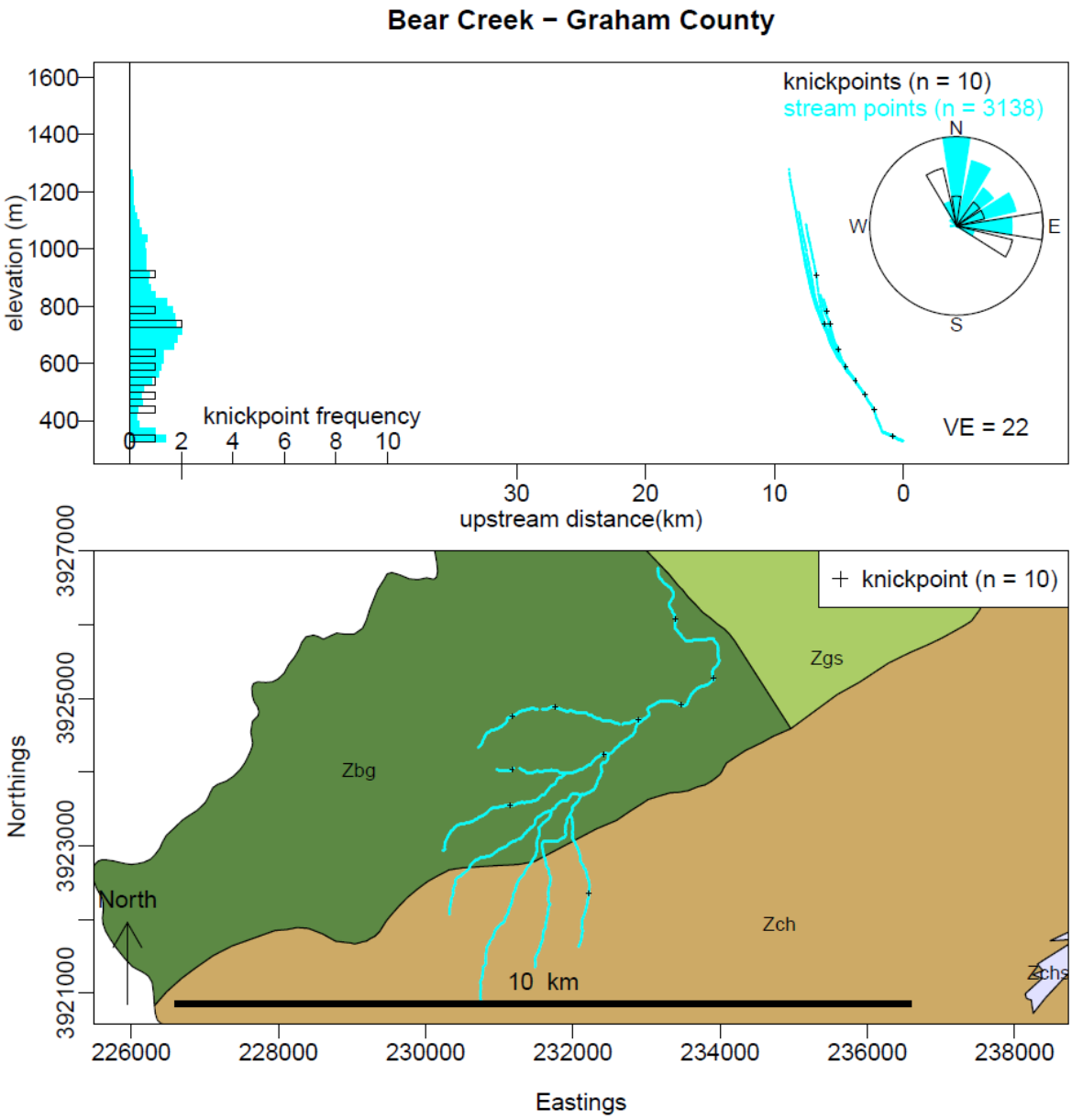

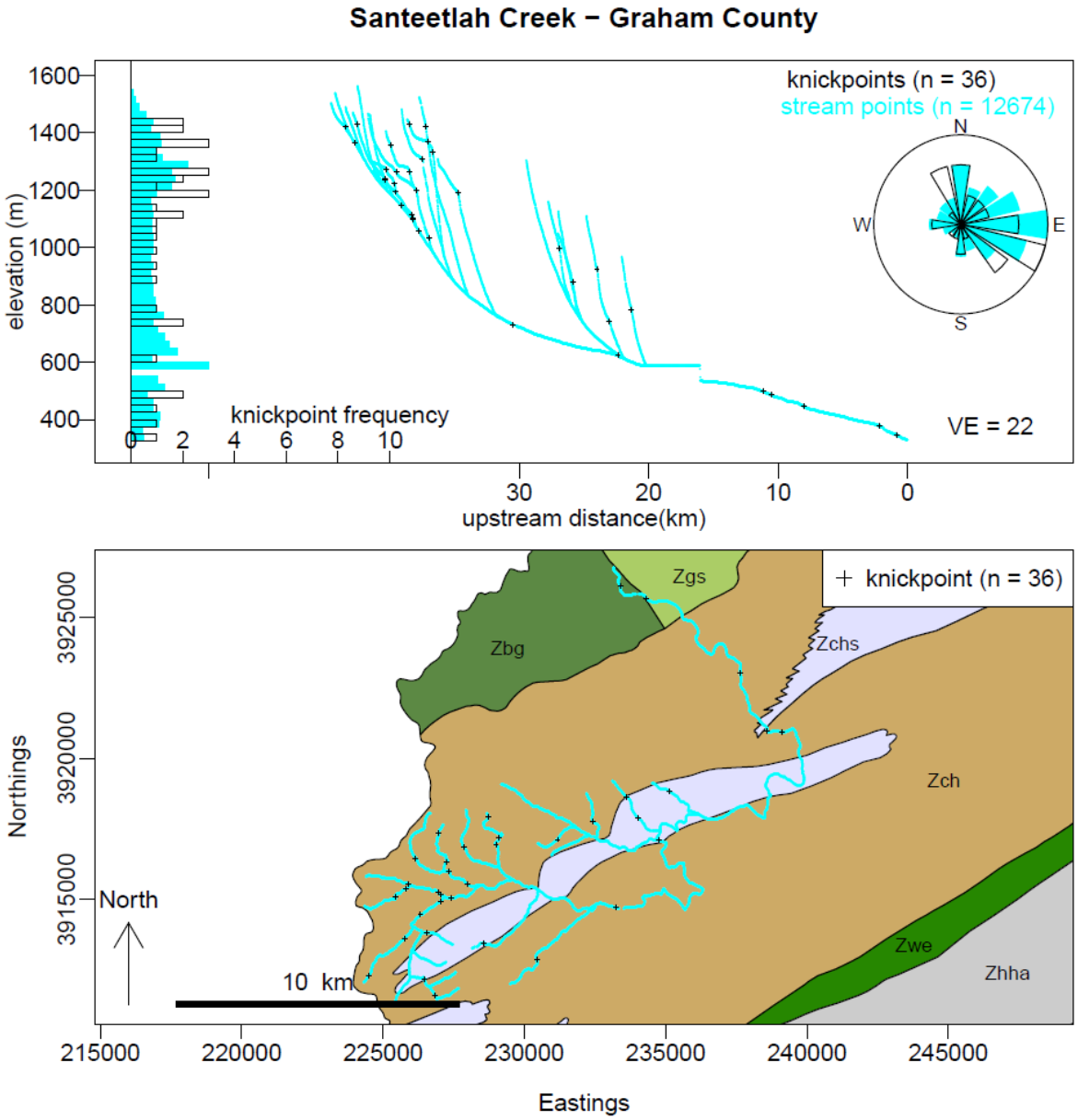
Santeetlah Creek − Graham County
knickpoints (n = 36)
stream points (n = 12674)
N
W
E
S
elevation (m)
1600
1400
1200
1000
800
600
400
knickpoint frequency
0
2
4
6
8
10
VE = 22
30
20
10
0
upstream distance(km)
+ knickpoint (n = 36)
Zgs
Zbg
Zchs
Zch
Zwe
Zhha
Northings
3925000
3920000
3915000
North
10 km
215000
220000
225000
230000
235000
240000
245000
Eastings

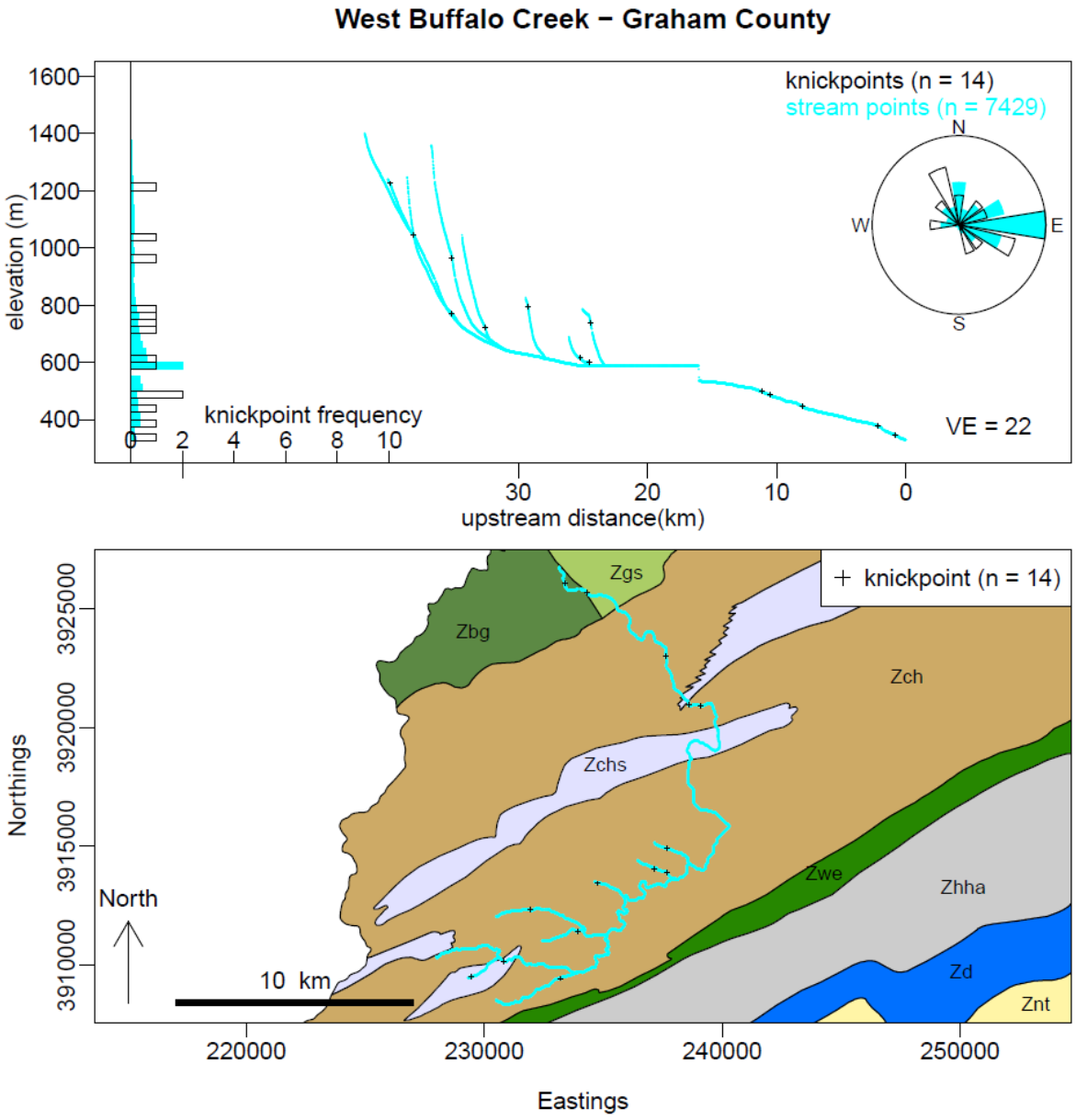
West Buffalo Creek − Graham County
knickpoints (n = 14)
stream points (n = 7429)
N
W
E
S
elevation (m)
1600
1400
1200
1000
800
600
400
knickpoint frequency
0
2
4
6
8
10
VE = 22
30
20
10
0
upstream distance(km)
+ knickpoint (n = 14)
Zgs
Zbg
Zch
Zchs
Zwe
Zhha
Zd
Znt
Northings
3925000
3920000
3915000
3910000
North
10 km
220000
230000
240000
250000
Eastings

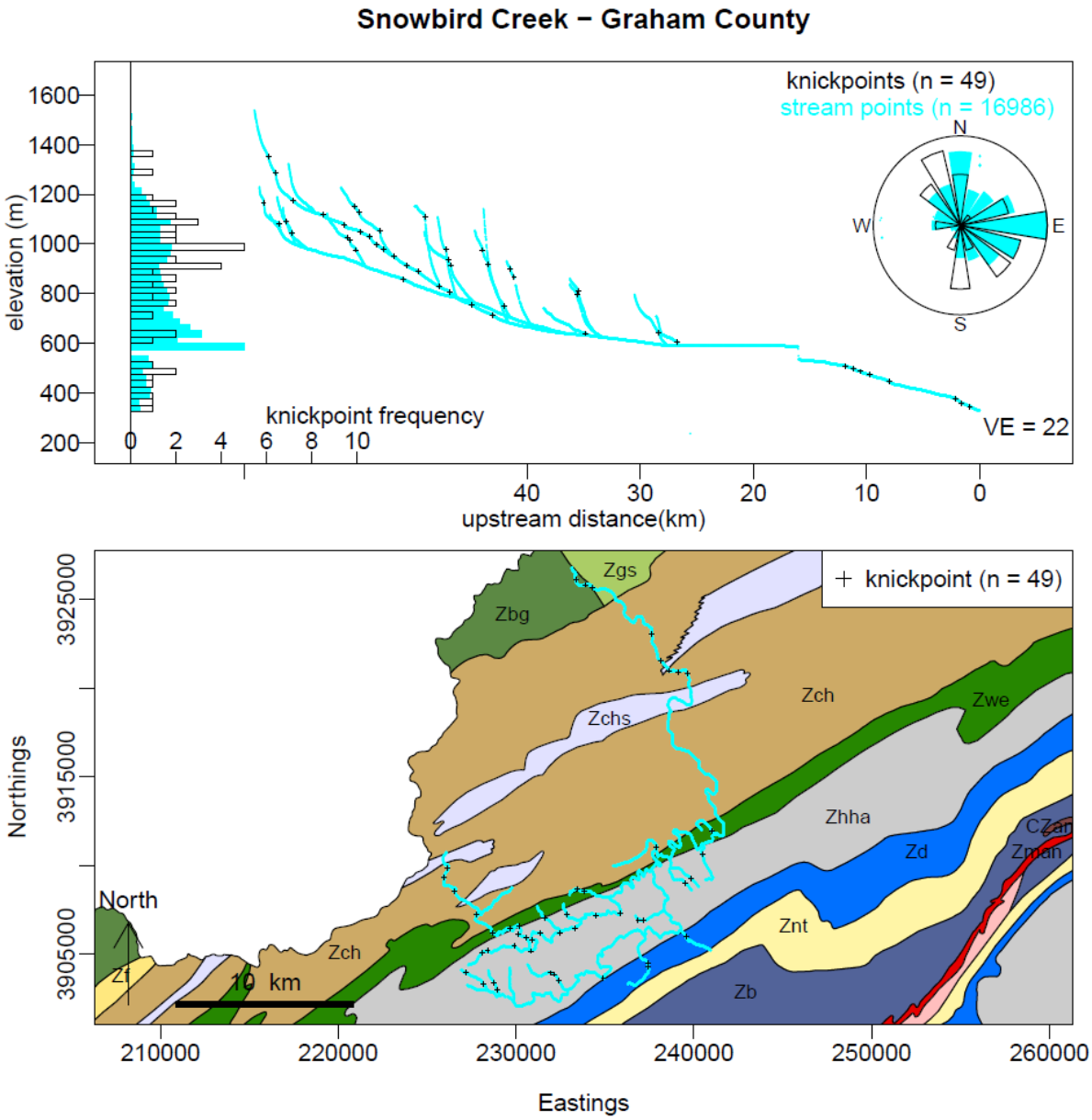
Snowbird Creek – Graham County
knickpoints (n = 49)
stream points (n = 16986)
N
E
S
W
elevation (m)
1600
1400
1200
1000
800
600
400
200
knickpoint frequency
0 2 4 6 8 10
VE = 22
40 30 20 10 0
upstream distance(km)
knickpoint (n = 49)
Zgs
Zbg
Zch
Zchs
Zwe
Zhha
Zd
CZan
Zman
Znt
Zb
North
Zf
10 km
Northings
3925000
3915000
3905000
210000 220000 230000 240000 250000 260000
Eastings

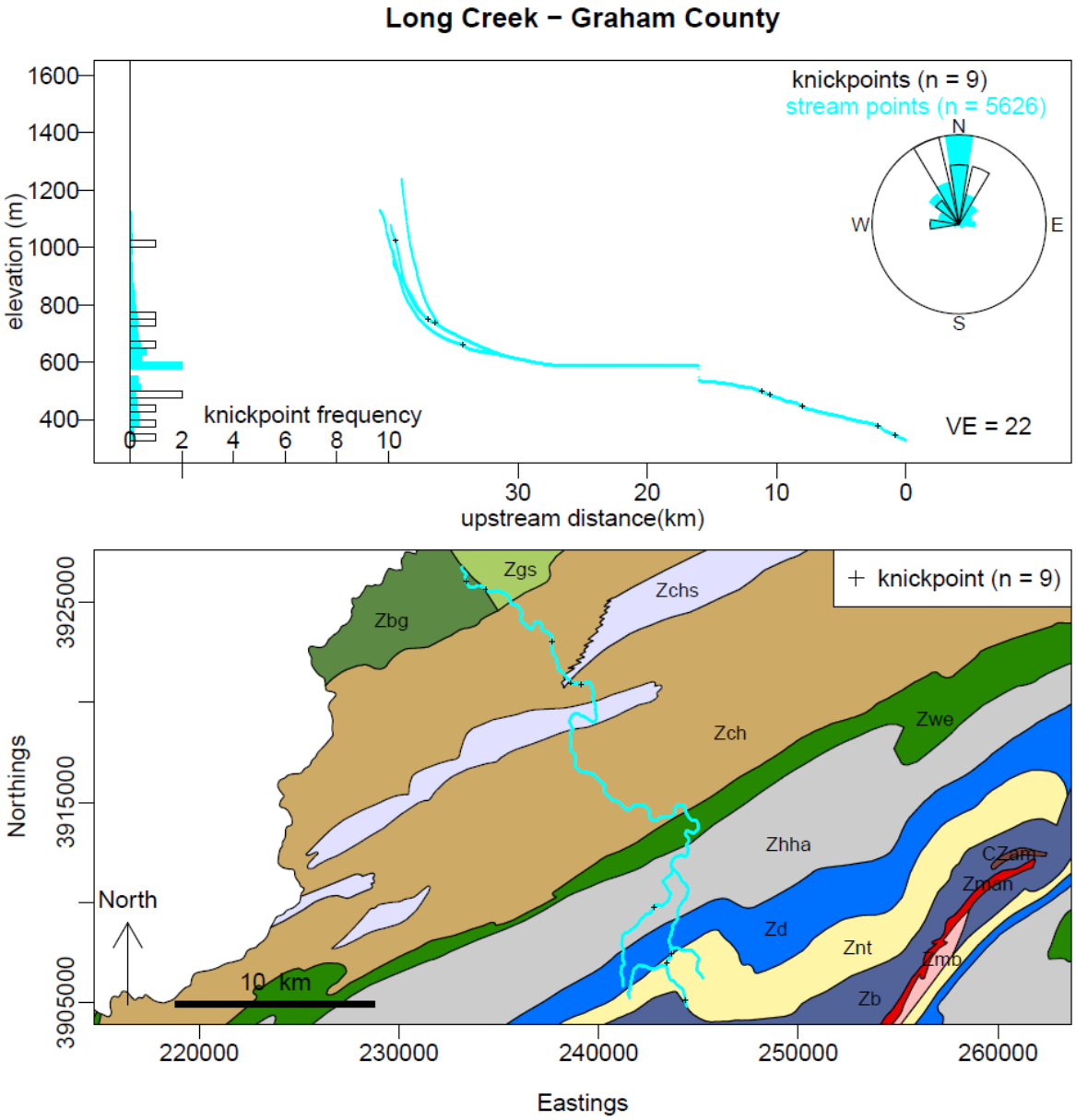
Long Creek – Graham County
knickpoints (n = 9)
stream points (n = 5626)
N
W
E
S
elevation (m)
1600
1400
1200
1000
800
600
400
knickpoint frequency
0
2
4
6
8
10
VE = 22
30
20
10
0
upstream distance(km)
knickpoint (n = 9)
Zgs
Zchs
Zbg
Zch
Zwe
Zhha
CZam
Zmam
Zd
Znt
Zmb
Zb
North
10 km
Northings
3925000
3915000
3905000
220000
230000
240000
250000
260000
Eastings

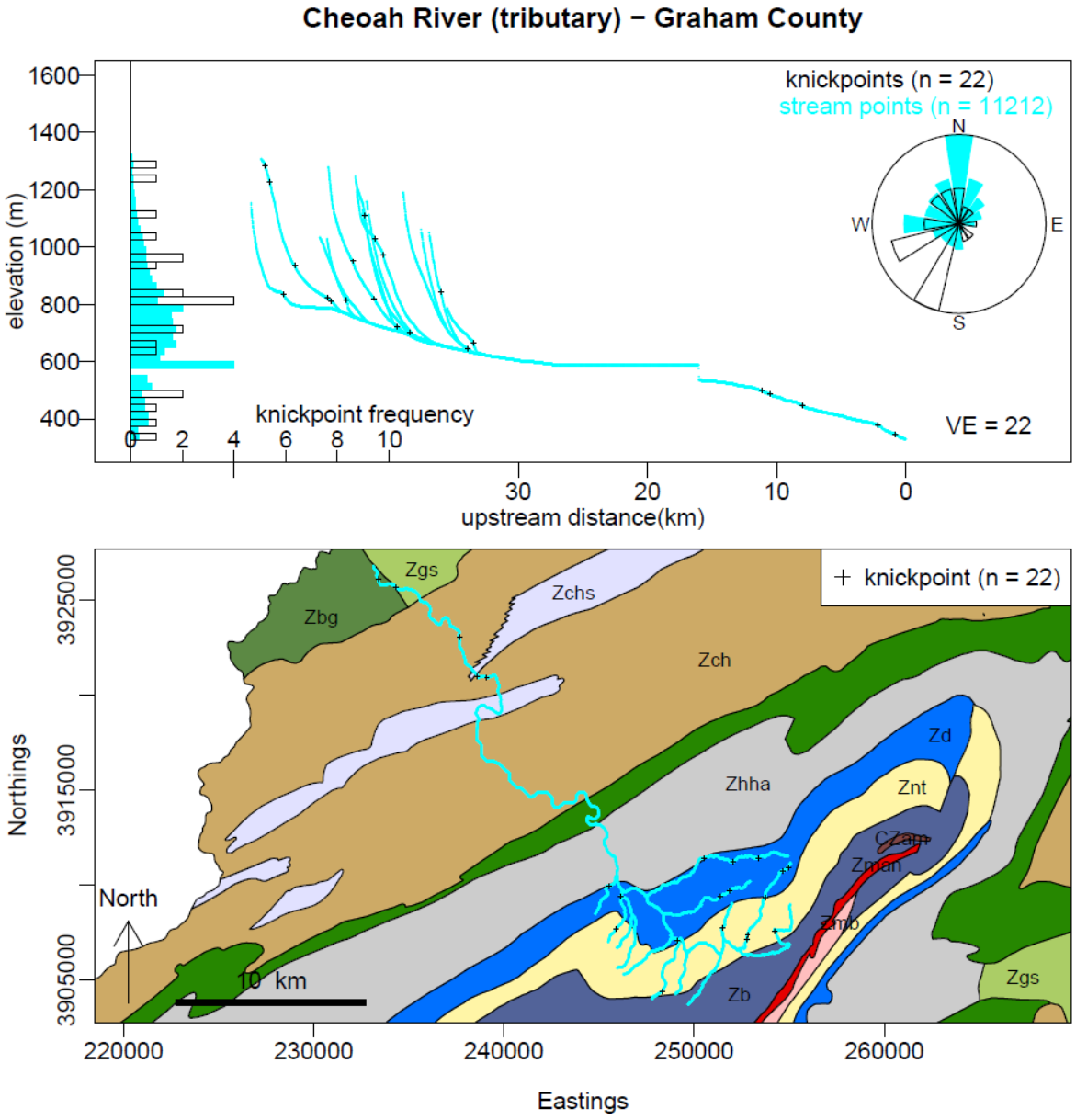
Cheoah River (tributary) − Graham County
knickpoints (n = 22)
stream points (n = 11212)
N
W
E
S
elevation (m)
1600
1400
1200
1000
800
600
400
knickpoint frequency
0
2
4
6
8
10
VE = 22
30
20
10
0
upstream distance(km)
+ knickpoint (n = 22)
Zgs
Zchs
Zbg
Zch
Zd
Zhha
Znt
CZam
Zmam
Zmb
Zb
Zgs
North
10 km
Northings
3925000
3915000
3905000
220000
230000
240000
250000
260000
Eastings

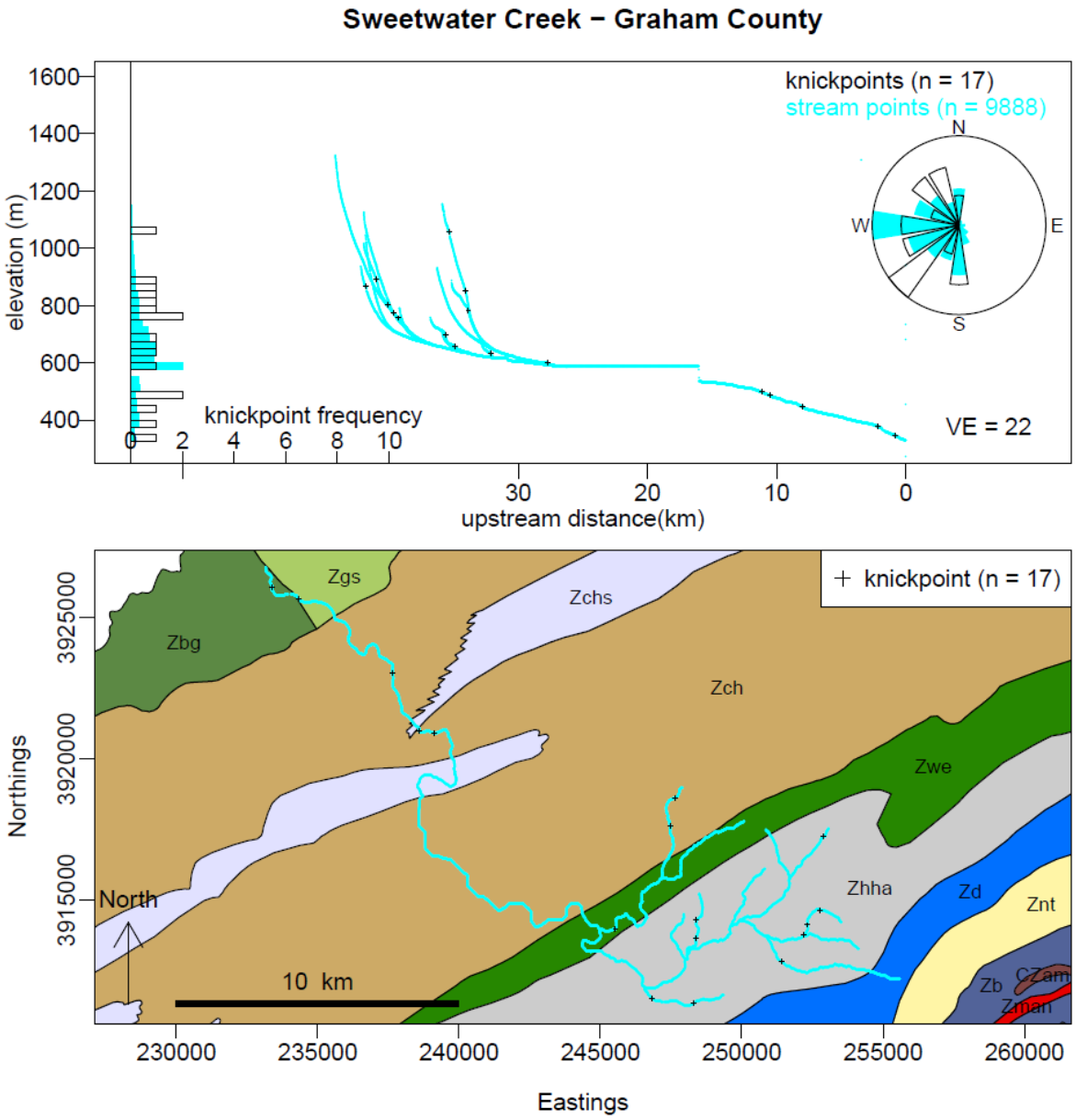
Sweetwater Creek − Graham County
knickpoints (n = 17)
stream points (n = 9888)
N
W
E
S
elevation (m)
1600
1400
1200
1000
800
600
400
knickpoint frequency
0
2
4
6
8
10
VE = 22
30
20
10
0
upstream distance(km)
+ knickpoint (n = 17)
Zgs
Zchs
Zbg
Zch
Zwe
Zhha
Zd
Znt
Zb
CZam
Znam
Northings
3925000
3920000
3915000
North
10 km
230000
235000
240000
245000
250000
255000
260000
Eastings

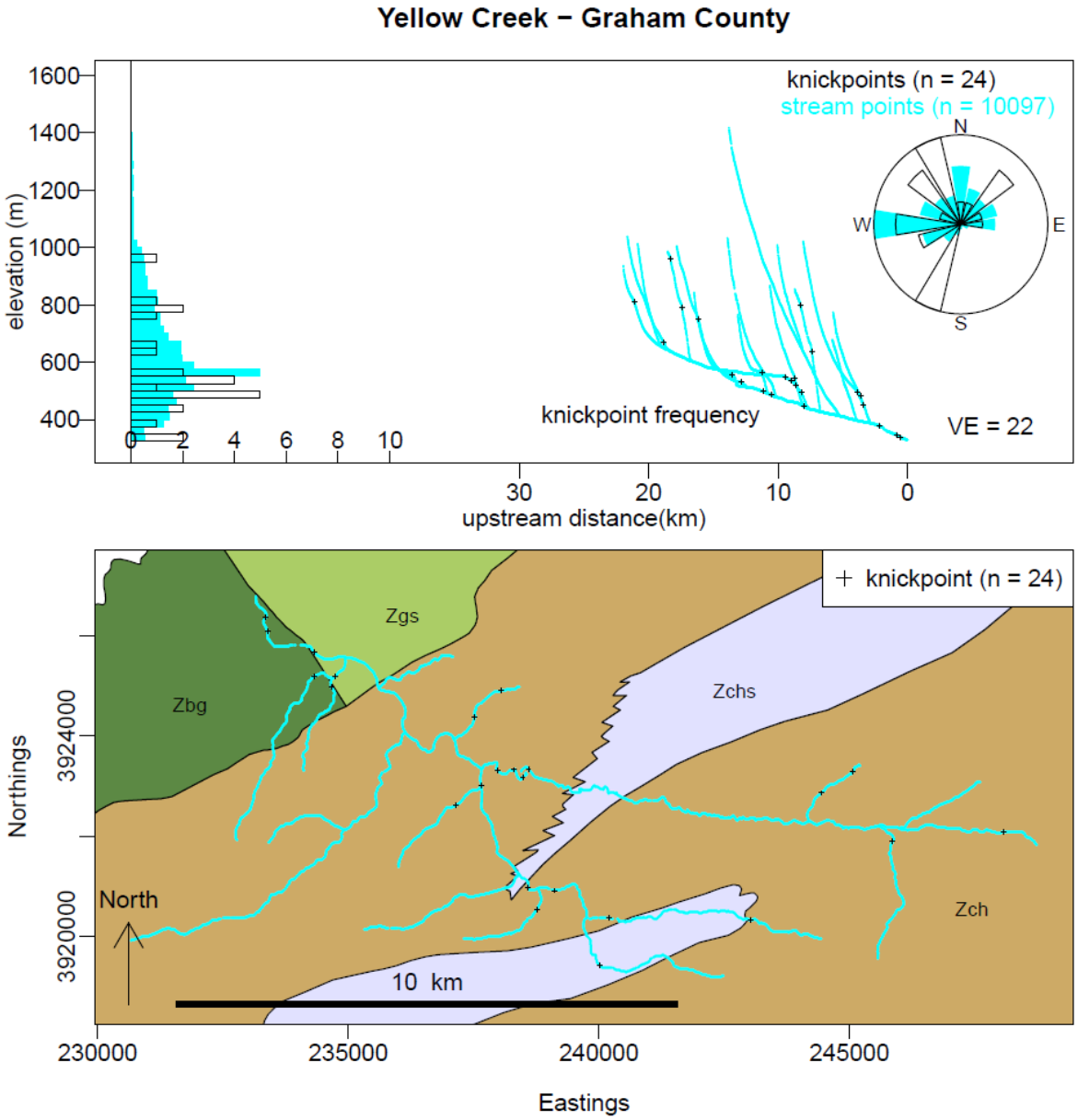
Yellow Creek – Graham County
knickpoints (n = 24)
stream points (n = 10097)
N
W
E
S
elevation (m)
1600
1400
1200
1000
800
600
400
0
2
4
6
8
10
knickpoint frequency
VE = 22
30
20
10
0
upstream distance(km)
+ knickpoint (n = 24)
Zgs
Zbg
Zchs
Zch
Northings
3924000
3920000
North
10 km
230000
235000
240000
245000
Eastings

A1.2 Swain County streams

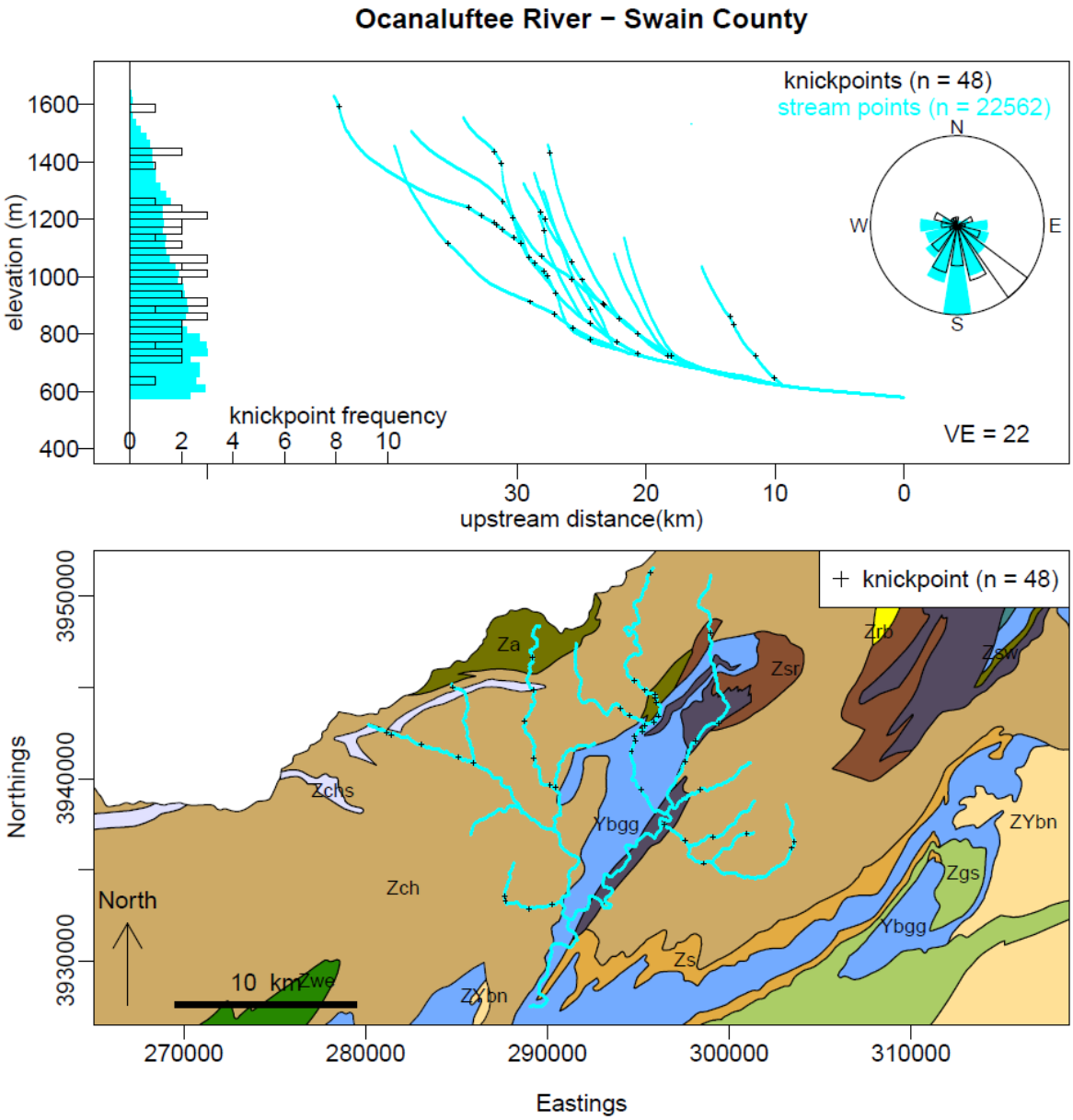

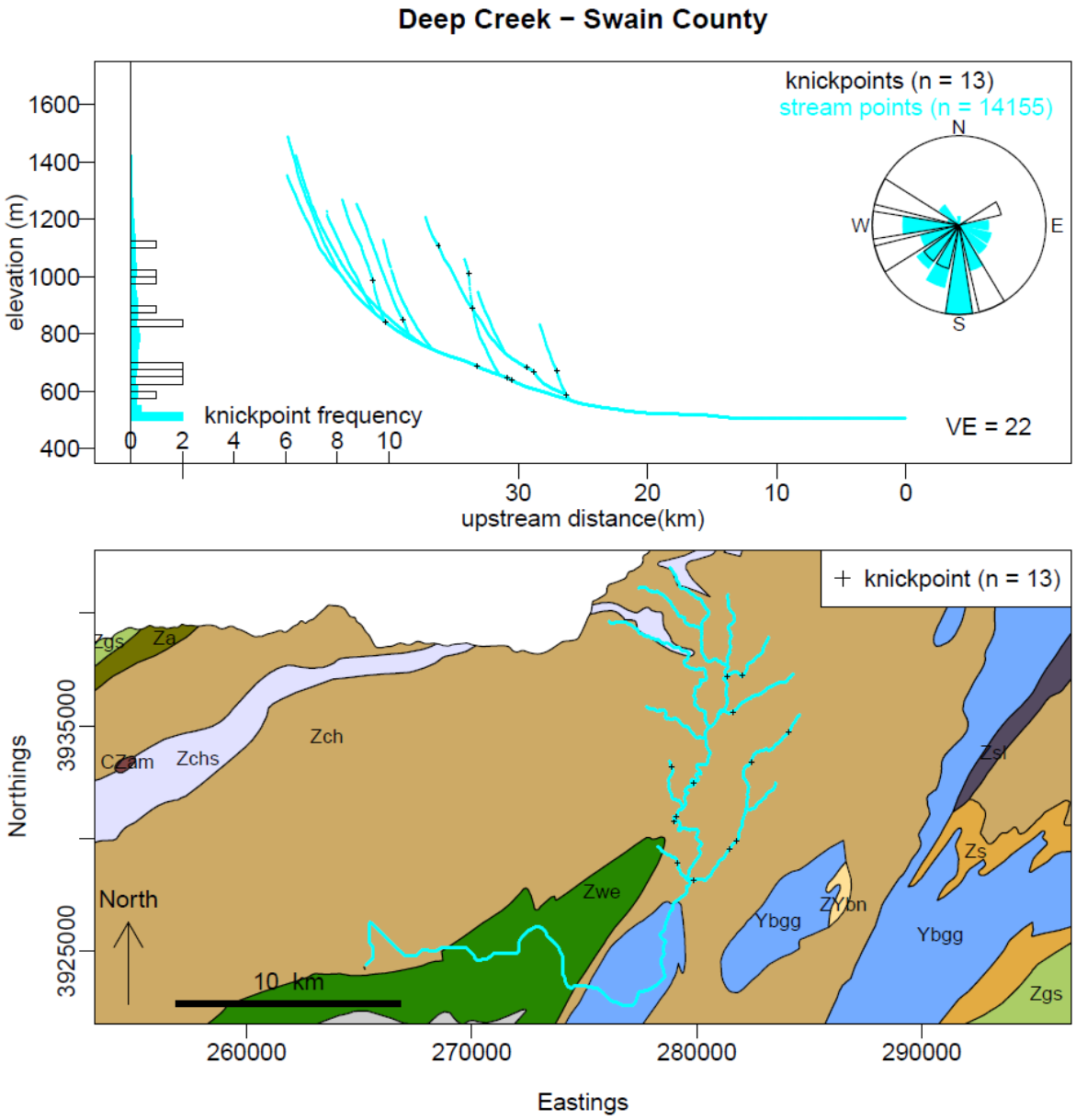
Deep Creek – Swain County
knickpoints (n = 13)
stream points (n = 14155)
N
W
E
S
elevation (m)
1600
1400
1200
1000
800
600
400
knickpoint frequency
0 2 4 6 8 10
VE = 22
30 20 10 0
upstream distance(km)
knickpoint (n = 13)
Zgs
Za
Zch
CZam
Zchs
Zsl
Zs
Zwe
Ybgg
ZYbn
Ybgg
Zgs
North
10 km
Northings
3935000
3925000
260000
270000
280000
290000
Eastings

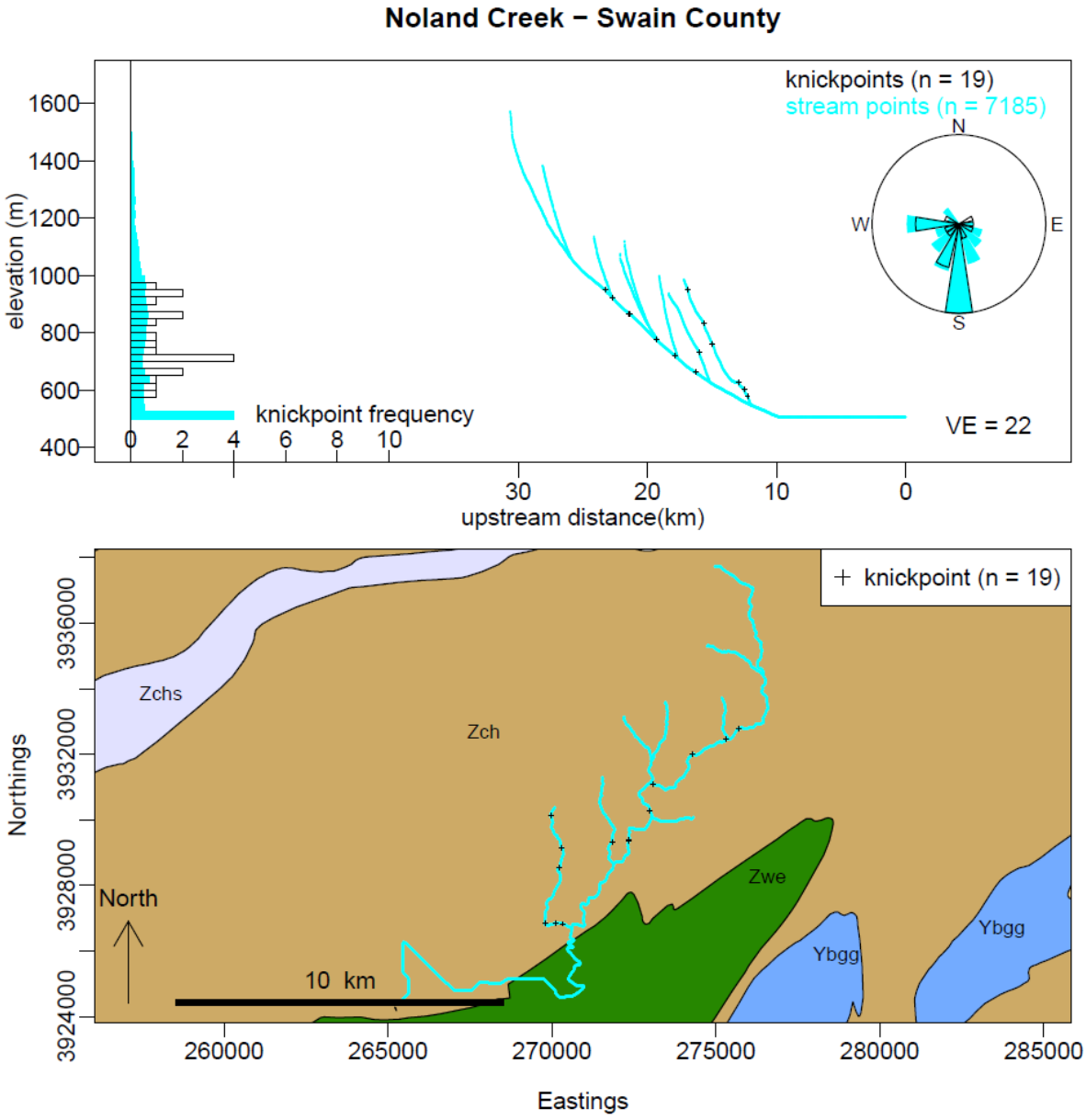
Noland Creek – Swain County
knickpoints (n = 19)
stream points (n = 7185)
N
W
E
S
elevation (m)
1600
1400
1200
1000
800
600
400
knickpoint frequency
0 2 4 6 8 10
VE = 22
30 20 10 0
upstream distance(km)
+ knickpoint (n = 19)
Zchs
Zch
Zwe
Ybgg
Ybgg
North
10 km
Northings
3936000
3932000
3928000
3924000
260000 265000 270000 275000 280000 285000
Eastings

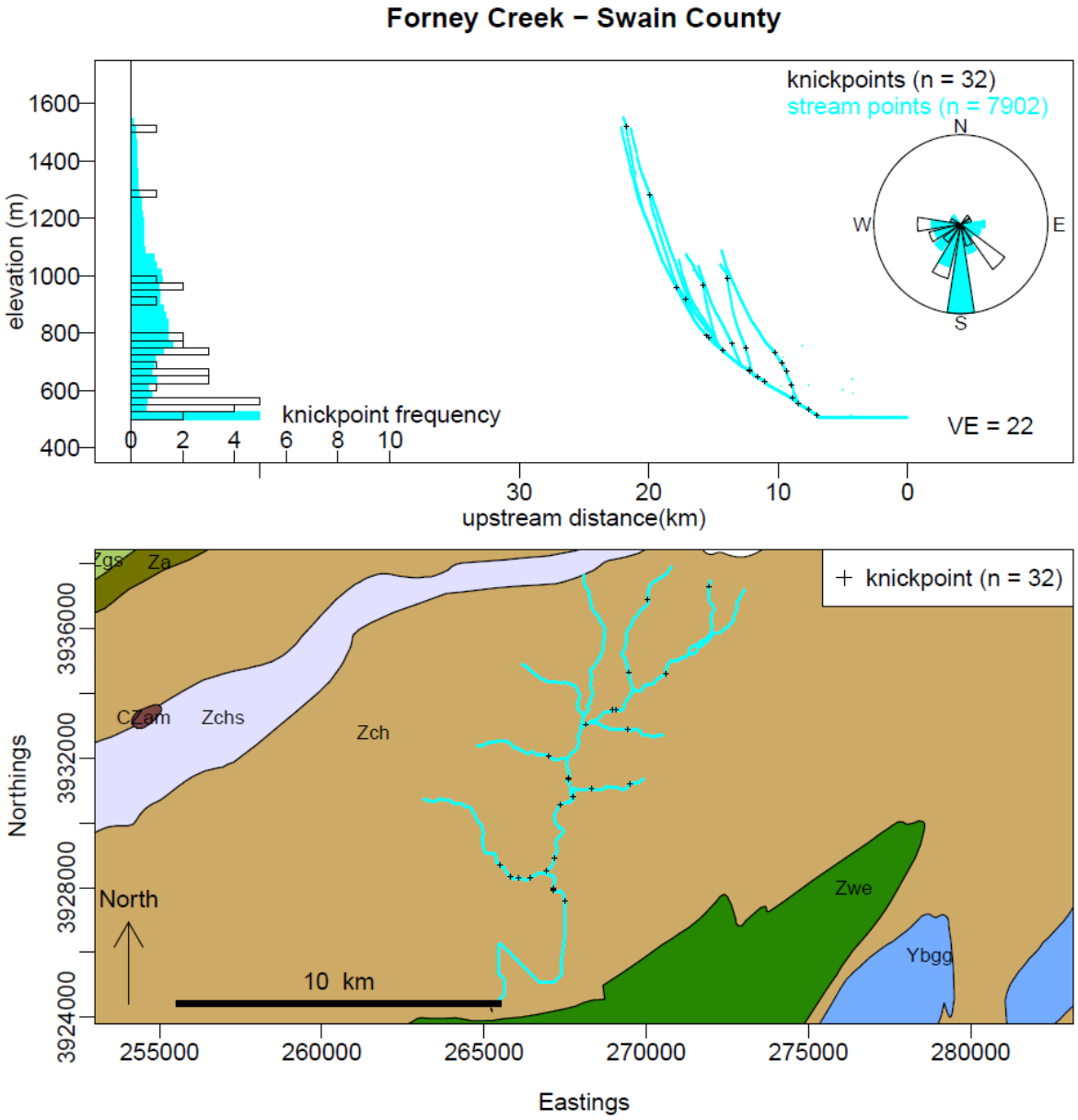
Forney Creek – Swain County
knickpoints (n = 32)
stream points (n = 7902)
N
W
E
S
elevation (m)
1600
1400
1200
1000
800
600
400
knickpoint frequency
0 2 4 6 8 10
VE = 22
30 20 10 0
upstream distance(km)
knickpoint (n = 32)
Zgs
Za
CZam
Zchs
Zch
Zwe
Ybgg
North
10 km
Northings
3936000
3932000
3928000
3924000
255000 260000 265000 270000 275000 280000
Eastings

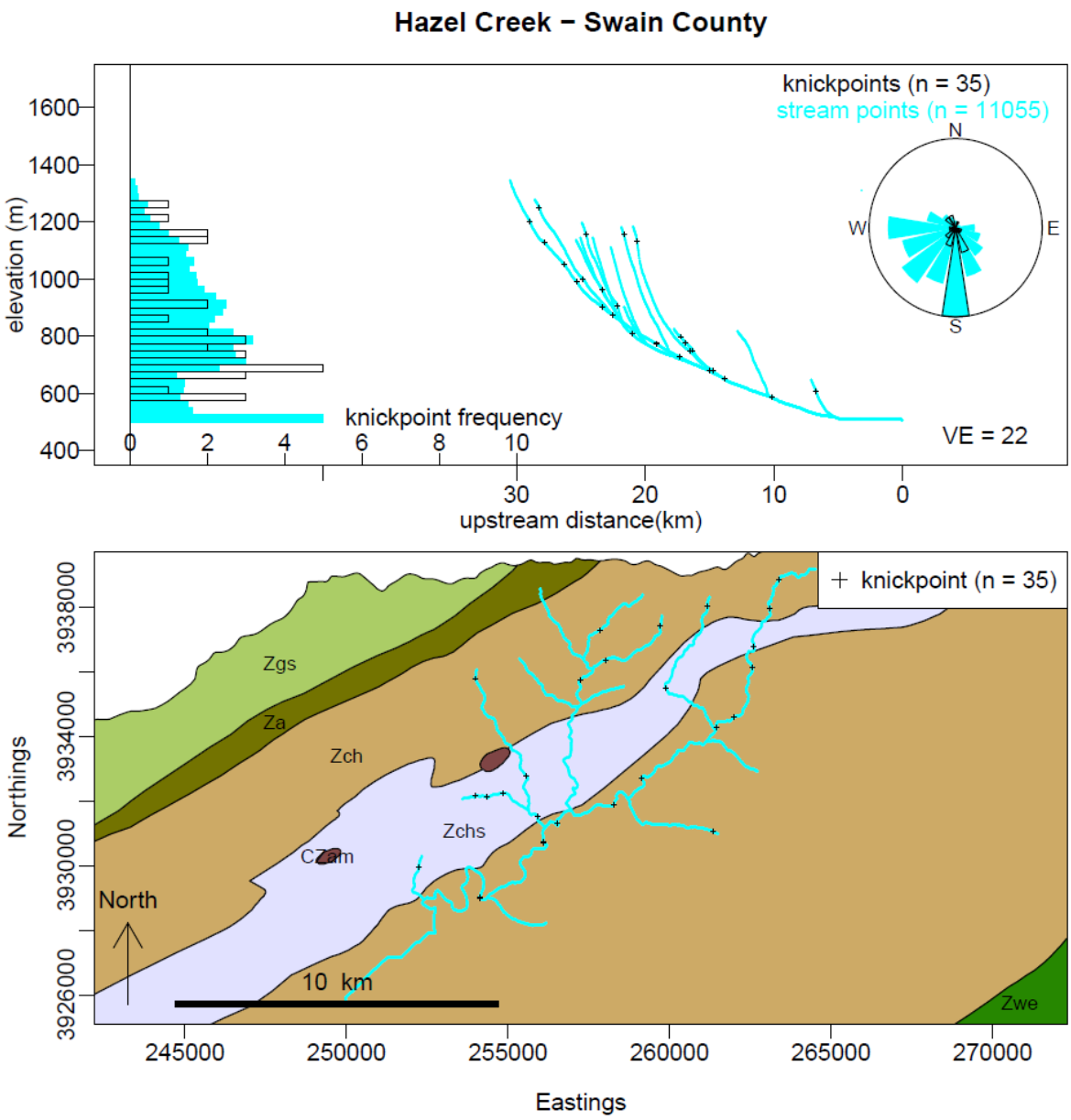
Hazel Creek – Swain County
knickpoints (n = 35)
stream points (n = 11055)
N
W
E
S
elevation (m)
1600
1400
1200
1000
800
600
400
0
2
4
6
8
10
knickpoint frequency
VE = 22
30
20
10
0
upstream distance(km)
knickpoint (n = 35)
Zgs
Za
Zch
Zchs
CZam
North
10 km
Zwe
Northings
3938000
3934000
3930000
3926000
245000
250000
255000
260000
265000
270000
Eastings

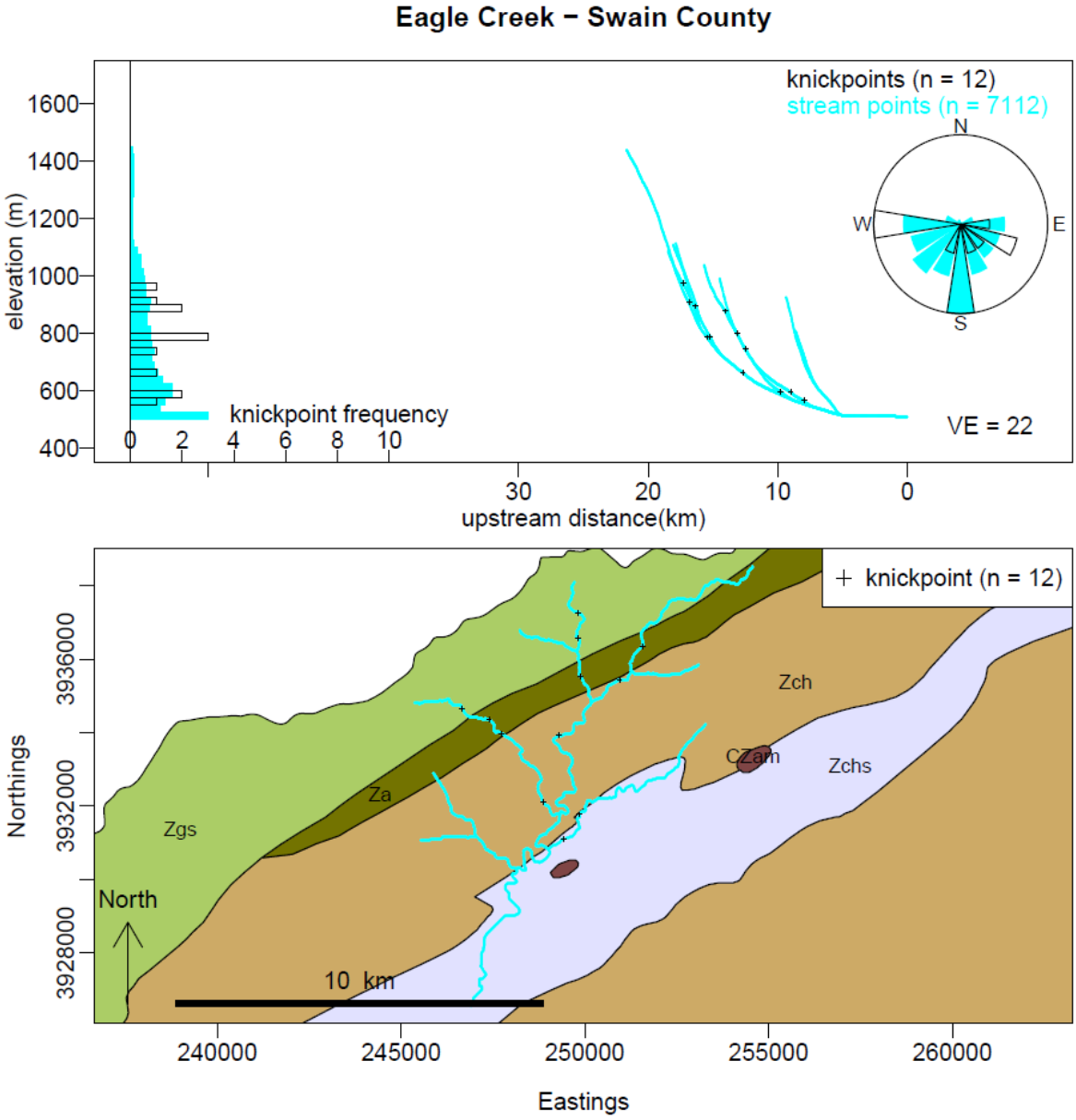
Eagle Creek – Swain County
knickpoints (n = 12)
stream points (n = 7112)
N
W
E
S
elevation (m)
1600
1400
1200
1000
800
600
400
knickpoint frequency
0 2 4 6 8 10
VE = 22
30 20 10 0
upstream distance(km)
+ knickpoint (n = 12)
Zch
CZam
Zchs
Za
Zgs
North
10 km
Northings
3936000
3932000
3928000
240000 245000 250000 255000 260000
Eastings

A1.3 R script used for knickpoint selection

```
#### This code is designed to find knickpoints along stream profiles
####  from dbf files with columns containing: x,y,z,length,accumulation
####  the units of elevation are converted from ft to m in this example.

####  The user must first scan in the *.dbf file then decide a plot TITLE, header,
####  and upstream/downstream directions of the basin which must be entered
####  character strings in quotation marks.

###   The dbf file has six columns:  index(useless) ,x,y,z,flowlength, and flow accum.

###   !!!  This code is for one stream at a time  !!!
library(foreign)  ## this library must be installed before using the following code

#####################################################################
##  Function used to put streams in descending order of length and
##  remove any non-positive elevation values

orderstream = function(stream,negs)
{
if (missing(negs))
{
negs=FALSE
}

if (negs==FALSE)
{
 stream = stream[order(stream[,5],decreasing=TRUE),]
 NAelev = which(stream[,4]<=0)
 NAlens = which(stream[,5]<=0)
 toohighs = which(stream[,4]>=6685) # elevation of Mt Mitchell in feet

 Ra =  range(stream[,5])
 Rw = which (stream[,5]<= Ra[1])

 rejects = c(NAelev,NAlens,toohighs,Rw)

 NL = length(rejects)
 if(NL>0)
 {
  streamfix = stream[-rejects,]
 }
 if(NL==0)
 {
```

```
 streamfix = stream
 }
 }

if (negs==TRUE)
 {
 stream = stream[order(stream[,5],decreasing=TRUE),]
 NAelev = which(stream[,4]<=0)
 NAlens = which(stream[,5]<=-100000) ## 100 km limit
 toohighs = which(stream[,4]>=6685) # elevation of Mt Mitchell in feet; nothing  #in our study area could
be any higher

 Ra =  range(stream[,5])
 Rw = which (stream[,5]<= Ra[1])

 rejects = c(NAelev,NAlens,toohighs,Rw)

 NL = length(rejects)
 if(NL>0)
 {
 streamfix = stream[-rejects,]
 }
 if(NL==0)
 {
 streamfix = stream
 }
 }

return(streamfix)

}


################################################################################
# take out the empty data rows that may result from the Arcmap extraction process
MTEE = function (datmat)
{
L = length (datmat[,1])
RS=vector()
for (i in 1:L)
 {
 RS[i] = sum(datmat[i,(3:5)])
 }
empties  = which(RS==0)
if(length(empties)==0)
```

```
{
return(datmat)
stop()
}
fulldat = datmat[-empties,]
return(fulldat)
}
################################################################################


###  This is the main code used for finding the knickpoints

findknixdir =function (stream,wfilt,wdiff,TITLE,METERS,A,B,C,D,FIXED)
{
        ######################################################################
##  inputs to the code
##  stream : a matrix containing 6-columns of data IN THIS ORDER
##  stream[,1] = index (ignored)
##  stream[,2] = x
##  stream[,3] = y
##  stream[,4] = z
##  stream[,5] = flow length
##  stream[,6] = flow accmumulation
##  windo = size of smoothing window in meters
##  FIXED = whether or not to reduce knickpoint clusters into single points
##  First, a matrix will be made from the dbf file described above
##  The matrix will be sorted so that the rows are in decreasing order of
##  flow length
######################################################################

stream = orderstream(stream)
if (METERS == FALSE)
{
        stream[,4] = stream[,4]*0.3048 ## this scaling is optional; my original
                                       ##  elevation was in ft
}
else
{
stream[,4] = stream[,4]
}

dmax = max(stream[,5])
dmin = min(stream[,5])
Xlim = c(dmin,dmax)
ymax = max(stream[,4])
```

```
ymin = min(stream[,4])
Ylim = c(ymin,ymax)

nn = length (stream[,1])

winrow = wfilt*(nn/(dmax-dmin))
winro  = round(winrow,digits=0)


#####################################################################
###  functions used within this function
#####################################################################
#####################################################################
### function for finding slope
slope = function (x,y)
{
n = length(x)
dxdy=matrix(ncol=1, nrow=n)
for(i in 1:n-1)
 {
 dxdy[i,1] = (y[i]-y[i+1])/(x[i] - x[i+1])
 }
dxdy[1]=dxdy[2]
return(cbind(x,dxdy))
}
#####################################################################
#####################################################################
### function for smoothing time series
### and to convert the indices (rows) into distance

smooth=function(x,y,w,TITLE)
{
w= winro
n= length (x)
hw=w/2  #half-window
smth=  matrix(ncol=2,nrow=n-w)    # subtract the window length to eliminate  ###   edge effects
smth[,1] =rbind(x[hw:(n-(hw)-1)])
{
k=1
for (i in ((hw):(n-w)))
{
 smth[k,2] = (sum(y[(i-hw):(i+hw)])) / w
 k=k+1
 }
 }
```

```
smth[1,2]=smth[2,2]    ####  this makes the second row equal the first to remove ### spike
return(smth)
}

#####################################################################
### ksn_calculator

####################
# ksn = slope / (drainage area ^ ( concavity index) )

dbf2ksn=function(stream)
{

stream[,4]=stream[,4]
stream = stream[order(stream[,5],decreasing=TRUE),]

S = slope(stream[,5],stream[,4])

nn = length (S[,1])
winrow = 1000*(nn/(max(S[,1])-min(S[,1])))
winro  = round(winrow,digits=0)
hw=winro/2

Sm =smooth(S[,1],S[,2],1000)
nn=length(Sm[,1])

                        Ar = stream[hw+1:(nn),6]*( (20*0.3048)^2)   ### specific to 20 ft x 20 ft DEMs

#XYlm = lm(log10(Sm) ~ log10(Ar))
#theta= XYlm$coefficients[1]

ksn = Sm[,2]/(Ar ^-.45)  ## concavity = 0.45

newxyz=cbind(stream[,2:5])
newxyz = newxyz[hw+1:(nn),]

headsup=c("x","y","z","len","ksn")
newtest=(cbind(newxyz,ksn))
return(newtest)

}

#####################################################################
##  fxn for calculating sum of sides' differences
##########
```

```
sumdiffs=function(x,y,w)
{
stream = cbind(x,y)
stream = stream[order(stream[,1],decreasing=TRUE),]
dmax = max(stream[,1])
dmin = min(stream[,1])

n= length (x)
hw=w/2  #half-window
ss=  matrix(ncol=6,nrow=n-w)
updiffs =vector()
downdiffs=vector()

ss[,1] =rbind(x[hw:(n-(hw)-1)])

for (i in ((hw):(n-w)))
{
updiffs[i] = sum(diff(y[(i-hw):i]))
downdiffs[i]= sum(diff(y[i:(i+hw)]))

ss[i,2] = updiffs[i]
ss[i,3] = downdiffs[i]
ss[i,4] = downdiffs[i]-updiffs[i]
ss[i,5] = updiffs[i]-downdiffs[i]
ss[i,6] = downdiffs[i]/updiffs[i]
}

ss[1,]=ss[2,]    ####  this makes the second row equal the first to remove spike
return(ss)

}

### call the internal functions

streamsmuth = smooth(stream[,5],stream[,4],wfilt)
streamSD= sumdiffs(streamsmuth[,1],streamsmuth[,2],wdiff)
medelev = median (stream[,4])
testdydx = slope(stream[,5],stream[,4])
smuthdydx= smooth(testdydx[,1],testdydx[,2],wfilt)
test2dydx= slope(smuthdydx[,1],smuthdydx[,2])
streamksn= dbf2ksn(stream)

#####################################################################
if (missing(FIXED))
{
```

```
FIXED = FALSE
}

#####################################################################
##
### default selection parameters if you don't set them when calling the function:
if (missing(A))
{
A = 70
}
Aa=A+130
if (missing(B))
{
B = 1.5
}
if (missing(C))
{
C = 0.01
}
if (missing(D))
{
D = -6
}
## picks for each parameter if you set them when calling the function
PIXA  = which (streamksn[,5] >= A & streamksn[,5] <=Aa)
PIXB  = which (streamSD[,6]  >= B)    # downdiffs[i]/updiffs[i]
PIXC  = which (smuthdydx[,2] >= C)   # abs. value of smoothed slope
PIXD  = which (streamSD[,3]  <= D )   # downdiffs[i]

## These are the picks found by all tests -  think of a venn diagram
PIXAB = intersect(PIXA,PIXB)
### if not using ksn change this to : PIXAB = (PIXB)
PIXCD = intersect(PIXC,PIXD)
PIX   = intersect(PIXAB,PIXCD)


## This converts clusters of very close knickpoints into one point
diffPIX = abs(diff(PIX))
revdiffPIX= abs(diff(rev(PIX)))
loners  = which(diffPIX >15 )
trupix  = c(PIX[loners],max(PIX))
#
#FIXED is set as TRUE when you want knickzones reduced to the bottom knickpoint of #each zone
if (FIXED ==TRUE)
{
```

```
 trupix = PIX
}

## These are the captions for the six plots that will be made
capA =  paste(Aa,"> ksn >",A)
capB =  paste("Sum of differences >", B )
capC =  paste("Smoothed slope >",C)
capD =  paste("Vertical drop in ", wdiff,"m > ",abs(D),"m",sep="")
capE =  "First picks"
capF =  "True picks - no clusters"

## These print the results to the R console for user supervision
print(capA )
PIXAlen = length(PIXA)
print(PIXAlen)
print(capB)
PIXBlen= length(PIXB)
print(PIXBlen)
print(capC)
PIXClen = length(PIXC)
print(PIXClen)
print(capD)
PIXDlen = length(PIXD)
print(PIXDlen)
print("PIX")
PIXlen = length(PIX)
print(PIXlen)
print("trupix")
trupixlen=length(trupix)
print(trupixlen)

## avoid an empty return
if (length(PIX) == 0)
{
 knixdir = matrix(rep(0,times=5),ncol=5)
 return(knixdir)
 stop()
}

###  write the coordinates of the knickpoint to a dbf file
eastings = stream[trupix,2]
northings= stream[trupix,3]
knixelev = stream[trupix,4]
knixdist = stream[trupix,5]
```

```
 knixmat = cbind(eastings,northings,knixelev,knixdist)

 ##  make the plots
 graphics.off()
 dev.new()
### choose a file location to save the selected knickpoints and the pdf plots of each stream
out1=paste('C:/UNC/PhD/R/profiles/images/auto_picks/graham_co/',TITLE, "_", A, "_", B, "_", C, "_",
D, ".pdf",sep="")
 ###  this defines the dimension of the .pdf file in inches

 pdf(file=out1,width=8,height=6)
 par(mfrow=c(3,2))          ## this makes a 3x2 plot
 par(mai = c(0.15,.2,.1,.1))   ## these are the margins
 par( mgp = c(0, -1.4, 0)  ) ## this puts the labels inside

 XLIM = c(50,0)
 YLIM = c(300,1500)

 colstream = "black"
 colpix = "black"
## ksn – normalized steepness
plot(stream[,5]/1000,stream[,4],type='l',xlab= 'distance (km)',ylab= 'elevation (m)',
xlim=XLIM,col=colstream,cex=2,cex.lab=1.2,cex.axis=1,ylim = YLIM,main =  "",tck=.04)
 points(stream[PIXA,5]/1000,stream[PIXA,4],typ='p',col=colpix,pch=2,cex=.6)
 hwayx = (XLIM[1]/2)

 hwayy = YLIM[2]
 text(hwayx,hwayy,capA,pos=1,cex=1.5)

### sum of diffs
plot(stream[,5]/1000,stream[,4],type='l',xlab= 'distance (km)',ylab= 'elevation (m)',
xlim=XLIM,col=colstream,cex=2,cex.lab=1.2,cex.axis=1,ylim = YLIM,main =  "",tck=.04)
 points(stream[PIXB,5]/1000,stream[PIXB,4],typ='p',col=colpix,pch=2,cex=.6)
text(hwayx,hwayy,capB,pos=1,cex=1.5)

##smoothed slope
plot(stream[,5]/1000,stream[,4],type='l',xlab= 'distance (km)',ylab= 'elevation (m)',
xlim=XLIM,col=colstream,cex=2,cex.lab=1.2,cex.axis=1,ylim = YLIM,main =  "",tck=.04)
 points(stream[PIXC,5]/1000,stream[PIXC,4],typ='p',col=colpix,pch=2,cex=.6)

text(hwayx,hwayy,capC,pos=1,cex=1.5)

## vertical drop
plot(stream[,5]/1000,stream[,4],type='l',xlab= 'distance (km)',ylab= 'elevation (m)',
xlim=XLIM,col=colstream,cex=2,cex.lab=1.2,cex.axis=1,ylim = YLIM,main =  "",tck=.04)
```

```
 points(stream[PIXD,5]/1000,stream[PIXD,4],typ='p',col=colpix,pch=2,cex=.6)

 text(hwayx,hwayy,capD,pos=1,cex=1.5)

## first round picks
plot(stream[,5]/1000,stream[,4],type='l',xlab= 'distance (km)',ylab= 'elevation (m)',
xlim=XLIM,col=colstream,cex=2,cex.lab=1.2,cex.axis=1,ylim = YLIM,main =  "",tck=.04)
 points(stream[PIX,5]/1000,stream[PIX,4],typ='p',col=colpix,pch=2,cex=.6)

text(hwayx,hwayy,capE,pos=1,cex=1.5)

## second round picks -  remove clusters
plot(stream[,5]/1000,stream[,4],type='l',xlab= 'distance (km)',ylab= 'elevation (m)',
xlim=XLIM,col=colstream,cex=2,cex.lab=1.2,cex.axis=1,ylim = YLIM,main = "",tck=.04)
 points(stream[trupix,5]/1000,stream[trupix,4],typ='p',col=colpix,pch=2,cex=.6)

text(hwayx,hwayy,capF,pos=1,cex=1.5)

graphics.off()

######  This is an internal function used to find stream directions
streamdir2  = function (stream, knick,GEOL)
{
TITLE <- deparse(substitute(knick))
Rw = 1
XLIM = c((knick[1]-50),(knick[1]+50))
YLIM = c((knick[2]-50),(knick[2]+50))
plot(stream[,2],stream[,3],asp=1, xlim = XLIM,ylim=YLIM, xlab = "Latitude",
ylab = "Longitude",main=TITLE,type='n')
if(missing(GEOL))
{
GEOL=FALSE
}
if(GEOL==TRUE)
{
for(i in 1:length(polyLAT) )
{
w = which(mapunit[i] == umapunit)
polygon(polyLON[[i]], polyLAT[[i]] ,   col=finalrgbcols[w] )
}
}
points(stream[,2],stream[,3],type='l')
## find the index of the knickpoint in the original stream database
knixind = which (stream[,5]== knick[4])
upseq = seq(from  = (knixind - Rw), to = (knixind), by = 1)
```

```
downseq = seq(from  = (knixind), to = (knixind + Rw), by = 1)
####  These are the neighboring pixels along the stream
upnorth = stream[(knixind-Rw),3]
upeast  = stream[(knixind-Rw),2]
downnorth = stream[(knixind+Rw),3]
downeast  = stream[(knixind+Rw),2]

points(stream[upseq,2],stream[upseq,3],type='l',col=4,lwd=2)
points(stream[downseq,2],stream[downseq,3],type='l',col=4,lwd=2)
points(knick[1],knick[2],pch=16,col=2)
points(upeast,upnorth,pch=16,col=3)
points(downeast,downnorth,pch=16,col=5)
arrows(upeast,upnorth,downeast,downnorth,lty=2,col='black')


fitN = c(upnorth,downnorth)
fitE = c(upeast, downeast)
fitline = lm(fitN ~ fitE)
SLP = abs(atan(fitline$coefficients[2])*(180/pi))

if (upeast < downeast&upnorth<downnorth)
{  # Q1
 SLP =  90 - SLP
}
if (upeast > downeast&upnorth<downnorth)
{  # Q2
 SLP = 270 + SLP
}
if (upeast > downeast&upnorth>downnorth)
{  # Q3
 SLP = 270 - SLP
}
if (upeast < downeast&upnorth>downnorth)
{  # Q4
 SLP =  90 + SLP
}

if (upeast==downeast)
{
 if (upnorth>downnorth)
 {
 SLP = 180
 }
 if (upnorth<downnorth)
 {
```

```
 SLP = 0
 }
 }
if (upnorth==downnorth)
 {
 if (upeast>downeast)
 {
 SLP = 270
 }
 if (upeast<downeast)
 {
 SLP = 90
 }
 }

SLP = (round(SLP,digits=0))
FIN = c(knick,SLP)
return(FIN)

}

KL = length(knixmat[,1])
knixdir =matrix(ncol=5,nrow=KL)

for (i in 1:KL)
 {
 knixdir[i,] = streamdir2(stream,knixmat[i,])
 }
### choose a location to save *.dbf files of the knickpoint locations and directions
setwd('C:/UNC/PhD/R/profiles/images/auto_picks/graham_co')
outname = paste(TITLE, "_", A, "_", B, "_", C, "_", D, "knixUTM.dbf",sep="")
write.dbf(knixdir,file= outname, factor2char = TRUE, max_nchar = 254)
return(knixdir)
#END OF CODE    ############################
}

##############################################################################################
##
##  function to calculate the stream direction distribution

wholestreamdir = function (stream)
{
 stream = as.matrix(stream)
 stream = orderstream(stream)
 N = length(stream[,1])
```

```
SLP = vector()
upnorth = vector(length =N)
upnorth[1] =NA

upeast = vector(length =N)
upeast[1] =NA

downnorth = vector(length =N)
downnorth[1] =NA

downeast = vector(length =N)
downeast[1] =NA

Rw=1
knixind = (1:(N))
upnorth[2:(N-1)] = stream[(knixind[2:(N-1)]-Rw),3]
upeast[2:(N-1)]  = stream[(knixind[2:(N-1)]-Rw),2]
downnorth[2:(N-1)] = stream[(knixind[2:(N-1)]+Rw),3]
downeast[2:(N-1)]  = stream[(knixind[2:(N-1)]+Rw),2]
upnorth[N] =NA
upeast[N] =NA
downnorth[N] =NA
downeast[N] =NA

for (i in 2:(N-1))
{
 fitN = c(upnorth[i],downnorth[i])
 fitE = c(upeast[i], downeast[i])
 fitline = lm(fitN ~ fitE)
 SLP[i] = abs(atan(fitline$coefficients[2])*(180/pi))

 if (upeast[i] < downeast[i]&upnorth[i]<downnorth[i])
 {  # Q1
 SLP[i] =  90 - SLP[i]
 }
 if (upeast[i] > downeast[i]&upnorth[i]<downnorth[i])
 {  # Q2
 SLP[i] = 270 + SLP[i]
 }
 if (upeast[i] > downeast[i]&upnorth[i]>downnorth[i])
 {  # Q3
 SLP[i] = 270 - SLP[i]
 }
 if (upeast[i] < downeast[i]&upnorth[i]>downnorth[i])
 {  # Q4
```

```
 SLP[i] =  90 + SLP[i]
 }

if (upeast[i]==downeast[i])
 {
 if (upnorth[i]>downnorth[i])
 {
 SLP[i] = 180
 }
 if (upnorth[i]<downnorth[i])
 {
 SLP[i] = 0
 }
 }
if (upnorth[i]==downnorth[i])
 {
 if (upeast[i]>downeast[i])
 {
 SLP[i] = 270
 }
 if (upeast[i]<downeast[i])
 {
 SLP[i] = 90
 }
 }
}  ## CLOSE FOR LOOP

SLP = (round(SLP,digits=0))
FIN = stream[c(1:(N-1)),c(2:5)]

FINFIN = cbind(FIN,SLP)

return(FINFIN)

}
```

APPENDIX 2: MAPS AND STREAM GROUPS

A2.1 Rock descriptions for 1:12,000 scale bedrock map

Grandfather Mountain Formation

meta-basalt (Zgb): greenstone; dark-gray to green-black; fine-grained; massive and uniform texture; locally contains amygdules of white feldspar(?); contains chlorite and epidote, some secondary chalcopyrite; resembles Montezuma member.

meta-gabbro (Zgg): porphyritic; black-gray to dark-brown, fine-grained basaltic matrix with euhedral white feldspars (3mm to 3 cm); feldspars weather to orange-brown; weakly foliated.

meta-siltstone (Zgs): blue-gray to rusty-tan-brown; schistose to phyllonitic texture; fissile; fine-grained; strongly foliated and locally folded; contains muscovite, chlorite, plagioclase and potassium feldspars, some quartz; some outcrops are meta-conglomeratic with feldspar clasts up to 5mm; weathers to create a "chippy" soil and many slope failures initiate in this unit; original bedding is cryptic and often is parallel to foliation.

meta-sandstone (Zgq): green-gray to blue-gray color; typically massive in outcrop especially along ridgelines; varies from green quartzite with indistinct grain boundaries to schistose, meta-arkose with gray sandy quartz matrix and sheared feldspar grains; some outcrops are meta-conglomeratic with feldspar (3mm – 2 cm); contains lithic fragments (5mm – 10 cm); strongly foliated, locally folded, and bedding is cryptic and often is parallel to foliation.

Crossnore Plutonic Suite

Bakersville meta-gabbro (Zcgb): amphibolite; black and white color; locally strongly foliated and lineated; some massive outcrops; contains mostly plagioclase feldspar, amphibole and biotite; minor pyroxene.

Basement Rocks

Blowing Rock gneiss (Ybrg): megacrystic and porphyritic; foliated; has a green-gray to silver-blue-gray muscovite and chlorite matrix with large pink potassium feldspar (5mm – 5 cm); some feldspar is euhedral and some is highly sheared, contains minor quartz.

Pumpkin Patch Metamorphic Suite (Yppg): mostly biotite-gneiss in study area; zone of interlayered mylonitic granitic and mafic gneisses; texture ranges from migmatitic to schistose; biotite gneiss contains biotite, plagioclase feldspar, amphibole, quartz, and garnet; locally contains augen gneiss and felsic pegmatite with large feldspar (1 – 4 cm) and some large muscovite crystals (3-5 cm)

Cranberry gneiss (divided):

quartz monzonite (Ymz): red-brown to pink; gneissic texture; contains mostly pink and white feldspar (5mm to 2 cm); some quartz (5-10%); strongly foliated.

chlorite feldspar gneiss (Ycg): green-gray to silvery gray; mainly schistose to locally gneissic texture; contains mostly chlorite, muscovite, and feldspar, some biotite and quartz; strongly foliated and mylonitic in some outcrops; locally contains pods of granitic gneiss

granitic gneiss (Ygg): heterolithic, but mostly granitic gneiss with some biotite gneiss; pink-brown to smoky-gray color; contains abundant plagioclase feldspar (3mm – 3 cm) and quartz with potassic feldspar; locally highly sheared and mylonitic in places; strongly foliated and banded; forms massive outcrops where foliation dips opposite of topography

biotite amphibole gneiss (Ybg): heterolithic, but mostly biotite gneiss with some granitic gneiss; locally schistose; intermediate to mafic composition; contains biotite, amphibole, plagioclase, quartz; difficult to distinguish from Pumpkin Patch Metamorphic Suite near fault zones.

A2.2 Qualitative analysis of streams in the Boone fault study area

We separated the streams that drain into the valley around Boone into six groups based on general location and geometric properties. Only the trunk streams are considered in this discussion. Group 1 streams drain north into map area, transitioning from Grandfather Mountain window metasedimentary rocks to Cranberry Gneiss at the Boone fault. These streams feed into the New River and drain to the northeast out of the study area. The headwaters contain abundant knickpoints, as well as hook-shaped map patterns, suggesting that these sections of stream once flowed off to another river to the southwest and that the lower relief area south of the Boone fault is an uplifted plateau. Group 1 contains Aho Branch, George Hayes (unnamed), Sorrento (unnamed 1,2), Flannery Fork, Winkler Creek, Friendship Church (unnamed), S. New River, and Parkway Peak (unnamed).

Group 2 streams drain southwest, northwest out to Watauga River. These streams cross from Grandfather Mountain window formation to the Cranberry Gneiss at the Boone faults, where the main drainage is captured within the Boone valley. There are some small knickpoints upstream of major knickpoints at ~27 km upstream distance (~900 m elevation). The headwaters may be part of uplifted plateau. Group 2 contains: Watauga River, Beetree Creek, Cannon Branch, Maple Ridge (unnamed), Hayes Branch, Laurel Fork, and Harrison Branch.

Group 3 streams drain southward from Rich Mountain and Snake Den Mountain into the Boone Valley, across the Gosslan Lead and Fries thrust faults. They contain no knickpoints in headwaters and display graded longitudinal profiles.

Group 3 includes: Boone Creek (1,2,3), and Hodges Creek. Group 4 streams drain eastward from Rich Mountain and Snake Den Mountain to the northeast and drain out the South New River. These streams contain knickpoints. Group 4 includes Trivett Branch, Howard Creek, and Doe Fork.

Group 5 streams drain to the south across Snake Den Mountain/Elk Knob and flow to the northwest to the South New River. This group does not reach the Boone fault, rather it joins the South New River a few kilometers north of the Boone Valley. These streams are graded and contain no knickpoints. Group 5 contains: Norris Fork, Rittle Fork, and Meat Camp creek.

Group 6 streams drain to the west from Snake Den Mountain/Rich Mountain and out the Watauga River. These streams flow across smooth topography and contain no knickpoints. Group 6 contains Vanderpool Creek, Linville Creek, and Brushy Fork.

APPENDIX 3: DATA TABLE FROM MAP ZONES

Zone	max. elev. (m)	min. elev. (m)	mean elev. (m)	std. dev. elev. (m)	area (km^2)	total relief(m)	max. local relief (m)	mean local relief(m)	max. crustal thickness (km)	min. crustal thickness (km)	mean crustal thickness (km)	std. dev. crustal thickness (km)
AP1	431	21	200	68	18235	410	225	62	48.8	41.6	44	1.6
VR1	643	62	222	69	18363	581	405	73	50.2	40.6	46.6	2.5
BR1	1000	65	304	81	17517	935	463	63	51.9	40.3	47.9	2.6
PI1	551	0	195	58	55770	551	287	42	51.5	34.5	40.4	3.8
AP2	919	104	431	144	12014	815	548	128	52.3	47.2	49.3	1.1
VR2	1102	136	296	83	14856	966	579	88	51.5	44.6	48	1.5
BR2	2025	191	786	287	24786	1834	807	244	54.2	44.1	48.3	2.2
PI2	1335	0	234	135	51986	1335	632	56	47.4	34.8	40.1	3
AP3	1081	189	510	142	18465	892	614	192	49.5	38.7	44.8	1.6
VR3	1434	223	584	188	28035	1211	646	173	46.5	36.8	43.3	2.4
BR3	1913	110	564	318	22461	1803	692	138	45.7	34.5	40.7	3.8
PI3	768	0	156	73	29620	768	441	41	44.5	32.4	36.2	3.2
AP4	1435	141	643	219	17174	1294	545	208	44.6	38.7	42.5	1.2
VR4	1483	121	654	261	21677	1362	608	197	44.1	36.7	39.6	1.6
BR4	1237	0	226	188	15107	1237	723	105	37.6	33.3	35.6	1.1
PI4	221	0	97	23	4999	221	122	39	35.4	33	34.2	0.6
AP5	914	257	587	119	8281	657	498	126	46.1	44.4	45.5	0.5
VR5	1237	13	380	215	25996	1224	583	136	45.8	36.2	41.5	2.6
BR5	654	0	153	72	22248	654	372	64	41.2	33.3	36.2	2.3

Table 1 Values extracted from the 19 different zones we produced by splitting the study area into 5 bands of ~1.5° of latitude and by the 4 major geologic provinces.